

**THE UNIVERSITY OF CALGARY**

**Characterization of a Mycophenolic Acid-Resistant  
Mouse Inosine 5'-Monophosphate Dehydrogenase Possessing  
Two Amino Acid Substitutions by Determination of the  
Effect of Each Mutation on the Kinetic Parameters of the Enzyme**

by

**Cary F. Cuncic**

**A THESIS**

**SUBMITTED TO THE FACULTY OF GRADUATE STUDIES**

**IN PARTIAL FULFILMENT OF THE REQUIREMENTS FOR THE**

**DEGREE OF MASTER OF SCIENCE**

**DEPARTMENT OF BIOCHEMISTRY AND MOLECULAR BIOLOGY**

**CALGARY, ALBERTA**

**JULY, 1997**

**©Cary F. Cuncic 1997**



**National Library  
of Canada**

**Acquisitions and  
Bibliographic Services**

**395 Wellington Street  
Ottawa ON K1A 0N4  
Canada**

**Bibliothèque nationale  
du Canada**

**Acquisitions et  
services bibliographiques**

**395, rue Wellington  
Ottawa ON K1A 0N4  
Canada**

*Your file Votre référence*

*Our file Notre référence*

**The author has granted a non-exclusive licence allowing the National Library of Canada to reproduce, loan, distribute or sell copies of this thesis in microform, paper or electronic formats.**

**The author retains ownership of the copyright in this thesis. Neither the thesis nor substantial extracts from it may be printed or otherwise reproduced without the author's permission.**

**L'auteur a accordé une licence non exclusive permettant à la Bibliothèque nationale du Canada de reproduire, prêter, distribuer ou vendre des copies de cette thèse sous la forme de microfiche/film, de reproduction sur papier ou sur format électronique.**

**L'auteur conserve la propriété du droit d'auteur qui protège cette thèse. Ni la thèse ni des extraits substantiels de celle-ci ne doivent être imprimés ou autrement reproduits sans son autorisation.**

**0-612-24652-3**

**Canada**

## **Abstract**

Inosine 5'-monophosphate dehydrogenase (IMPDH) catalyzes the first committed step in the *de novo* production of guanine nucleotides. Mycophenolic acid (MPA) is an inhibitor of IMPDH and a derivative of it is used in immunosuppressive drug therapy. A mouse MPA-resistant IMPDH was isolated from neuroblastoma cells which possessed two amino acid substitutions: Thr 333 was replaced with Ile and Ser 351 was replaced with Tyr. In this study, IMPDHs containing each single mutation were generated and assayed in addition to the wild-type and double mutant. The effect of each mutation on the  $K_m$ IMP,  $K_m$ NAD<sup>+</sup>,  $K_i$ XMP,  $K_i$ MPA and  $k_{cat}$  of IMPDH was determined. Each mutation affected some kinetic parameters, the most striking results were produced by the T333I mutation which was the main if not sole cause of the MPA resistance and caused a 10-fold reduction in  $k_{cat}$ .

## **Acknowledgments**

I would like to thank the department of Biochemistry and Molecular Biology, University of Calgary for multiple Graduate Research Scholarships and acknowledge the Medical Research Council of Canada, who's funding made my project possible.

Thank you to my committee members: Dr. Goren, Dr. Huber and Dr. Stevenson. I appreciate the time you took over the years to help me with my project and your words of advice and encouragement. Thank you also to Dr. Severson for being my external examiner.

I would like to thank my supervisor, Dr. Floyd Snyder, for all of his advice and support over the years. He had confidence in me to write my thesis while I was working across the country. It took an extra effort on his part to continue his supervision of my thesis under these circumstances and I greatly appreciate it.

My friends Glenis Wiebe, Shari Gallant, and Mauer Chiarello have given me a lot of emotional support. Glenis was a fellow graduate student in Dr. Snyder's lab. We became close friends and I miss working with her on a daily basis. Shari and I have shared endless cups of coffee and conversations; often, a Saturday morning cafe au lait with her got me through the week. Mauer and I have been friends since we were six years old. He was always there to throw some cash in my bank account at the end of the month if I needed it. Mauer has supported me through everything in life.

Finally, I would like to express my gratitude to my parents for their patience and financial and emotional support throughout the course of graduate school. They have always been behind me 100% and I truly appreciate all of the help that they have given.

## Table of Contents

	Page
<u>Abstract</u> .....	iii
<u>Acknowledgments</u> .....	iv
<u>Table of Contents</u> .....	v
<u>List of Tables</u> .....	viii
<u>List of Figures</u> .....	ix
<u>List of Abbreviations</u> .....	xi
<u>CHAPTER 1: Introduction</u> .....	1
Function of IMP Dehydrogenase.....	1
Mechanism of IMP Dehydrogenase.....	1
Cell Proliferation Dependence on [IMPDH].....	5
Utilizations of IMPDH Inhibitors in Drug Therapy.....	6
Human IMPDH Exists as Two Isozymes.....	7
Expression Patterns of Human IMPDH.....	11
IMPDH Enzyme Kinetics.....	14
Mycophenolic Acid, an Inhibitor of IMPDH.....	15
Mechanism of Mycophenolic Acid Inhibition.....	16
A MPA-Resistant Mouse IMPDH.....	16
Active-Site Amino Acids in IMPDH.....	19
MPA Interaction with IMPDH Mutants.....	24
Objectives of Study.....	24
<u>CHAPTER 2: Materials</u> .....	26
<u>CHAPTER 3: Methods</u> .....	30
General Protocols.....	30
Maintenance and storage of bacterial strains.....	30
Agarose gel electrophoresis of DNA.....	30
Purification of DNA from agarose gel.....	31

Restriction endonuclease digestion of DNA.....	32
Phosphatase treatment of DNA.....	32
Cloning insert DNA into plasmid DNA.....	33
Transformation of <i>E. Coli</i> with plasmids.....	33
Preparation of competent <i>E. Coli</i> for transformation.....	33
Preparation of <i>E. Coli</i> for electroporation.....	34
Transformation of competent <i>E. Coli</i> .....	34
Transformation of <i>E. Coli</i> by electroporation.....	35
Selection of <i>E. Coli</i> colonies to screen for gene insertion.....	35
Large scale preparation of plasmid DNA.....	36
Small scale preparation of plasmid DNA.....	37
Spectrophotometric quantitation of DNA and RNA.....	38
RNA-based Methodology.....	38
Preparation of DEPC-H <sub>2</sub> O.....	38
Isolation of total RNA from mouse neuroblastoma cells.....	38
Formaldehyde gel electrophoresis of RNA.....	39
Isolation of polyA <sup>+</sup> RNA.....	40
Generation of cDNA by reverse transcription.....	40
PCR-based Methodology.....	41
PCR to generate full-length IMPDH genes.....	41
Restriction fragment length polymorphism analysis.....	41
PCR to generate 985 bp product.....	41
Restriction fragment length polymorphism analysis.....	42
Site-Directed Mutagenesis of IMPDH.....	42
Purification of plasmid DNA for site-directed mutagenesis.....	42
Site-directed mutagenesis procedure.....	44
Expression, Purification and Assay of IMPDH.....	46
Large-scale induction and purification of IMPDH-MBP.....	46
Cleavage of fusion protein by factor Xa.....	47
Bradford protein assay.....	47
SDS-polyacrylamide gel electrophoresis.....	47
IMPDH assay and Analysis.....	48
<b><u>CHAPTER 4: Results</u></b> .....	<b>50</b>

Confirmation of Site-Directed Mutants.....	50
Purification of Recombinant IMPDH.....	54
IMPDH Kinetic Assays.....	57
Calculated Kinetic Parameters.....	70
<u>CHAPTER 5: Discussion</u> .....	74
Wild-Type IMPDH Kinetics.....	75
Wild-Type and Double Mutant IMPDH Comparison.....	76
Consequences of Mutations of IMPDH.....	77
$K_i$ M <sub>PA</sub> .....	77
$K_m$ NAD <sup>+</sup> and $K_i$ NAD <sup>+</sup> .....	78
$K_m$ IMP.....	79
$K_i$ XMP.....	80
$k_{cat}$ and $K_m$ IMP/ $k_{cat}$ .....	80
IMPDH Amino Acids Thr 333 and Ile 351 Across Species.....	81
Conclusions.....	82
<u>References</u> .....	84
<u>Appendix: Enzyme Kinetics</u> .....	97

## **List of Tables**

	Page
Table 1	Kinetic Parameters of Human Types I and II IMPDH.....14
Table 2	Kinetic Parameters of Mouse Type II and Mouse Type II MPA-Resistant IMPDH.....18
Table 3	Mutational Events in Mouse Type II MPA-Resistant IMPDH.....19
Table 4	Amino Acid Homology of IMPDH Across Species.....20
Table 5	Table of Primers used in PCR and Site-Directed Mutagenesis.....27
Table 6	Kinetic Parameters of Four Species of Mouse Type II IMPDH.....71
Table 7	Mycophenolic Acid Inhibition of IMPDH.....72
Table 8	Summary of Kinetic Parameters of the Four IMPDHs.....73

## List of Figures

	Page
Figure 1	Structures of IMP and XMP.....2
Figure 2	Purine Metabolic Pathway .....3
Figure 3	Reaction Mechanism of IMPDH.....4
Figure 4	Structures of Inhibitors of IMPDH.....8
Figure 5	Structures of Mycophenolic Acid and Mycophenolate mofetil.....9
Figure 6	Molecular Mechanism of IMPDH.....17
Figure 7	Amino Acids of IMPDH which Interact with IMP(ox).....22
Figure 8	Amino Acids of IMPDH which Interact with MPA.....23
Figure 9	Binding Sites of Primers on Mouse Type II IMPDH .....29
Figure 10	PMAL Vector.....43
Figure 11	Site-Directed Mutagenesis Scheme.....45
Figure 12	RFLP Analysis of IMPDH Genes.....51
Figure 13	IMPDH Restriction Map for <i>Bsa</i> I and <i>Bsa</i> J1.....53
Figure 14	SDS-PAGE of Fusion and Cleaved IMPDHs.....55
Figure 15a)	Initial Velocity of T333/S351 IMPDH.....58
15b)	Initial Velocity of I333/S351 IMPDH.....58
15c)	Initial Velocity of T333/Y351 IMPDH.....58
15d)	Initial Velocity of I333/Y351 IMPDH.....58
Figure 16a)	NAD <sup>+</sup> Uncompetitive Inhibition of T333/S351 IMPDH.....61
16b)	NAD <sup>+</sup> Uncompetitive Inhibition of I333/S351 IMPDH.....61
16c)	NAD <sup>+</sup> Uncompetitive Inhibition of T333/Y351 IMPDH.....61
16d)	NAD <sup>+</sup> Uncompetitive Inhibition of I333/Y351 IMPDH.....61
Figure 17a)	XMP Competitive Inhibition of T333/S351

		IMPDH.....	64
17b)	XMP Competitive Inhibition of I333/S351	IMPDH.....	64
17c)	XMP Competitive Inhibition of T333/Y351	IMPDH.....	64
17d)	XMP Competitive Inhibition of I333/Y351	IMPDH.....	64
Figure 18a)	MPA Uncompetitive Inhibition of T333/S351	IMPDH.....	67
18b)	MPA Uncompetitive Inhibition of I333/S351	IMPDH.....	67
18c)	MPA Uncompetitive Inhibition of T333/Y351	IMPDH.....	67
18d)	MPA Uncompetitive Inhibition of I333/Y351	IMPDH.....	67

## List of Abbreviations

A	Absorbance
ATP	Adenosine triphosphate
BSA	Bovine serum albumin
CaCl <sub>2</sub>	Calcium chloride
cDNA	Complementary DNA
ddH <sub>2</sub> O	Double distilled water
DEPC	Diethyl pyrocarbonate
DMSO	Dimethyl sulfoxide
DNA	Deoxyribonucleic acid
dNTP	Deoxyribonucleotide
DTT	Dithiothreitol
EDTA	Ethylenediamine tetraacetic acid
g	Gram
g	Force of gravity
HCl	Hydrochloric acid
I	Isoleucine
Ile	Isoleucine
IMP	Inosine 5'-monophosphate
IMPDH	Inosine 5'-monophosphate dehydrogenase
IPTG	Isopropylthio-β-galactoside
KCl	Potassium chloride
M	Moles per litre
MBP	Maltose binding protein
MgCl <sub>2</sub>	Magnesium chloride
ml	Millilitre
mM	Millimoles per litre
m m	millimetre
MPA	Mycophenolic acid
MOPS	3-(N-Morpholino)propanesulfonic acid
NAD <sup>+</sup>	Nicotinamide adenine dinucleotide
NaCl	Sodium chloride
NaI	Sodium iodide

NaOAc	Sodium acetate
OD.	Optical density
$\Omega$	Ohms
PAGE	Polyacrylamide gel electrophoresis
PMSF	Phenylmethylsulfonyl flouride
ppsi	Pounds per square inch
RFLP	Restriction fragment length polymorphism
RNA	Ribonucleic acid
rpm	Rotations per minute
S	Serine
SDS	Sodium dodecyl sulphate
Ser	Serine
T	Threonine
TEMED	N, N, N', N'-tetramethylethylenediamine
Thr	Threonine
Tris	Tris-(hydroxymethyl)-aminomethane
Tyr	Tyrosine
$\mu$ F	Microfarad
$\mu$ L	Microlitre
UV	Ultraviolet
Xgal	5-bromo-4-chloro-3-indolyl- $\beta$ -D-galactoside
XMP	Xanthosine 5'-monophosphate
Y	Tyrosine

## **CHAPTER 1: Introduction**

### **Function of IMP Dehydrogenase**

Inosine 5'-monophosphate dehydrogenase (IMPDH) (IMP:NAD<sup>+</sup> oxidoreductase, EC 1.1.1.205) catalyzes the oxidation of inosine 5'-monophosphate (IMP) to xanthosine 5'-monophosphate (XMP) (Figure 1) (Abrams and Bentley, 1959). This reaction is the first committed step in the *de novo* production of guanine nucleotides in the purine metabolic pathway (Figure 2) (Crabtree and Henderson, 1971; Snyder and Henderson, 1973; Jackson and Weber, 1975). IMP is the end-product of the *de novo* biosynthesis of purines and has three potential fates. IMP can be dephosphorylated to inosine by a 5'-nucleotidase (on the path to uric acid production), converted to adenylosuccinate by adenylosuccinate synthase (on the path of adenine nucleotide biosynthesis), or oxidized to XMP by IMPDH. The oxidation of IMP to XMP by IMPDH is not only the first committed step of *de novo* guanine nucleotide biosynthesis, it is also the rate-limiting step. NAD<sup>+</sup> is reduced during the reaction and mammalian IMPDH has been reported to require potassium ion (Anderson and Sartorelli, 1968).

### **Mechanism of IMP Dehydrogenase**

The kinetics of IMPDH has been studied in a wide variety of species including human (Holmes *et al.*, 1974; Carr *et al.*, 1993; Hager *et al.*, 1995), mouse (Anderson and Sartorelli, 1968; Hodges *et al.*, 1989), Chinese hamster (Huberman *et al.*, 1981; Sintchak *et al.*, 1996), rat (Jackson *et al.*, 1977; Yamada *et al.*, 1988), parasitic protozoa (Hupe *et al.*, 1986; Verham *et al.*, 1987; Hedstrom and Wang, 1990), *Aerobacter aerogenes* (Brox and Hampton, 1968), *Escherichia coli* (Gilbert *et al.*, 1979), and the nitrogen-fixing nodules of cowpea (Atkins *et al.*, 1985). The elucidated enzyme mechanism is an ordered bi-bi reaction (Figure 3; taken from Link and Straub, 1996

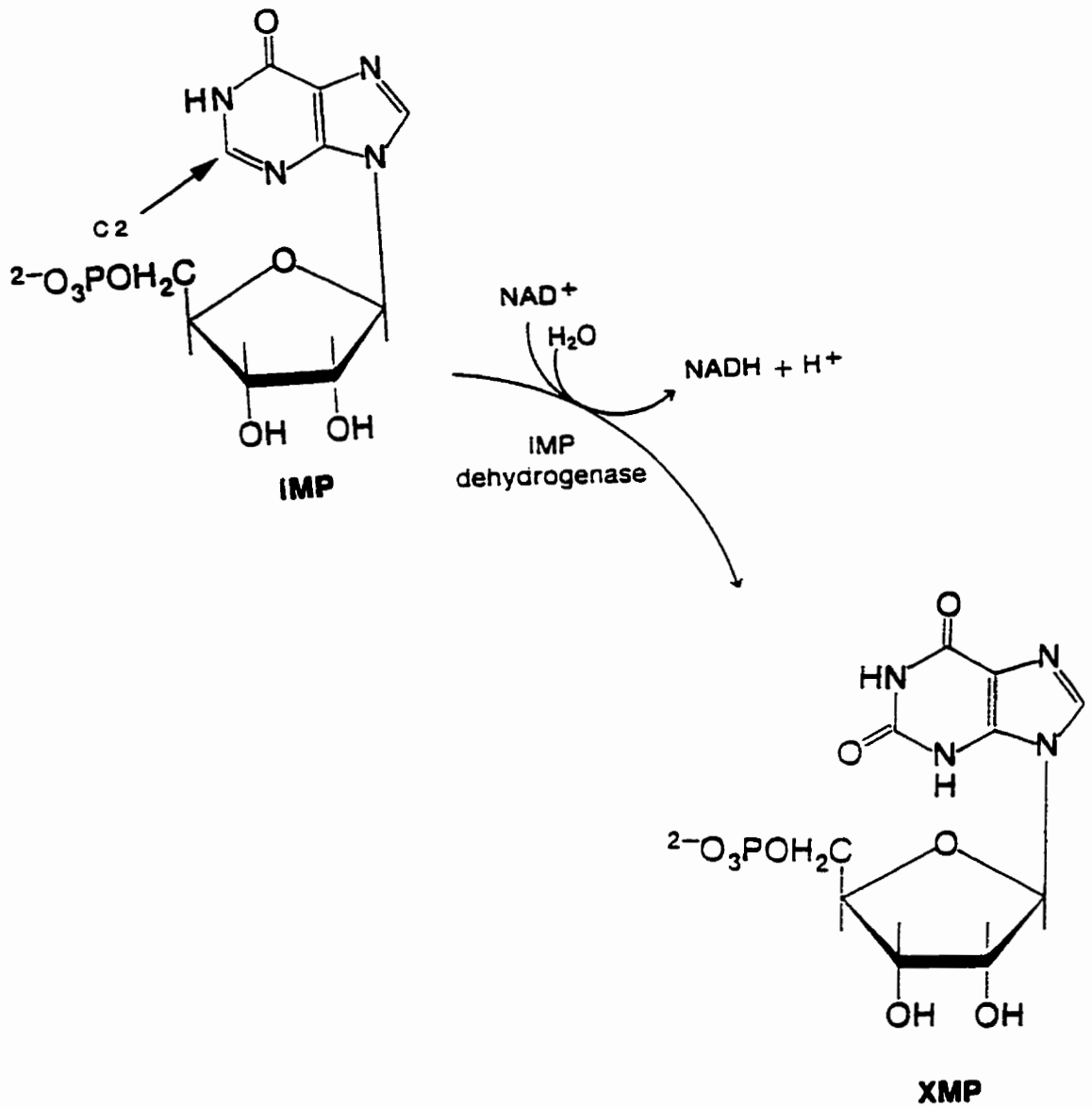


**Figure 1.** Oxidation of IMP to XMP by IMPDH

C2 of the purine ring forms a covalent bond with IMPDH.

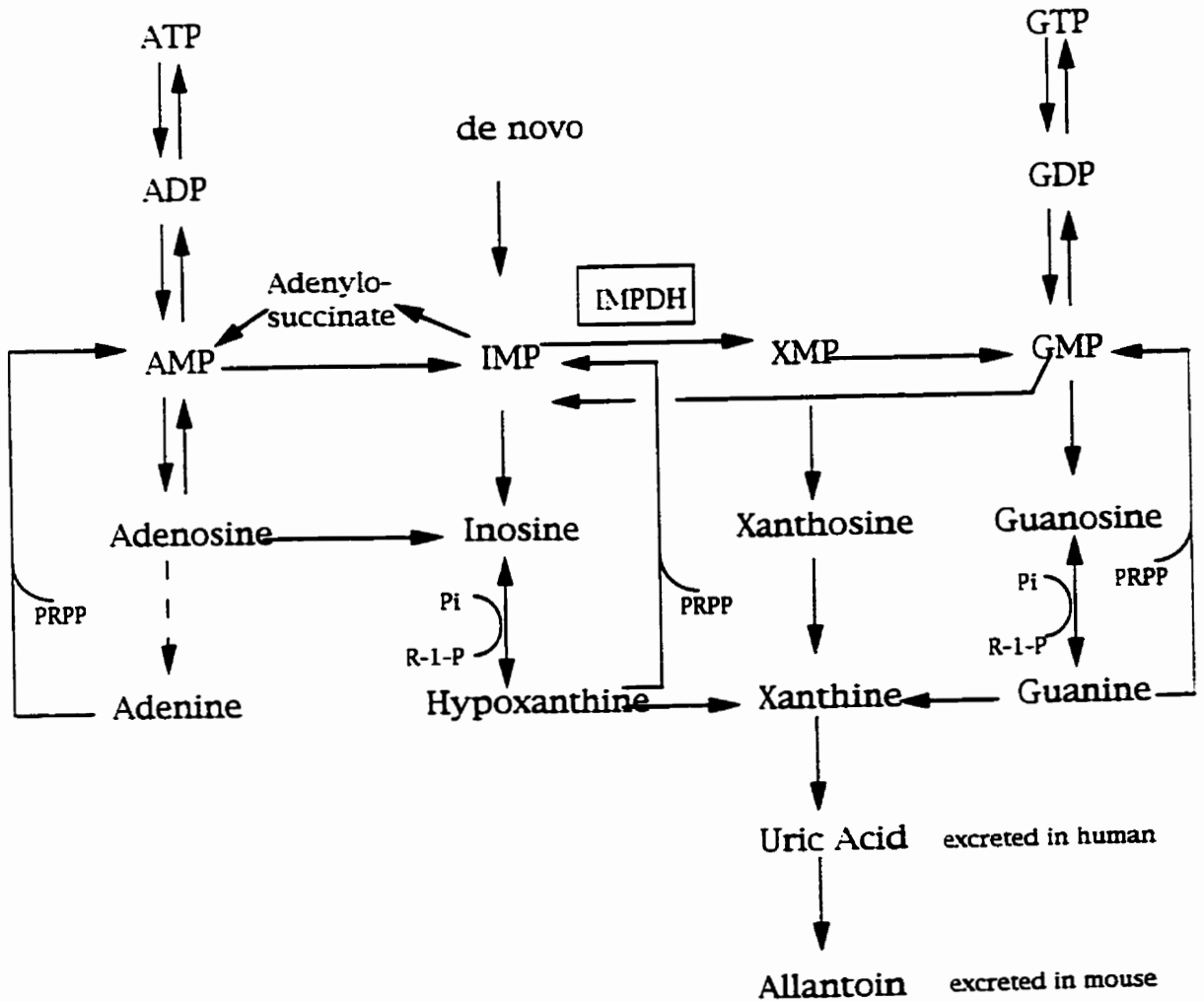


**Figure 2. Pathways of Purine Metabolism and Interconversion**

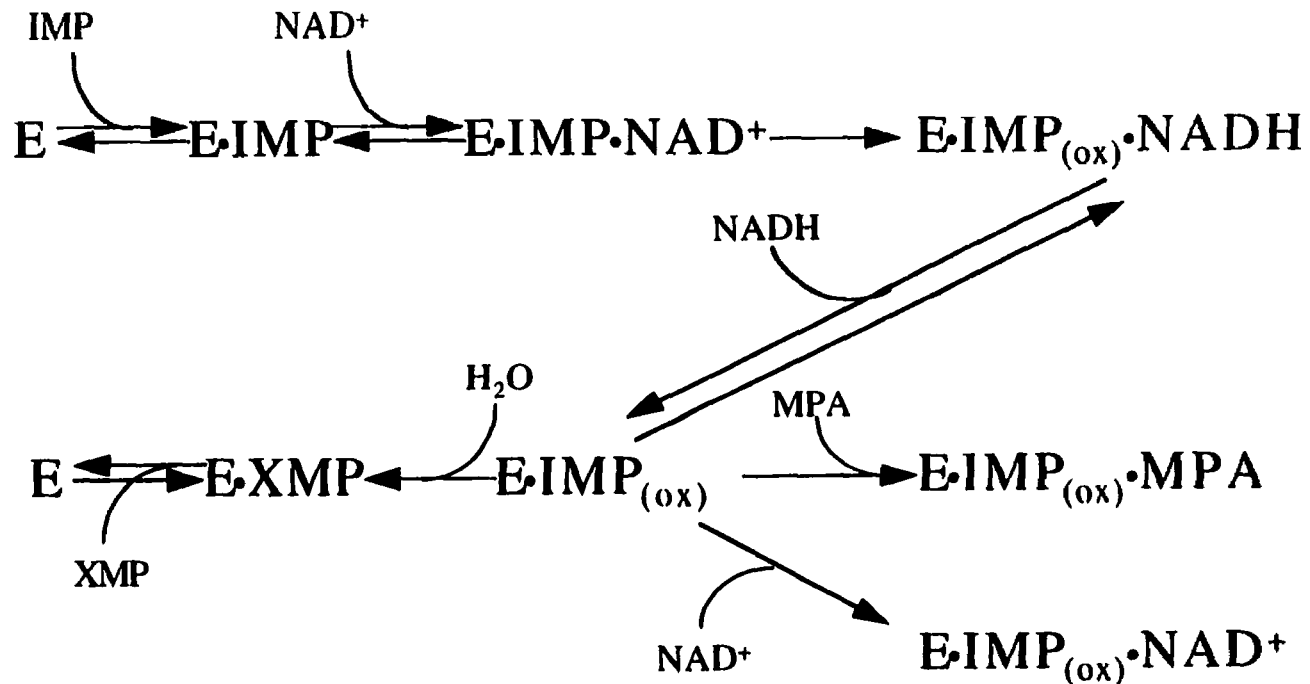


**Figure 3. Reaction Mechanism of IMPDH**

“E” denotes the enzyme IMPDH. IMP binds first, followed by NAD<sup>+</sup> binding, forming a ternary complex. A covalent bond is formed between Cys 331 of IMPDH and C-2 of the purine ring of IMP with hydride transfer from IMP to NAD<sup>+</sup>. “E·IMP<sub>(ox)</sub>” represents a chemical intermediate between IMP and XMP which is covalently bound to IMPDH.

(“E·IMP<sub>(ox)</sub>” is denoted as “E·XMP” in some literature.) NADH is released, the chemical intermediate undergoes hydrolysis and the XMP product is released. MPA (or NAD<sup>+</sup>) binds to E·IMP<sub>(ox)</sub>, leading to a dead-end ternary complex.

and used with permission). IMP first binds to IMPDH, then  $\text{NAD}^+$  binds. IMP is oxidized to XMP while  $\text{NAD}^+$  is reduced to NADH, then NADH is released, and this is followed by the release of XMP. IMP binding to IMPDH occurs by likely many enzyme-substrate interactions and results in a covalent bond between the cysteine amino acid residue on IMPDH at position 331 in the human enzyme (Antonino *et. al.*, 1994) and the corresponding Cys at position 319 in the protozoan enzyme (Huete-Perez *et. al.*, 1995). IMP bound to IMPDH via this bond is the covalent intermediate. Mutation of Cys 331 in human type II IMPDH to Ala or Ser abolishes the activity of the enzyme (Wu *et. al.*, 1996).  $\text{NAD}^+$  is a substrate inhibitor of IMPDH, inhibiting at high (>0.5 mM) concentrations (Anderson and Sartorelli, 1968; Jackson *et. al.*, 1977; Hodges *et. al.*, 1989; Wang *et. al.*, 1990). Substrate inhibition by  $\text{NAD}^+$  appears to proceed by the sequestering of the covalent intermediate into a dead-end complex (Wu *et. al.*, 1996). The monovalent cation involvement in the mechanism has been studied. Purified recombinant human type II IMPDH possesses less than 1% of maximal activity in the absence of monovalent cation (Xiang *et. al.*, 1996).  $\text{K}^+$  is the most potent monovalent activator, likely due to the size of its ionic radius (Xiang *et. al.*, 1996). IMP can bind to IMPDH in the absence of potassium, but the monovalent cation is required for the reaction to proceed. IMPDH is thought to bind  $\text{K}^+$  before it binds IMP (Xiang *et. al.*, 1996) and it has been hypothesized that  $\text{K}^+$  helps to organize protein conformation around the active site and position Cys-331 for catalysis (Sintchak *et. al.*, 1996). It is not known if the monovalent cation dissociates in each catalytic cycle because no inhibitors which compete with  $\text{K}^+$  are known (Xiang *et. al.*, 1996).

### Cell Proliferation Dependence on [IMPDH]

IMPDH is a tetramer composed of four 56-58 kDa monomers (Gilbert *et. al.*, 1979; Yamada *et. al.*, 1988; Carr *et. al.*, 1993). Intracellular concentrations of IMPDH are positively correlated with rates of cell

proliferation. A positive correlation was found between IMPDH activity and proliferation of rat hepatomas having varied growth rates. All rat hepatoma tissues possessed a much higher IMPDH activity than those of normal tissue (Weber, 1983). This positive correlation has been observed in human leukemic cell lines, solid tumor tissues (Jackson *et. al.*, 1975; Natsumeda *et. al.*, 1988; Collart and Hubermann, 1990; Konno *et. al.*, 1991; Nagai *et. al.*, 1991, 1992; Collart *et. al.*, 1992; Senda and Natsumeda, 1994), as well as in T lymphocytes upon activation in response to mitogen (Allison *et. al.*, 1975; Dayton *et. al.*, 1994). IMPDH activity also showed a positive correlation with the growth rate of nonmalignant human lymphoblasts (Gruber *et. al.*, 1985), suggesting that IMPDH is interdependent with conditions affecting growth rate rather than being a direct marker of malignant transformation or T cell activation. The association is likely due to the requirement of guanine nucleotides for cell growth; IMPDH inhibitors deplete GTP levels. This depletion is thought to block RNA-primed DNA synthesis which inhibits DNA synthesis and thus inhibits cell growth (Catapano *et. al.*, 1995). IMPDH plays an essential role in providing the replicating cell with the necessary precursors for DNA and RNA synthesis. When cells are treated with IMPDH inhibitors, DNA synthesis abruptly ceases and this cessation can be circumvented by the addition of exogenous guanosine (Cohen and Sadee, 1983).

#### Utilizations of IMPDH Inhibitors in Drug Therapy

Because IMPDH levels are linked to cellular proliferation, IMPDH is a target for antitumor (Jackson *et. al.*, 1975; Robins, 1982; Weber, 1983; Tricot *et. al.*, 1989; Gharehbaghi *et. al.*, 1994), antiviral (Streeter *et. al.*, 1973; Malinoski and Stollar, 1981), antiparasitic (Webster and Whaun, 1982; Hupe *et. al.*, 1986; Verham *et. al.*, 1987) and immunosuppressive (Jackson *et. al.*, 1975; Eugui *et. al.*, 1991; Dayton *et. al.*, 1994) drug therapy. Some IMPDH inhibitors which have been tested for their antiproliferative effects are tiazofurin

(Kharabanda *et. al.*, 1988; Tricot *et. al.*, 1989), ribavirin (Yamada *et. al.*, 1988; Hedstom and Wang, 1990), "virazole" (which is structurally identical to ribavirin and utilized for its antiviral effects) (Streeter *et. al.*, 1973; Lowe *et. al.*, 1977; Jayaram *et. al.*, 1982), selenazofurin (Gharehbaghi *et. al.*, 1994), benzamide riboside (Jayaram *et. al.*, 1992; Gharehbaghi *et. al.*, 1994), and mycophenolic acid (MPA) (Lowe *et. al.*, 1977; Eugui *et. al.*, 1991) (Figures 4 and 5). Inhibitors of IMPDH block *de novo* GTP biosynthesis which reduces the concentrations of guanylates required for DNA synthesis. Tiazofurin and MPA have been shown to strongly induce differentiation of various kinds of neoplastic cells such as leukemic cells (Tricot *et. al.*, 1989; Collart and Huberman, 1990), breast carcinoma (Sidi *et. al.*, 1988; Bacus *et. al.*, 1990), and melanoma (Kiguchi *et. al.*, 1990) tissues. This differentiation was shown to be due to decreased levels of guanine nucleotides in the cells; addition of exogenous guanosine (a precursor for synthesis of GMP via the salvage pathway) blocked the differentiation (Koloski *et. al.*, 1986; Olah *et. al.*, 1988; Yamaj *et. al.*, 1990). Tiazofurin has been utilized in clinical trials for leukemia chemotherapy (Tricot *et. al.*, 1989) and mycophenolate mofetil, a prodrug of MPA, has passed clinical trials for use as an immunosuppressive agent during transplantations (Shaw *et. al.*, 1995; Sollinger, 1995).

### Human IMPDH Exists as Two Isozymes: Comparison of Amino Acid and DNA Sequences

There are two isozymes of human IMPDHs: type I and type II (Natsumeda *et. al.*, 1990). Two distinct IMPDH cDNAs were isolated from a human spleen cDNA library. Both type I and type II IMPDH clones contain an open reading frame of 1542 base pairs encoding proteins of 514 amino acid residues. The amino acid sequences show 84% identity. Eighty-four amino acids differ between the two enzymes: 52 amino acids are conservative substitutions and 32 diverge with respect to the chemical properties of the side-chain of

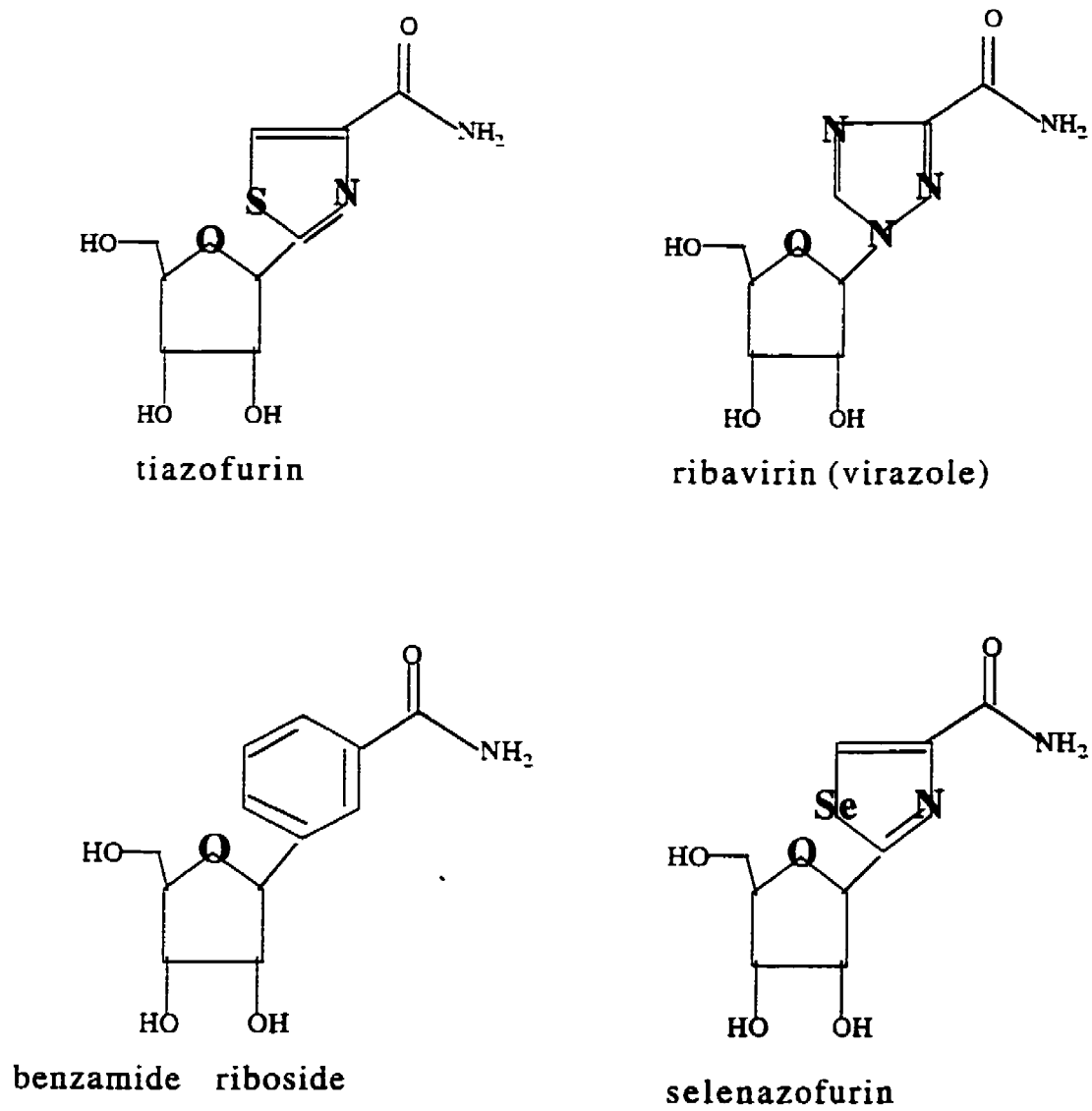
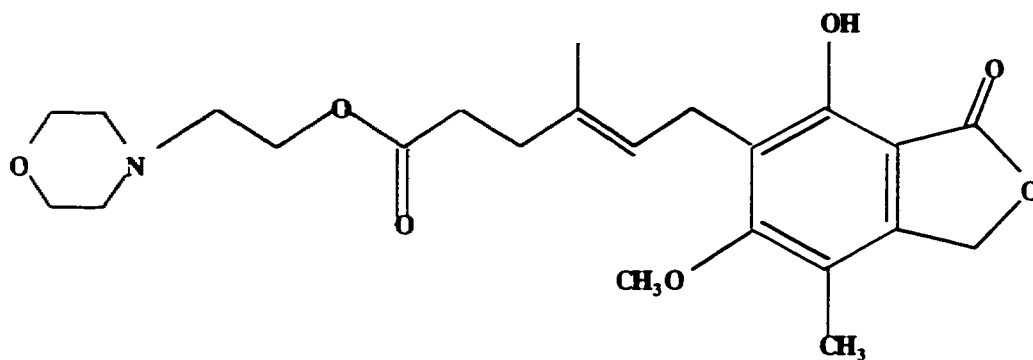
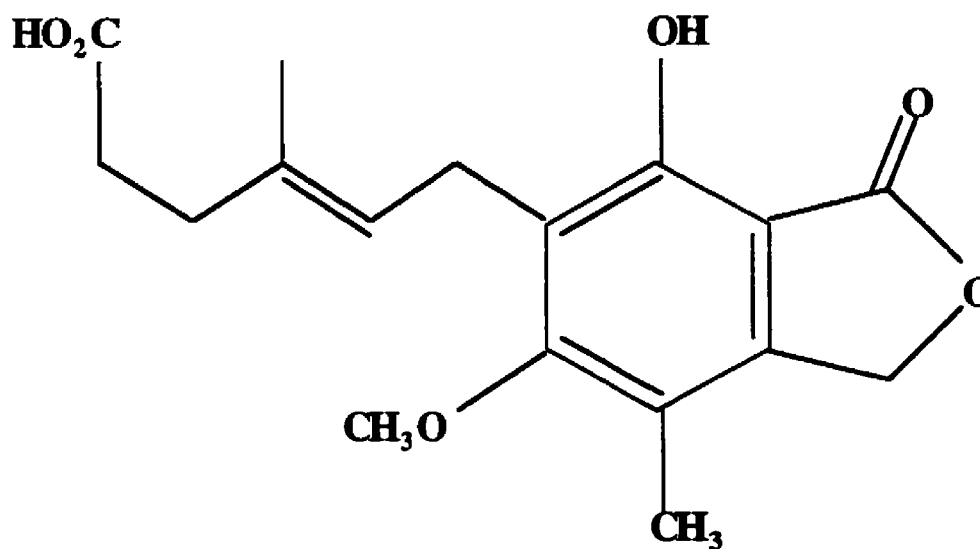


**Figure 4. Inhibitors of IMPDH**



**Mycophenolate mofetil**



**Mycophenolic Acid**

**Figure 5. Structures of Mycophenolate mofetil and Mycophenolic Acid**

the amino acids (Natsumeda *et. al.*, 1990). The calculated pI values based on amino acid sequence are 6.1 for type I and 6.7 for type II. The nucleotides in the coding region of the two cDNAs have 76.4% sequence identity while there wasn't any significant similarity between the two in the noncoding region. The gene for type II IMPDH has been sequenced (Zimmerman *et. al.*, 1994). It contains 14 exons and is approximately 5.8 kb in length. Potential binding sites for nuclear factors (AP2, ATF, CREB, Egr-1, Nm23, and Sp1) were found in the promoter, suggesting that some of the nuclear factors may play a role in the regulation of IMPDH type II gene transcription (Zimmermann *et. al.*, 1994). The type II IMPDH gene has been localized to the p21-24 region of chromosome 3, where a number of tumor suppressor genes have also been located (Glesne *et. al.*, 1993). The gene for type I IMPDH has been localized to chromosome 7 in the q31.3 to q32 region (Gu. *et. al.*, 1994). Type I IMPDH mRNA is 3.5 kb in size and type II IMPDH mRNA is 2.3 kb (Natsumeda *et. al.*, 1989). The IMPDH type I gene exists as multiple pseudogenes in the human and Rhesus monkey genomes but there is only a single functional gene. The type II IMPDH gene exists as a single copy in these species (Dayton and Mitchell, 1993). Single copy genes for each IMPDH were also found in rat, mouse, dog, cow, and chicken DNA. Distinct mRNAs for type I and type II IMPDH were identified in mouse and hamster (Dayton and Mitchell, 1993).

The amino acid sequences of IMPDH are highly conserved among species. Human type II IMPDH differs from mouse type II and a Chinese hamster IMPDH by only 6 and 8 out of 514 amino acids, respectively (Tiedeman and Smith, 1991; Natsumeda *et. al.*, 1990; Collart and Huberman, 1988) and human type I IMPDH is analogous to mouse type I IMPDH. *Drosophila melanogaster* possesses 65% amino acid identity with human type II IMPDH (Sifri *et. al.*, 1994). Considering conservative substitutions between amino acids, the parasitic protozoa *Leishmania donovani* (Wilson *et. al.*, 1991), yeast (Genbank accession number L28920), and plant (Collart *et. al.*, 1996)

IMPDHs exhibit 70% amino acid sequence homology with mammalian IMPDHs. The bacterial proteins possess 70% amino acid similarity among themselves and 60% with those of mammalian cells (Thomas and Drabble, 1985; Kanazki and Miyagawa, 1990; Collart *et. al.*, 1996). The parasitic protozoa *T. foetus*, however, differs in amino acid sequence by approximately 30% when compared to other species (Beck *et. al.*, 1994).

### Expression Patterns of Type I and Type II IMPDH

Human type I and type II IMPDH were found to differ in their expression patterns. Type I IMPDH was expressed at higher levels in normal leukocytes than in ovarian tumors and type II IMPDH was expressed at higher levels in ovarian tumors, leading to the conclusion that the two IMPDHs are differentially regulated (Natsumeda *et. al.*, 1989. This was an important finding, since drugs more potent for one isozyme over the other would potentially have fewer side-effects.

Differential expression for each IMPDH among 16 different human and 5 different fetal tissues was evident, suggesting that each enzyme may be expressed in a tissue-specific manner (Senda and Natsumeda, 1994). Type II IMPDH was the dominant species in every tissue except for peripheral blood leukocytes (Senda and Natsumeda, 1994) where the ratio of type II/type I mRNA was 0.7. Levels of mRNA and IMPDH protein were examined in normal lymphocytes and compared to levels in K563 and HL-60 leukemic cell lines. There was an increased level of IMPDH protein in the leukemic cell lines which corresponded with the observed increase in IMPDH enzyme activity (7.8 and 9.4-fold, respectively), due to specific upregulation of type II IMPDH activity.

Levels of IMPDH activity and expression were also examined in leukemic cells from patients and compared to normal lymphoblasts.

Again, the levels of increased type II mRNA in leukemic cells (1.5 to 5.1-fold relative to levels in normal lymphocytes) corresponded with increased IMPDH activity (1.8 - 7.8-fold compared to normal lymphocytes) (Nagai *et. al.*, 1991). Type I mRNA levels remained constant in leukemic cells compared to normal lymphocytes. The levels of type I mRNA and type II mRNA were approximately equal in normal lymphocytes (Nagai *et. al.*, 1991). Normal lymphocytes were stimulated with phytohemagglutinin or transformed with Epstein-Barr virus (EBV). Levels of type I mRNA remained constant in all three cell types while levels of type II mRNA were increased 3.2-fold and 5.7-fold respectively (Nagai *et. al.*, 1992). Stimulated HL-60 cells possessed 2.8-fold higher levels of IMPDH type II mRNA than quiescent HL-60 cells and the level decreased when replication of the cells declined. The levels of type I IMPDH were constant (Nagai *et. al.*, 1992). Type II IMPDH is the predominant species in HL-60 cells at the mRNA and protein levels (Konno *et. al.*, 1991). When HL-60 cells are induced to differentiate, levels of type II IMPDH are decreased to 5% of their levels in HL-60 cells and type I IMPDH levels are decreased to 79% and become the main species in the differentiated cells (Nagai *et. al.*, 1992). Differentiation by retinoic acid or DMSO proceeded by a different mechanism than differentiation induced by IMPDH inhibitors in that addition of exogenous guanosine failed to overcome the differentiation (Koloski *et. al.*, 1986; Yamaji *et. al.*, 1990).

Enhanced expression of type II mRNA (3 to 50- fold) was also found in various neuronal tumors compared to normal brain tissue and in sarcoma cells relative to normal fibroblasts (Collart, *et. al.*, 1992). The increase was not due to gene amplification and type I mRNA levels were not detectable (Collart *et. al.*, 1992). These results led to the proposal that type II IMPDH is associated with and perhaps necessary for cell growth while type I IMPDH is unrelated to the proliferative status of the cells and possesses more of a "housekeeping" function.

The profiles of the two IMPDH mRNA quantities upon T lymphocyte activation differ from those of neoplastic transformation and differentiation. Mitogen-activated T-cells showed a dose-dependent increase in IMPDH protein levels and activity. In this case, levels of both IMPDH mRNAs were increased 10-fold, indicating that type I and type II human IMPDH may be beneficial drug targets for immunosuppressive therapy.

The expression patterns of type I and type II IMPDH differ when melanoma cells, leukemic cells, or T-cells are treated with an inhibitor specific for IMPDH such as tiazofurin or mycophenolic acid (Kiguchi *et. al.*, 1990; Kiguchi *et. al.*, 1990; Dayton *et. al.*, 1994). The steady-state level of type I mRNA remained constant throughout while the levels of type II mRNA changed in a biphasic fashion. Initially, the gene expression of type II was up-regulated due to the depletion of guanine nucleotides; type II IMPDH expression is inversely regulated by intracellular guanine nucleotide concentrations via a post-transcriptional nuclear event in response to the intracellular level of guanine ribonucleotides (Glesne *et. al.*, 1991). Subsequent to this, differentiation occurred and with it the retardation of cell proliferation and lowered levels of type II IMPDH mRNA.

Differences in IMPDH type I and type II gene expression could mean that the two isoenzymes possess different regulatory mechanisms and play different biological roles in *de novo* guanine nucleotide biosynthesis. The different regulatory mechanisms will be able to be further explored when the type I IMPDH gene is characterized and its potential transcription factor binding sites are compared to those identified in the type II gene (Zimmermann *et. al.*, 1994). Both enzymes have been identified as immunosuppressive drug targets (Dayton *et. al.*, 1994) and it seems as though the type II IMPDH would be the logical drug target for antitumor chemotherapy due to its increased expression in leukemic and solid tumor cells (Konno *et.*

*al.*, 1991; Nagai *et. al.*, 1991; Nagai *et. al.*, 1992; Collart *et. al.*, 1992). A drug would potentially have fewer side-effects if it was targetted specifically against either type I or type II IMPDH, leaving the other to maintain a housekeeping function in the cell. Development of such a drug requires knowledge of the biochemical properties of the two enzymes.

### Enzyme Kinetic Studies of Human IMPDHs

Kinetic studies were performed on type I and type II IMPDH by two different groups. In both cases, the recombinant nonfusion proteins were expressed and purified from a strain of *E. coli* which lacks its own IMPDH (Carr *et. al.*, 1993; Hager *et. al.*, 1994.) The summarized kinetic data is shown in table 1.

Table 1. Summary of Comparison of Type I and Type II IMPDH Kinetic Parameters

Kinetic Parameter	Carr <i>et. al.</i> , 1993		Hager <i>et. al.</i> , 1994	
	Type I	Type II	Type I	Type II
$K_m$ IMP ( $\mu$ M)	18	9.3	14.2	9.2
$K_m$ NAD <sup>+</sup> ( $\mu$ M)	46	32	42	32
$K_i$ XMP ( $\mu$ M)	80	94	-	-
$K_i$ NADH ( $\mu$ M)	102	90	-	-
$K_i$ MPA (nM)	37	9.5	-	-
$K_i$ MPA* (nM)	33	7.0	11	6
$k_{cat}$ (sec <sup>-1</sup> )	1.5	1.3	1.8	1.4

\*  $K_i$  determined by the tight-binding inhibitor equation (Cha, 1975).

- not determined

The interesting finding from these kinetic studies was that MPA inhibited type II IMPDH more potently than type I (4.8-fold

lower  $K_i$ ) (Carr *et. al.*, 1993). Inhibition of type II IMPDH specifically by MPA may not be as promising as it would seem from the study, as another group determined that the  $K_i$ MPA was merely 2-fold higher for type II IMPDH than for type I IMPDH (Hager *et. al.*, 1994).

### Mycophenolic Acid, an Inhibitor of IMPDH

Mycophenolic acid (MPA) was first isolated from *Penicillium glaucum* in 1896 (Gosio, 1896). The work was repeated (Alsberg and Black, 1913) and the phenol was given the name mycophenolic acid. Structural studies led to the publication of the structure of MPA (Birkinshaw *et. al.*, 1952) (Figure 5). MPA was first found to have limited antibacterial and antifungal properties (Abraham, 1945; Florey *et. al.*, 1946) before being identified as an antitumor agent (Carter, 1966). MPA was identified as a nucleic acid synthesis inhibitor by specifically inhibiting the enzyme IMP dehydrogenase. The inhibition was found to be uncompetitive and reversible (Franklin and Cooke, 1969). Inhibition of IMPDH by MPA results in inhibition of cell proliferation and T-cell activation via depletion in guanosine nucleotide levels (Koloski *et. al.*, 1986; Mitchell *et. al.*, 1992). Depletion of GTP has antiproliferative effects, especially on lymphocytes, which seem to have an elevated requirement for guanine nucleotide flux compared to any other cell type. The drug mycophenolate mofetil (CellCept™) (Figure 5) is metabolised to MPA *in vivo* and is currently used as an immunosuppressant in kidney transplantation (Sollinger *et. al.*, 1995).

MPA is a more potent inhibitor of mammalian IMPDHs compared bacterial or protozoan IMPDHs.  $K_i = 9$  to  $18$  nM for human IMPDH (Carr *et. al.*, 1993),  $9$  nM for Chinese hamster (Sintchak *et. al.*, 1996),  $1.4$  nM for mouse (Hodges *et. al.*, 1989),  $500$  nM for *Bacillus subtilis*,  $20$   $\mu$ M for *Escherichia coli* (Wu and Scrimgeour, 1973) and  $14$   $\mu$ M for *T. foetus* (Hedstrom and Wang, 1990).

### Mechanism of MPA Inhibition of IMPDH

MPA inhibits IMPDH uncompetitively with respect to both IMP and NAD<sup>+</sup>; MPA binds to IMPDH after NADH is released but before XMP is produced. This was first shown in protozoa (Hupe *et. al.*, 1986; Headstrom and Wang, 1990) then in mammals (Hodges *et. al.*, 1989; Link and Straub, 1996) (Figure 3). MPA inhibits IMPDH specifically by preventing the step of an IMPDH-substrate covalent intermediate undergoing hydrolysis to form XMP (Figure 6; taken from Link and Straub, 1996 and used with permission). The IMPDH-substrate intermediate is IMP covalently bound via C-2 of the purine ring to Cys 331 in humans (Wu *et. al.*, 1994) or to the corresponding Cys-319 in the parasite *T. foetus* (Huete-Perez *et. al.*, 1995). In other words, IMP binds to IMPDH, then NAD<sup>+</sup> binds and is reduced to NADH with the simultaneous oxidation of IMP such that it is now bound via C-2 to Cys-331 of human IMPDH. NADH leaves, then in absence of inhibitor the covalent intermediate undergoes hydrolysis to produce XMP which then leaves; however, MPA binds to the covalent intermediate, preventing the hydrolysis (Link and Straub, 1996). The molecular details of MPA prevention of hydrolysis are still not understood (Link and Straub, 1996). Multi-inhibitor experiments and the structural similarities between nicotinamide and MPA led to the hypothesis that MPA binds to IMPDH in the nicotinamide sub-binding site (Wang *et. al.*, 1990). X-ray crystal studies are consistent with this proposal (Sintchak *et. al.*, 1996); however, it is still possible that MPA binds to IMPDH at a site distinct from that of NAD<sup>+</sup>.

### A MPA-Resistant IMPDH Identified in Mouse Neuroblastoma Cells

Mouse neuroblastoma (NB) cells were stepwise selected (without mutagenesis) for a 10000-fold increased resistance to MPA (Hodges *et. al.*, 1989). The work was originally performed to study the effects that altered levels of IMPDH on purine metabolism. The increased

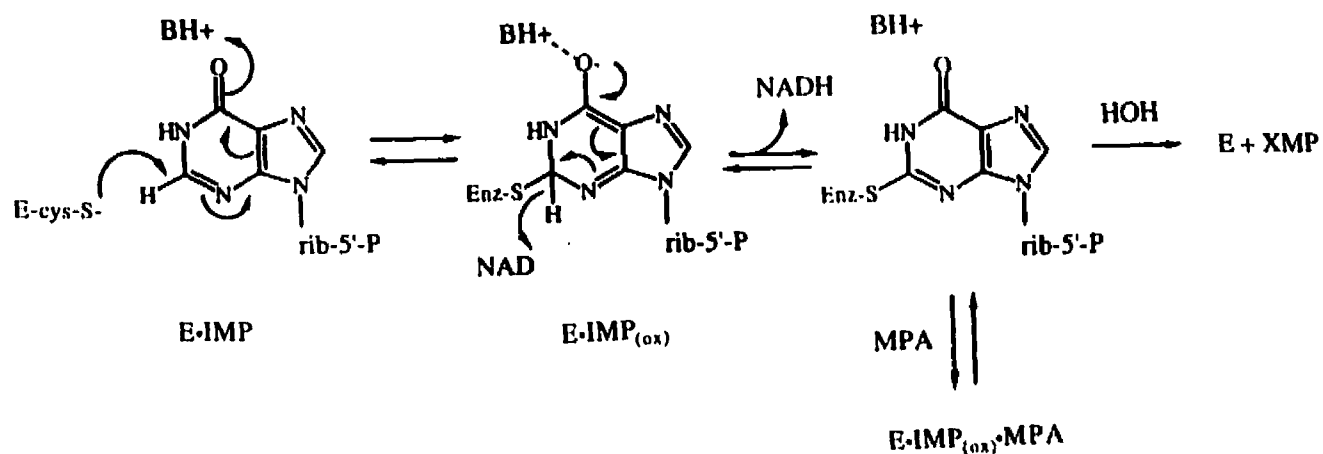


**Figure 6.** Proposed Molecular Mechanism of IMPDH

Cys 331 (331 in human type II) of IMPDH attacks IMP at the C-2 position which is followed by hydride transfer to NAD<sup>+</sup>. The result is the formation of a covalent intermediate, E-IMP<sub>(ox)</sub>. E-IMP<sub>(ox)</sub> is then hydrolyzed to E + XMP. MPA binds to E-IMP<sub>(ox)</sub> forming a dead-end complex and preventing the hydrolysis to products.

resistance to MPA was determined to be partly due to gene amplification and hypothesized increased transcription of the IMPDH gene; the MPA-resistant cell line had a 25-fold increased gene copy number for IMPDH and mRNA levels were 500-fold increased in the MPA-resistant cells (Lightfoot and Snyder, 1994). This is in agreement with an estimated 200-500-fold increase in quantity (approximately 20% of the soluble protein) of IMPDH protein in the MPA-resistant cells (Hodges *et. al.*, 1989). The increase in IMPDH abundance was not sufficient to account for the 10000-fold increased resistance to MPA. The kinetic evidence supported the theory that a mutational event(s) had occurred (Hodges *et. al.*, 1989).

Table 2. Kinetic Parameters for Wild-Type and MPA-Resistant Mouse NB Cells

Kinetic Parameter	Wild-Type NB	MPA-Resistant NB
$K_m$ IMP ( $\mu$ M)	14	13
$K_m$ NAD <sup>+</sup> ( $\mu$ M)	25	94
$K_i$ XMP ( $\mu$ M)	78	336
$K_i$ NAD <sup>+</sup> (mM)	1.3	1.5
$K_i$ MPA (nM)	1.4	3400
$V_{max}^*$ (nmols/min•mg protein)	3.1	75

\*For the IMPDH from wild-type NB cells, this parameter is acutally the specific activity since the enzyme was not pure; the cell lysate was assayed in this case.

Kinetic evidence supported a mutational event due in part to the 4-fold increased  $K_m$  NAD<sup>+</sup> and  $K_i$  XMP. The most striking evidence is the 2400-fold increased  $K_i$  MPA. The MPA-resistant IMPDH was able to be purified in two steps due to its increased abundance; the





(Sintchak *et. al.*, 1996). Glycolate oxidase, tryptophan synthase, and indole-3-glycerol phosphate synthase possess similar folds and C-terminal phosphate-binding sites as the core domain of IMPDH. The flanking (sub) domain (amino acid residues 110-244) protrudes from the N-terminal side of the barrel core and appears to be novel in sequence and structure (Sintchak *et. al.*, 1996).

The deduced quaternary structure of IMPDH suggests a  $K^+$  binding site such that  $K^+$  could help to position Cys 331 for catalysis as well as possibly stabilize the tetramer form of IMPDH (Sintchak *et. al.*, 1996). The IMPDH-IMP complex is actually the covalent intermediate, with C-2 of IMP covalently bound to Cys 331 of IMPDH, forming an oxidized IMP thioimidate intermediate. At this point, hydride transfer has occurred, NADH has been released, but hydrolysis of IMP has not occurred; thus, XMP has not been produced (Link and Straub, 1996; Fleming *et. al.*, 1996). The amino acids of IMPDH involved in IMP and MPA binding are shown (Figures 7 and 8; taken from Sintchak *et. al.*, 1996 and used with permission). The X-ray crystal structure of IMPDH-MPA supports the earlier proposal (Hedstrom and Wang, 1990) that MPA binds in the nicotinamide subsite portion of IMPDH, provided that no large conformational changes occur after NADH leaves and MPA binds. The nicotinamide moiety of  $NAD^+$  would form hydrogen bonds with Gly 324, Thr 333, Gly 326 and Asn 303 (Sintchak *et. al.*, 1996). MPA may also be a water molecule mimic, as the -OH forms hydrogen bonds with Thr 333 and Gln 441. If a water molecule were forming the hydrogen bonds instead of MPA, it would be properly positioned for nucleophilic attack at the C-2 carbon of the thioimidate intermediate, resulting in hydrolysis of the intermediate to form XMP (Sintchak *et. al.*, 1996). Des-hydroxy-MPA (Figure 5) is at least 1000-fold less potent an inhibitor of IMPDH (Or *et. al.*, 1995) which supports this hypothesis.

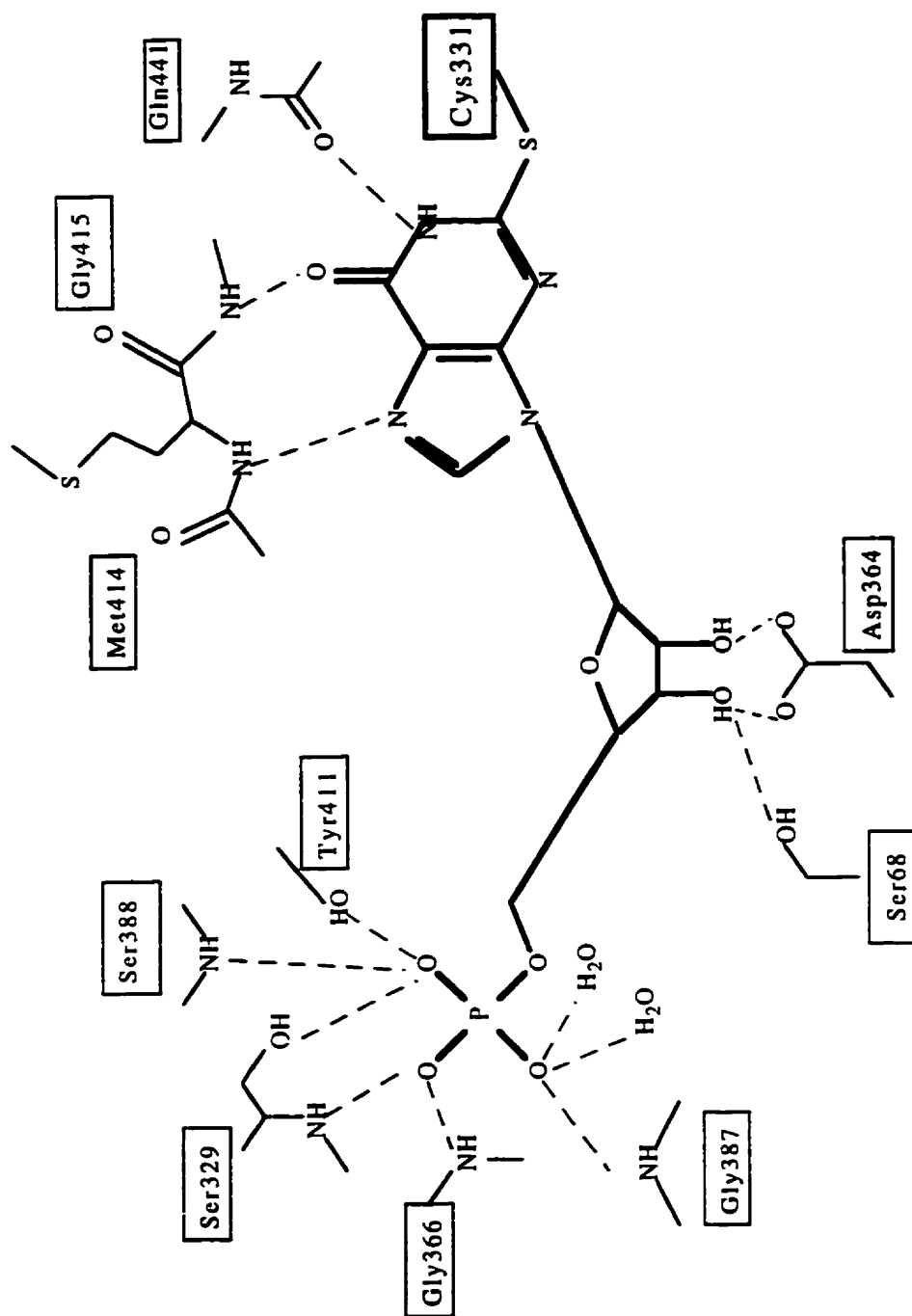


**Figure 7.** Amino Acids which Interact with IMP(ox)

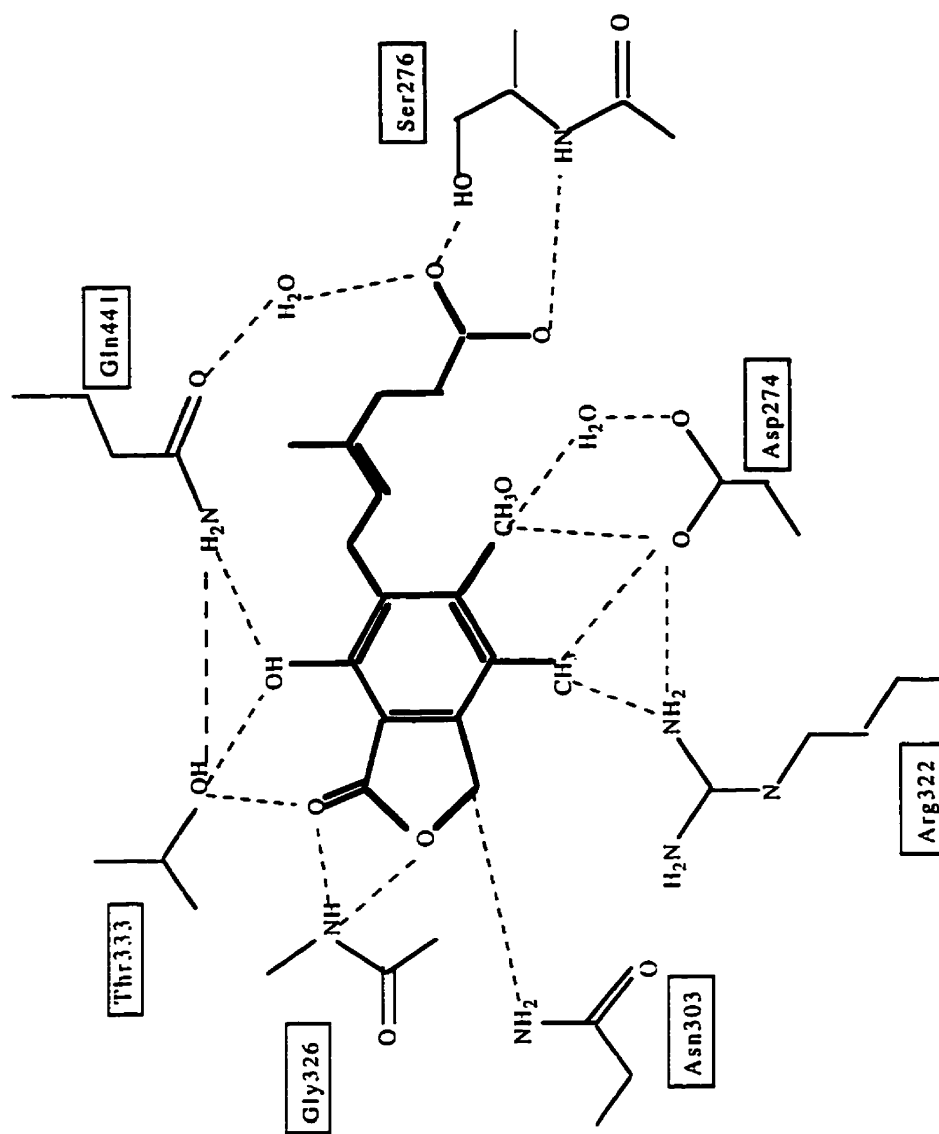


**Figure 8.** Amino Acids of IMPDH which Interact with MPA

### MPA Interaction with IMPDH Mutants

Several active-site mutants were constructed (and are currently being constructed; Sintchak *et. al.*, 1996) and their effects on catalysis and MPA binding were determined. The Thr-to-Ile substitution had previously been described (Lightfoot and Snyder, 1994) and it was found that this substitution increased the  $K_i$  MPA 300-fold while reducing the  $k_{cat}/K_m$  by approximately 3.5-fold. (Sintchak *et. al.*, 1996).

Three human type II IMPDHs were isolated from a randomly mutated IMPDH pool by their decreased affinity for MPA (Farazi *et. al.*, 1997). The three mutants were 1) Q277R 2) A462T 3) F465S/D470G. A fourth IMPDH, Q277R/A462T was also studied. None of the four amino acid positions had been implicated in direct binding to either IMP or MPA (Sintchak *et. al.*, 1996). The  $K_i$ MPA,  $K_m$ IMP,  $K_m$ NAD<sup>+</sup>, and  $k_{cat}$  were determined for the four IMPDH species to elucidate possible structural features which participate in the determination of species selectivity of MPA inhibition (Farazi *et. al.*, 1997). It was determined that increases in  $K_i$  MPA do not correlate with changes in  $K_m$ IMP,  $K_m$ NAD<sup>+</sup> nor  $k_{cat}$ . No inhibition experiments using XMP or NAD<sup>+</sup> as the inhibitor were performed in this investigation.

### Objectives of My Study

A mouse type II IMPDH (which is analogous to human type II) was identified with altered kinetic properties, one of which was an increased resistance to MPA (Hodges *et. al.*, 1989). Two amino acid substitutions had occurred (Lightfoot and Snyder, 1994): Ile 333 replaced Thr 333 and Tyr 351 replaced Ser 351. It was unknown which of the two was responsible for each altered kinetic parameter or if they were working synergetically. The objectives of my work

were to determine the kinetic effects of the amino acid substitutions at positions 333 and 351. This was performed in two major steps. Four purified recombinant mouse IMPDH type II proteins were obtained: wild-type IMPDH from mouse NB cells, MPA-resistant IMPDH (Lightfoot and Snyder, 1994) which was described to have two point mutations and each IMPDH containing only one of the mutations, which were generated by site-directed mutagenesis. The four IMPDHs were then assayed and their  $K_m$ IMP,  $K_m$ NAD<sup>+</sup>,  $K_i$ XMP,  $K_i$ NAD<sup>+</sup>,  $K_i$ MPA, and  $k_{cat}$  were determined. From these experiments, it was possible to determine the kinetic effects of each individual amino acid substitution as well as any combined effects. It was hoped that the information from this study would aid in the understanding of mycophenolic acid inhibition of IMPDH as well as give clues as to whether amino acids at positions 333 or 351 are also involved in other aspects of the enzyme mechanism, such as substrate binding or catalysis.

## **CHAPTER 2: Materials**

Butanol, phenol, isoamyl alcohol, methanol, ethanol, acetic acid, hydrochloric acid, boric acid, sodium hydroxide, potassium acetate, potassium chloride, sucrose, sodium chloride, EDTA, glycerol, MOPS, DTT, formamide, and molecular biology grade agarose were purchased from BDH Inc. IMP, XMP, NAD<sup>+</sup>, IPTG, BSA, ATP, DMSO, PMSF, chloramphenicol, maltose, N-lauryl sarcosine, glycine, magnesium chloride, magnesium sulphate,  $\beta$ -mercaptoethanol, lysozyme, RNase A, ampicillin, tetracycline, and standards for the Bradford protein assay were purchased from Sigma Chemical Co. SDS, ammonium persulphate, Bradford assay dye reagent, protein standards for electrophoresis, bromophenol blue, coomassie brilliant blue, and Triton-X-100 were purchased from Biorad Laboratories. Sodium acetate, isopropanol, chloroform, and D-glucose were purchased from Fisher Scientific. Reverse transcriptase, calf intestinal phosphatase, DNA ligase, oligo dT<sub>15</sub> primer, dNTPs, ethidium bromide, and electrophoresis grade bis-acrylamide were purchased from Boehringer Mannheim. Oligo-dT cellulose was purchased from Collaborative Research Inc. LB medium, agar, X-gal, electrophoresis grade acrylamide, and *Taq* polymerase were purchased from Gibco-BRL Life Technologies. Light mineral oil, lithium chloride, and formaldehyde were purchased from Mallinckrodt Co. Guanidinium thiocyanate was purchased from Merck-Schuchardt. Mycophenolic acid was purchased from Calbiochem. PFU polymerase was purchased from Strategene. PMAL-c2, factor Xa, *E. coli* TB1 and amylose resin was purchased from New England Biolabs.

Restriction enzymes were purchased from Boehringer Mannheim and New England Biolabs.

Reagents utilized for site-directed mutagenesis (10x one-phor-all

buffer PLUS, nuc mix, reaction mix, *E. coli* NM522 *mutS* ) were provided in a kit purchased from Pharmacia Biotech.

Reagents used for the isolation of DNA from agarose gel (glassmilk, NaI, newwash, TBE modifier) were purchased from Bio/Can Scientific.

DNA molecular weight markers were either purchased from Boehringer Mannheim or prepared in-house with lambda DNA purchased from Pharmacia Biotech and digested by restriction enzymes.

All oligonucleotide primers were custom synthesized at the DNA synthesis laboratory, University of Calgary, Alberta, Canada (with the exception of oligo-dT<sub>15</sub> primer).

IMPDHs which were assayed to determine kinetic parameters were prepared in-house (see also methods) as fusion proteins bound to maltose-binding protein (MBP). IMPDH was cleaved from MBP by factor Xa and it was this preparation which was assayed since neither maltose nor MBP was found to interfere with IMPDH activity. The cleaved fusion IMPDH had an extra 10 amino acids on its N-terminus which were from pMAL.

Table 5. Primers used for the polymerase chain reaction and site-directed mutagenesis.

Primer	Sequence	Restriction Site	Length	Location in IMPDH
5-IMP <sup>o</sup>	dCCG <u>TCGAC</u> ATGGCGGACTACCTG	<i>Sal</i> I	23	-8 to 15
3-IMP <sup>oo</sup>	dAAG <u>TCGAC</u> AAGGCATATACTGGATCTG	<i>Sal</i> I	27	1575 to 1549
IMP-2*	dCAAATGAAATTCTGCAGCGCAG	None	22	590 to 611

wt-1052*	pGCAGTGTACAAGGTGT <u>CTGAGTATGCCCG</u>	<i>Bsa</i> I	29	1036 to 1064
wt-998*	pCCATCTGCATCAC <u>CCAGGAAGTGTTGG</u>	<i>Bsa</i> J1	27	986 to 1012
mutnde*	pGGTATTTACACCG <u>CTTATG</u> GGTGC ACTCTC	<i>Nde</i> I	30	nonessential; in pMAL

---

Underlined sequences indicate the location of the restriction site. Nucleotide substitutions which induce a mutation utilized in site-directed mutagenesis are in bold italics. Locations in IMPDH are given relative to initiation of translation (Figure 9; IMPDH cDNA sequence was taken from Tiedman and Smith, 1991 and used with permission).

- ° primers used to generate full-length wild-type and double mutant IMPDH by PCR
- primers used to generate 985 bp products by PCR for RFLP analysis
- \* primers used to generate the two single mutant IMPDHs by site-directed mutagenesis



## **CHAPTER 3: Methods**

### **GENERAL PROTOCOLS**

#### **Maintenance and Storage of Bacterial Strains**

All cultures were grown in autoclaved (121°C, 15 psi for 20 minutes) LB medium (10 g/l peptone 140 (Gibco laboratories), 5 g/l yeast extract (Gibco laboratories), 10 g/l NaCl, pH 7.4 at 20°C) supplemented with the appropriate antibiotic unless otherwise indicated. Agar plates were prepared by adding 3 g of agar to 100 ml LB medium before autoclaving. The sterile solution was cooled to 50°C before addition of antibiotic. Plates were poured directly from the flask with approximately 25 ml per 78 mm plastic petri dish. Plates were inverted after the agar had solidified (1 hour) and stored wrapped in parafilm at 4°C. Bacterial strains to be kept long term were stored at -70°C in 50% glycerol and prepared in the following way: 2 ml LB medium supplemented with the appropriate antibiotic were inoculated with a single isolated colony from an agar plate. The culture was grown overnight at 37°C with shaking at 225 rpm. The cells (1.5 ml of each culture) were pelleted in a microcentrifuge tube by centrifugation at 14000g for 1 minute. The supernatant was discarded and the cell pellet was resuspended in sterile 50% glycerol. The suspension was frozen in dry ice, then immediately transferred to a -70°C freezer.

#### **Agarose Gel Electrophoresis of DNA**

Gels were prepared by boiling agarose in 1x TBE buffer (100 mM Tris-borate pH 8.3, 1 mM EDTA) until dissolved. The solution was cooled until it felt warm to the touch (60°C) and ethidium bromide (0.5 µg/ml) was added. The solution was poured into a gel tray (Bio-Rad Mini-Sub Cell apparatus for up to 8 samples) containing a comb for forming the wells. Thirty ml of solution was used for each



suspension was centrifuged again at 14 000g and the DNA-containing supernatant was transferred into a fresh tube. The elution process was repeated with 5  $\mu$ l sterile ddH<sub>2</sub>O and the fractions were pooled.

### Restriction Endonuclease Digestion of DNA

Restriction digests were performed in buffers supplied by the manufacturers. The amount of enzyme used was 1 to 2 units per  $\mu$ g DNA with the volume of enzyme never exceeding 10% of the total volume. Reactions were overlaid with light mineral oil and allowed to proceed for four to eighteen hours at the appropriate temperature in a water bath. The digests were monitored by agarose gel electrophoresis and then were extracted by an equal volume of phenol:chloroform = 1:1, then by an equal volume of chloroform. The DNA was precipitated by the addition of 1/10 volume of 3 M sodium acetate pH 5.2 and 2.5 volumes of 95% ethanol followed by incubation on ice for ten minutes. The DNA was collected by centrifugation at 15000g for 15 minutes at 4°C. The pellet was washed with 70% ethanol and dissolved in sterile ddH<sub>2</sub>O.

### Phosphatase Treatment of pMAL DNA Following Restriction Endonuclease Digestion

Calf intestinal phosphatase (Boehringer Mannheim) was added to pMAL expression vector in four consecutive aliquots of two units of phosphatase in each. The first immediately followed restriction endonuclease digestion and was incubated at 37°C for 30 minutes. The second was incubated for 15 minutes at 55°C, the third was incubated at 37°C for 30 minutes and the fourth was incubated at 55°C for 15 minutes. The phosphatase was heat inactivated at 65°C for 20 minutes. The DNA was purified from agarose gel using glass beads.

### Cloning Insert DNA into Plasmid DNA

Plasmid DNA (500 ng) which had been treated with calf intestinal phosphatase and purified from agarose gel was mixed with insert DNA at a molar ratio of 3:1 in 15  $\mu$ l of ligation buffer (66 mM Tris-HCl pH 7.4, 5 mM MgCl<sub>2</sub>, 1 mM DTT, 1 mM ATP). The reaction was started by the addition of 1 unit of T4 DNA ligase (Boehringer Mannheim) and was allowed to proceed at room temperature for eighteen hours. Two  $\mu$ l of the ligation was used to transform *E. coli* TB1 cells.

### Transformation of *E.Coli* with Plasmids

#### Preparation of Competent *E.Coli* for Transformation

Five ml of sterile LB medium was inoculated with one vial of *E.Coli* NM522 *mut S* cells (provided in site-directed mutagenesis kit by Pharmacia) and grown overnight at 37°C with shaking at 250 rpm. One ml of the overnight culture was aseptically added to 100 mls of sterile LB medium and incubated at 37°C with shaking at 250 rpm until the O.D. was 0.25-0.5 at 600 nm. The cells were transferred to two sterile 50 ml centrifuge tubes and chilled on ice for 15 minutes. The cells were then centrifuged at 2500 rpm in a Sorval SS34 rotor for 15 minutes at 4°C. The supernatant was discarded and the cells were gently resuspended in 30 ml of cold sterile Buffer #1 (one hundred ml ddH<sub>2</sub>O added to 20 ml of 1 M KCl, 1.2 ml of 5 M potassium acetate, 12 ml of 1 M CaCl<sub>2</sub> and 30 ml of ultrapure glycerol; the pH was titrated to 5.8 with acetic acid and the final volume brought to 200 ml with distilled H<sub>2</sub>O). The cells were incubated on ice for 1 hour and then centrifuged at 3000 rpm in a Sorval SS34 rotor at 4°C. The supernatant was removed and the cells were gently resuspended in 4 ml of cold, sterile Buffer #2 (100 ml ddH<sub>2</sub>O added to 4 ml of 0.5 M MOPS, 2 ml of 1 M KCl, 15 ml of 1 M CaCl<sub>2</sub> and 30 ml of ultrapure glycerol. The pH was titrated to 6.8 with 10 N NaOH and the final volume was brought to 200 ml distilled H<sub>2</sub>O.) The cells were incubated on ice for 15 minutes

Aliquots (0.5 ml) were transferred into 1.5 ml microcentrifuge tubes and frozen on dry ice. Cells were stored at  $-70^{\circ}\text{C}$  for no longer than six months.

#### Preparation of *E.Coli* for Electroporation

Centrifuge bottles and flasks were washed in 12 M HCl and rinsed thoroughly in sterile ddH<sub>2</sub>O before being used. Five ml of sterile LB medium were inoculated with one isolated colony of *E.Coli* DH5-alpha or TB1 cells and grown overnight at  $37^{\circ}\text{C}$  at 225 rpm. Sterile LB medium (500 ml) was inoculated with the 5 ml overnight culture and grown at  $37^{\circ}\text{C}$  with vigorous shaking to an O.D. of 0.5 to 0.8 at 600 nm (4 to 6 hours). The cells were chilled on ice for 15 minutes then centrifuged at 4000g for 15 minutes at  $4^{\circ}\text{C}$ . The supernatant was poured off and the cells were resuspended in cold sterile ddH<sub>2</sub>O (500 ml). The cells were centrifuged as above, the supernatant was poured off and the cells were resuspended in 250 ml of cold sterile ddH<sub>2</sub>O. The cells were again centrifuged as above, the supernatant was poured off and the cells were resuspended in cold sterile 10% glycerol (25 ml). The cells were centrifuged as above, the supernatant was poured off and the cells were resuspended in 10% glycerol (1.4 ml). The cell concentration at this point was at least  $3 \times 10^{10}$  cells/ml. The cells were transferred into 0.1 ml aliquots, frozen on dry ice and stored at  $-70^{\circ}\text{C}$  for no longer than six months.

#### Transformation of Competent *E.Coli* NM522 mut S Cells

Competent *E. Coli* (200  $\mu\text{L}$ ) were added to a 17 x 100 mm culture tube and placed on ice. Digested DNA (30  $\mu\text{L}$ ) from the mutagenesis reaction mix was added and the mixture was incubated on ice for 30 minutes. The tubes were incubated for 45 seconds at  $42^{\circ}\text{C}$  then chilled on ice for 2 minutes. One ml of SOC medium (LB supplemented with 2.5 mM KCl, 10 mM MgCl<sub>2</sub>, 10 mM MgSO<sub>4</sub> and 20 mM D-glucose) was added to the transformed cells. They were mixed gently and incubated for 2 hours at  $37^{\circ}\text{C}$  with shaking at 180 rpm. Three ml of SOC + 100  $\mu\text{g/ml}$  ampicillin was added and the

cells were incubated overnight at 37°C with shaking at 250 rpm.

Transformation of *E. Coli* DH5-alpha and TB1 cells by Electroporation  
Electroporation was performed with a Bio-Rad Gene Pulser™ (model 1652076) according to the manufacturer's protocol. Cells were thawed and 40 µl were mixed with 2 µl of each ligation mixture in a 0.5 ml microcentrifuge tube and incubated on ice for 10 minutes. Each mixture was transferred to a cold 0.1 cm electroporation cuvette. Electroporation was performed at 25 µF, 2.5 kV and 200 Ω. One ml of SOC medium was added to each electroporation cuvette and the cell suspension was transferred to a 17 x 100 mm culture tube. The cells were incubated for 1 hour at 37°C with shaking at 225 rpm. Fifty to 200 µl of cell suspensions were plated on LB supplemented with 100 µg/ml ampicillin and incubated at 37°C 12-20 hours.

#### Selection of *E. Coli* Colonies to Screen for Gene Insertion

After transformation, 200µl of cell culture was spread on LB-agar plates supplemented with 100 µg/ml ampicillin. These plates were left to grow inverted overnight at 37°C. The following day, individual colonies were picked and plated on two different plates: #1) LB-agar plates supplemented with 100 µg/ml ampicillin #2) LB-agar plates supplemented with 100 µg/ml ampicillin overlaid with IPTG (4 µl of 200 mg/ml) and X-gal (40 µl of 20 mg/ml). Insertion of the desired gene in pMAL inactivates the β-galactosidase alpha-fragment activity. Because TB1 cells are an alpha-complementing host, colonies containing pMAL only turn blue and colonies containing pMAL with a gene inserted remain white on IPTG/X-gal plates. Colonies corresponding to white colonies on plate #2 were picked from plate #1 for miniplasmid preparation (see below). Plasmids containing the IMPDH gene were identified by restriction enzyme digestion and visualized by agarose gel electrophoresis.

### Large Scale Preparation of pMAL Plasmid DNA

Twenty-five ml of LB medium + 100 µg/ml ampicillin were inoculated with a single bacterial colony containing the plasmid and grown overnight at 37°C with shaking at 225 rpm. Ten ml were used to inoculate 250 ml LB containing 100 µg/ml ampicillin and grown until the O.D. was 0.6 at 600 nm (4 to 7 hours). Chloramphenicol (170 µg/ml) and D-glucose (0.2%) was added and the culture was grown overnight (12 to 18 hours) at 37°C with shaking at 225 rpm. The cells were harvested by centrifugation at 4000g and resuspended in 7.5 ml of cold STE (8% sucrose, 100 mM Tris-HCl pH 8.0, 40 mM EDTA). STEL (4.5 ml) (STE supplemented with 10 mg lysozyme per 4.5 ml) was added and the mixture was incubated at room temperature for 10 minutes. Four ml of lysis buffer (100 mM Tris-HCl pH 8.0, 40 mM EDTA, 0.2% SDS) were added and incubated at 37°C until the solution cleared (5 minutes). Five M potassium acetate (4 ml) was added and mixed by inversion. The mixture was incubated on ice for 30 minutes then centrifuged at 35000g for 45 minutes. The flocculated top layer was removed with Kimwipes™ and the supernatant was collected. Absolute isopropanol (0.6 volumes) were added and mixed by inversion, then the mixture was centrifuged at 12000 g for 10 minutes at room temperature. The supernatant was discarded and the pellet was air-dried (10 to 30 minutes). The pellet was dissolved in sterile dd H<sub>2</sub>O (9.5 ml) and then solid CaCl<sub>2</sub> (10.2 g) was added and dissolved by inversion. Ethidium bromide (1.2 ml of a 5 mg/ml solution) was added and mixed by inversion. The mixture was heat-sealed in an ultracentrifuge tube (Beckman quick-seal) and centrifuged for 24 hours at 210 000g at 25°C in a Beckman 80 Ti rotor. The bands of DNA were visualized using a long wave hand held UV lamp. The lower band consisted of covalently closed circular DNA and it was removed using a 21 gauge needle. The DNA was extracted 4 times with an equal volume (approximately 2 ml) of H<sub>2</sub>O-saturated n-butanol. The volume was brought to 8 ml with sterile ddH<sub>2</sub>O.



A was added, the mixture was incubated for two hours at 37°C and then re-extracted with phenol/chloroform. The DNA was precipitated by two volumes of ethanol at room temperature and collected by centrifugation at 15000g for 15 minutes at 4°C. The supernatant was removed by gentle aspiration and the DNA was washed with 70% EtOH, then dissolved in sterile ddH<sub>2</sub>O.

### Spectrophotometric Quantitation of DNA and RNA

DNA and RNA were diluted in ddH<sub>2</sub>O and 50 µl to 100 µl was placed in a cuvette. The A<sub>260</sub> was determined in a spectrophotometer with ddH<sub>2</sub>O as the blank. The concentrations were determined by the following formulas. 1 absorbance unit of DNA is equal to 0.05 mg/ml and 1 absorbance unit of RNA is equal to 0.04 mg/ml.

### RNA-BASED METHODOLOGY

#### Preparation of DEPC-H<sub>2</sub>O

All ddH<sub>2</sub>O used in RNA-based methodologies was prepared with DEPC in the following way. DEPC in ddH<sub>2</sub>O (0.1%) was incubated overnight at room temperature with stirring and this was autoclaved (121°C, 15 ppsi for 20 minutes) the next day.

#### Isolation of Total RNA from Mouse Neuroblastoma Cells

Total RNA was prepared by a modified protocol of Chomczynski and Sacchi (1987). The following protocol is per 30 ml flask of mouse neuroblastoma cells (Seeds *et. al.*, 1970) harvested and frozen at 1 aliquot per flask. Each aliquot was thawed and to each was added 1 ml of solution D (25 mM sodium citrate, pH 7.0, 0.5% w/v N-Laurylsarcosine, 4 M guanidinium thiocyanate freshly supplemented with 0.73% β-mercaptoethanol). This was mixed and transferred to a 15 ml sterile polypropylene tube. Sodium acetate at 2 M, pH 5.2 (0.1

ml), H<sub>2</sub>O-saturated phenol (1 ml), and chloroform:isoamyl alcohol = 24:1 (0.2 ml) were added sequentially with vortexing after each addition. The final suspension was mixed by vortex for 10 seconds. The mixture was cooled on ice for 10 minutes and then centrifuged at 12000g for 20 minutes at 4°C. The aqueous (top) phase was transferred into a fresh tube, mixed with isopropanol (1 ml), incubated at -20°C for 1 hour and then centrifuged at 12 000g for 20 minutes. The supernatant was discarded and the pellet was dissolved in solution D (0.3 ml) and transferred into a 1.5 ml microcentrifuge tube. The RNA was precipitated by addition of absolute isopropanol (0.3 ml) and incubation for 1 hour at -20°C. The RNA was collected by centrifugation at 12 000g for 10 minutes at 4°C. The supernatant was discarded and the pellet was washed with 70% ethanol (600 µl). The pellet was recentrifuged briefly at 12000g and the supernatant was discarded. The pellet was air-dried for 5 minutes and dissolved in sterile ddH<sub>2</sub>O (25 µl).

#### Formaldehyde Gel Electrophoresis of RNA

The 50 ml gel was run in a Bio-Rad Mini-Sub Cell apparatus and prepared in the following way. Agarose (0.56 g) was boiled in 37 ml ddH<sub>2</sub>O then cooled to 60°C. 37% formaldehyde (8 ml) and 5 ml of 10x running buffer (0.1 M MOPS pH 7.0, 40 mM NaOAc, 5 mM EDTA) were added, the solution was mixed and poured into a gel tray. The final concentration of agarose was 1.2%. RNA samples (up to 30 µg) were diluted to 20 µl with 10 µl formamide, 3.5 µl formaldehyde, 2.0 µl 5x running buffer and ddH<sub>2</sub>O. The mixture was incubated at 55°C for 15 minutes and 2 µl of RNA loading buffer (50% glycerol, 1 mM EDTA, 0.4% bromophenol blue) was added. The samples were added to the wells of the gel and the gel was electrophoresed in 1x running buffer at 50 mA until the dye front had migrated 8 cm (several hours). The gel was stained in 200 ml TAE buffer (40 mM Tris-acetate, 1 mM EDTA) containing 0.5 µg/ml ethidium bromide for two hours. The gel was destained in ddH<sub>2</sub>O. The RNA was

visualized under ultraviolet light.

### Poly A<sup>+</sup> RNA Isolation from Total RNA

Poly A<sup>+</sup> RNA was isolated by a modified method of Aviv and Leder (1972). A minimum of 1 mg total RNA was used as starting material and diluted to 0.4 mg/ml in sterile ddH<sub>2</sub>O. The solution was incubated at 65°C for 10 minutes, cooled on ice and 1/10 volume of 5 M LiCl was added. Oligo dT cellulose (50 mg/mg RNA, Collaborative Research Inc.) was suspended in 1 ml of elution buffer (10 mM Tris-HCl pH 7.5, 1 mM EDTA, 0.05% SDS) and the suspension was poured into a 10 ml sterile, disposable Polyprep column. The column was washed with 10 volumes of binding buffer (20 mM Tris-HCl pH 7.6, 1 mM EDTA, 0.1% SDS, 0.5 M LiCl<sub>2</sub>). The RNA was applied to the column one drop at a time. The eluent was collected and reapplied to the column one drop at a time. The eluent was discarded and the column was washed with binding buffer until the eluent A<sub>260</sub> was below 0.1 (at least four volumes). Elution buffer was heated to 65 °C and applied to the column. The eluent was collected and precipitated by addition of 3 M NaOAc pH 5.2 ( 1/10 volume) and 95% ethanol (2.5 volumes). The Poly A<sup>+</sup> RNA was incubated at -20°C overnight. The precipitated Poly A<sup>+</sup> RNA was collected by centrifugation at 10000g for 15 minutes at 4°C. The pellet was washed in 70% ethanol, recentrifuged briefly at 10000g, air-dried and dissolved in sterile ddH<sub>2</sub>O (50 µl per mg starting RNA).

### Generation of cDNA by Reverse Transcription

A 50 µl reaction mix was prepared containing H<sub>2</sub>O, 2 µg poly A<sup>+</sup> RNA, 1x cDNA buffer (50 mM Tris-HCl pH 8.2 at 41°C, 40 mM KCl, 6 mM MgCl<sub>2</sub>, 1 mM DTT), 1.5 mM of each dNTP, 1 µg oligo-dT<sub>15</sub> primer (Boehringer Mannheim), 25 units RNase inhibitor and 45 units avian myeloblastosis virus reverse transcriptase (Boehringer Mannheim). The reaction was incubated at 42°C for 2 hours. The final product

was stored at -20°C.

### PCR-BASED METHODOLOGY

#### PCR to Generate Full Length T333/S351 (wild-type) and I333/Y351 (double mutant) IMPDH Genes

A 49  $\mu$ l reaction containing 1x PCR buffer (20 mM Tris-HCl pH 8.75, 10 mM KCl, 10 mM  $(\text{NH}_4)_2\text{SO}_4$ , 2 mM  $\text{MgCl}_2$ , 1% Triton-X-100, 100  $\mu$ g/ml bovine serum albumin), 0.2 mM of each dNTP, 20 pmol each primer (5-IMP and 3-IMP, each containing a *Sal* I restriction site for cloning purposes; table 5), and template DNA (2  $\mu$ l NB cDNA or 1  $\mu$ l of 1:100 miniprep of I333/Y351 IMPDH cloned into pBluescript) was mixed and overlaid with 30-50  $\mu$ l light mineral oil. The mixture was heated at 94°C for two minutes and 2.5 units (1  $\mu$ l) of PFU polymerase (Stratagene) was added below the mineral oil. The mixture was amplified for 30 cycles using a Perkin-Elmer-Cetus DNA Thermal Cycler with the following parameters: 94°C for 40 seconds, 55°C for 50 seconds and 72°C for 2 minutes.

All PCR products were diluted 1:2 in sterile dd H<sub>2</sub>O and extracted once with one volume of phenol:chloroform = 1:1, then with one volume of chloroform. The DNA was precipitated by the addition of 1/10 volume of 3 M sodium acetate pH 5.2 and 2.5 volumes of ethanol. The DNA was collected by centrifugation at 15000g for 15 minutes at 4°C. The pellet was washed with 70% ethanol and dissolved in sterile ddH<sub>2</sub>O.

#### Restriction Fragment Length Polymorphism Analysis

##### PCR to Generate 985 bp Product

A 49.5  $\mu$ l reaction containing 1xPCR buffer (20 mM Tris-HCl pH 8.4, 1.0 mM  $\text{MgCl}_2$ , 50 mM KCl), 0.2 mM of each dNTP, 20 pmol each primer (IMP-2 and 3-IMP; table 5), and 1  $\mu$ l template DNA (1:100 dilution of IMPDH in pMAL from a miniprep) was mixed and overlaid

with 30-50  $\mu$ l light mineral oil. The mixture was heated at 94°C for two minutes and 2.5 units (0.5  $\mu$ l) *Taq* polymerase (Gibco-BRL) was added to each below the mineral oil. The mixture was amplified for 30 cycles using a Perkin-Elmer-Cetus DNA Thermal Cycler with the following parameters: 94°C for 40 seconds, 55°C for 50 seconds, and 72°C for 70 seconds.

All PCR products were diluted 1:2 in sterile dd H<sub>2</sub>O and extracted once with one volume of phenol:chloroform = 1:1, then with one volume of chloroform. The DNA was precipitated by the addition of 1/10 volume of 3 M sodium acetate pH 5.2 and 2.5 volumes of ethanol. The DNA was collected by centrifugation at 15000g for 15 minutes at 4°C. The pellet was washed with 70% ethanol and dissolved in sterile ddH<sub>2</sub>O.

#### Restriction Fragment Length Polymorphism Analysis

DNA (980 bp) generated by PCR was digested by *Bsa* I and *Bsa* J1 (New England Biolabs) using the buffers supplied. Products were separated and visualized on a 2% agarose gel by electrophoresis using TBE as the buffer.

### SITE-DIRECTED MUTAGENESIS OF IMPDH

#### Purification of Plasmid DNA for Site-Directed Mutagenesis

Two miniplasmid preparations which included digestion by RNase A were performed on TB1 cells containing double mutant IMPDH cloned into pMAL expression vector (Figure 10; taken from a New England Biolabs instructions manual). The two preparations were combined. One Qiagen™ -5 tip was equilibrated with 1 ml of buffer QBT (750 mM NaCl, 50 mM MOPS, 15% ethanol, pH 7.0, 0.15% Triton-X-100). The miniplasmid preparations were added to the column and left to flow by gravity. The column was washed with 3 ml buffer QC (1.0 M NaCl, 50 mM MOPS, 15% ethanol, pH 7.0). The DNA was eluted from the column with 1 ml buffer QF (1.25 M NaCl, 50 mM Tris-HCl,

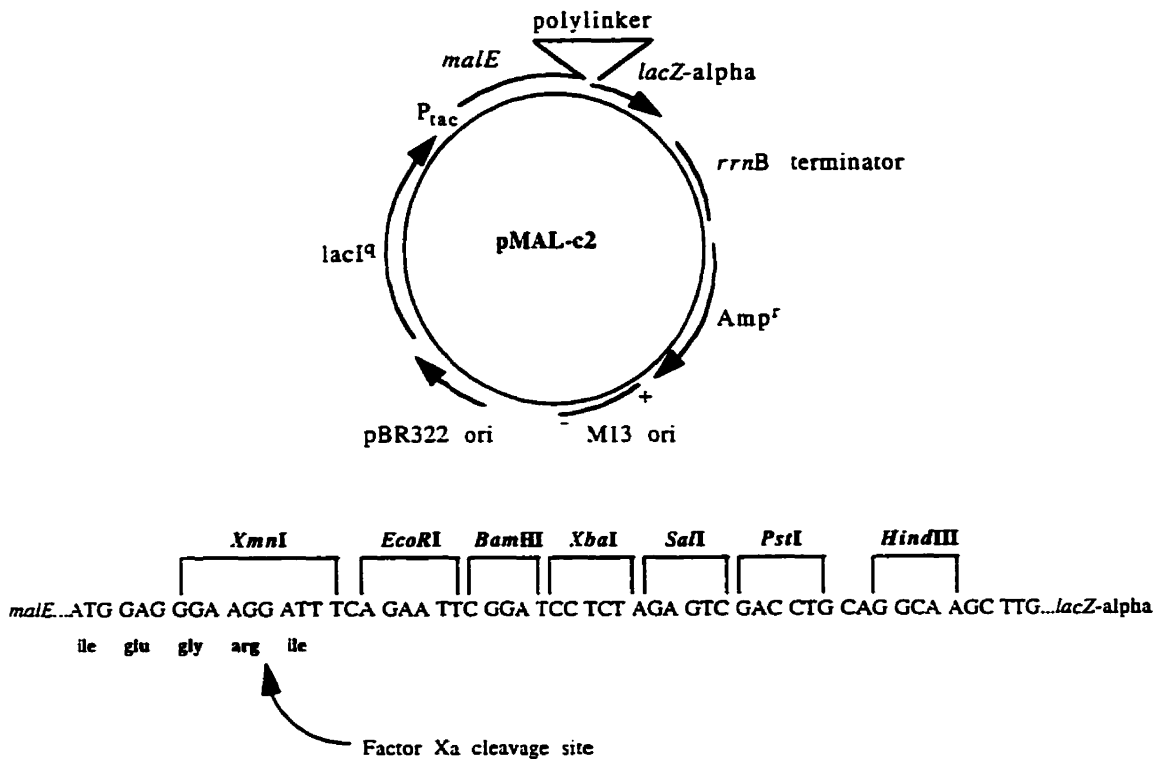


### **Figure 10. PMAL-c2 Expression Vector**

PMAL (6646 base pairs) contains the maltose-binding protein (MBP) encoding gene from *E. coli*, resulting in the expression of a MBP-fusion protein. Unique restriction sites between *malE* and *lacZ-alpha* are available for inserting the gene of interest. The *lacI<sup>q</sup>* gene encodes the Lac repressor which keeps expression of the gene from *P<sub>tac</sub>* low in the absence of IPTG; gene expression is induced by the addition of IPTG. Insertion of the gene inactivates the  $\beta$ -galactosidase alpha-fragment activity of the *malE-lacZ-alpha* fusion, which results in a white colony on Xgal plates when the host is alpha-complementing (eg. TBI) as opposed to a blue colony occurring when there is no inserted gene.

15% ethanol, pH 8.5). The DNA was precipitated by addition of 0.7 volumes of isopropanol and collected by centrifugation at 15000g for 30 minutes at 4°C. The DNA pellet was washed with 70% ethanol, recentrifuged briefly, air-dried and dissolved in sterile ddH<sub>2</sub>O.

### Site-Directed Mutagenesis Procedure

Site-directed Mutagenesis was performed with a kit (Pharmacia) based on the unique site elimination procedure developed by Deng and Nickoloff (1992) (Figure 11; taken from a Pharmacia instructions manual). The starting material was the double mutant IMPDH which had been cloned into pMAL and purified using a Qiagen™ column. Two primers for each mutagenesis reaction were used (wt-998 and mutnde or wt-1052 and mutnde; table 5). One abolished a nonessential restriction enzyme site (*Nde* I in this case) and the other contained the desired mutation. They both bound to the same (antisense) strand.

A 20 µl reaction containing 0.025 pmol of plasmid DNA, 1.25 pmol of each primer and 1/10 volume of 10x One-Phor-All Buffer PLUS (100 mM Tris acetate, 100 mM magnesium acetate, 500 mM potassium acetate, pH 7.5) was set up in a microcentrifuge tube. The mixture was incubated at 100°C for 5 minutes, then immediately chilled on ice for 5 minutes. The mixture was centrifuged briefly, then incubated at room temperature for 30 minutes. The mutagenesis reaction was started by the addition of 7 µl of nucleotide mix (2.86 mM each dATP, dCTP, dGTP and dTTP, 4.34 mM ATP, 1.43x One-Phor-All-Buffer PLUS) and 3 µl of reaction mix (0.83-1.17 units/µl T4 DNA ligase, 0.83-1.17 units/µl T4 DNA polymerase and 0.2-2.8 mg/ml T4 Gene 32 Protein). The mixture was incubated at 37°C for 1 hour then stopped by incubation at 85°C for fifteen minutes. The mixture was centrifuged briefly and placed on ice. The plasmids were digested with the restriction endonuclease *Nde*I (New England Biolabs) and 200 µl of competent NM522 (*mutS*) *E. Coli* cells were

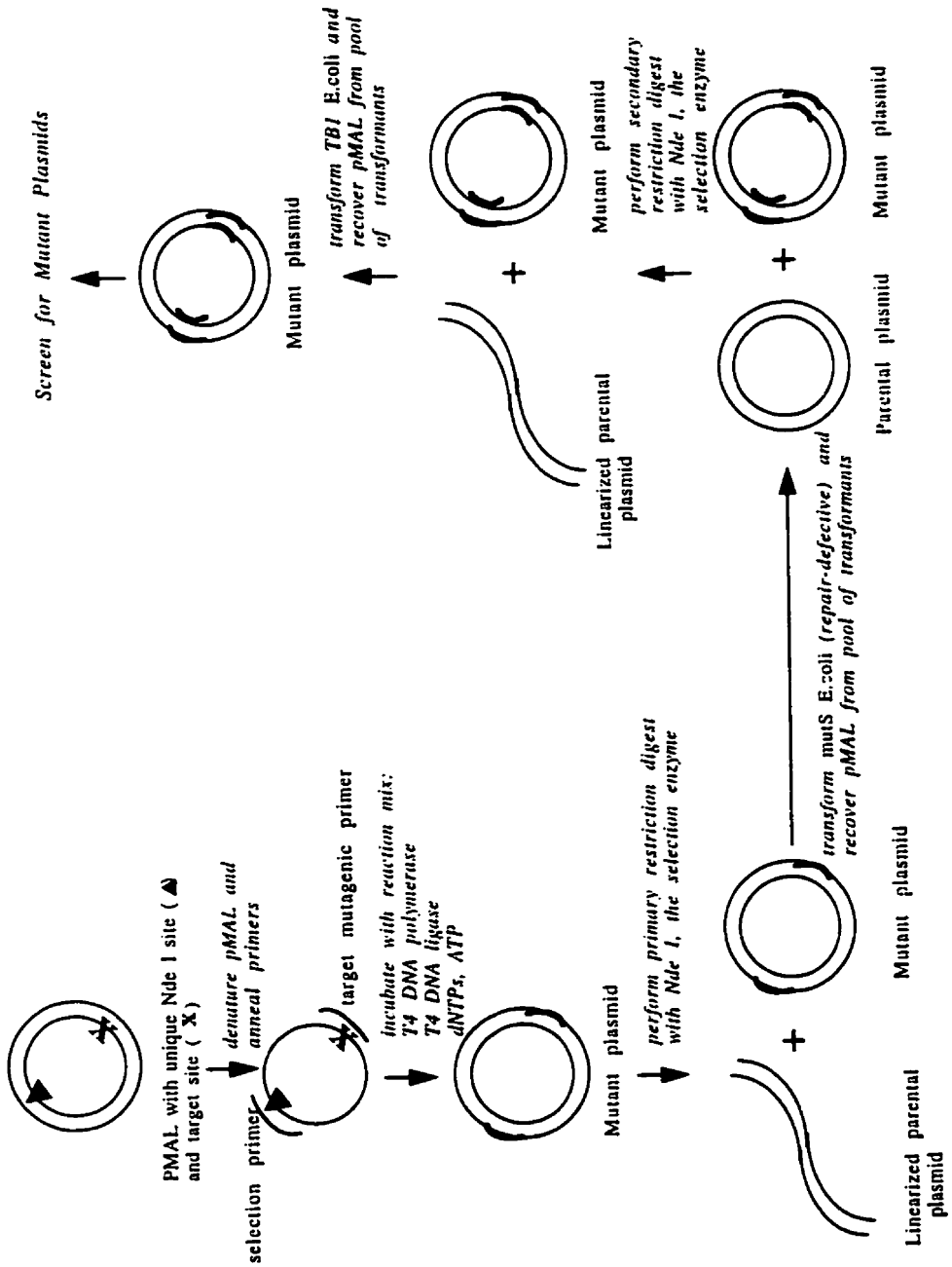


**Figure 11. Site-Directed Mutagenesis Scheme**

transformed with the entire (30  $\mu$ l) enzyme digestion. Miniplasmid preparations were performed on the overnight cultures of transformed NM522 cells. Plasmids were subjected to a second round of *Nde* I restriction endonuclease digestion. The digested plasmid DNA was dissolved in 30  $\mu$ l of sterile dd H<sub>2</sub>O. 1  $\mu$ l was used to transform TB1 cells by electroporation. 100  $\mu$ l and 10  $\mu$ l of transformed cells were plated on LB-agar plates supplemented with 100  $\mu$ g/ml ampicillin. Colonies were screened for the desired mutation by miniplasmid preparation followed by RFLP analysis.

### IMPDH EXPRESSION, PURIFICATION AND ASSAY

#### Large-Scale Induction and Purification of IMPDH-MBP

One litre of rich broth (LB supplemented with 2 g/litre glucose) containing 100  $\mu$ g/ml sterile ampicillin was inoculated with 10 ml of an overnight culture of *E. Coli* TB1 cells containing the fusion plasmid. The cells were grown to an O.D<sub>600</sub> of 0.5 ( $2 \times 10^8$  cells/ml). Filter-sterilized 100 mM IPTG (10 ml) was then added and the culture was grown at 37°C for two hours. The cells were harvested by centrifugation at 4000g for 20 minutes and the supernatant was discarded. The cells were resuspended in 50 ml of column buffer (20 mM Tris-HCl pH 7.4, 200 mM KCl, 1 mM EDTA, 1 mM fresh DTT) supplemented with 1 mM PMSF. The cells were frozen at -20°C overnight. The cells were thawed in cold water and then placed in an ice-water bath and sonicated in 8x15 second pulses. The sonicate was centrifuged at 9000g for 30 minutes at 4°C. Fifteen ml of amylose resin was poured into a 20 ml syringe plugged with silanized glass wool and was washed with 8 volumes of column buffer. The supernatant was applied to the amylose column at a flow rate of 0.8 ml/min. The column was washed with 12 volumes of column buffer. The fusion protein was then eluted with column buffer supplemented with 10 mM maltose. Fractions (approximately 3 ml) were collected and assayed for protein content by the Bradford

(Biorad) protein assay. The protein-containing fractions were pooled, divided into 1 ml aliquots and stored at  $-70^{\circ}\text{C}$ .

### Cleavage of Fusion Protein by Factor Xa

The concentration of fusion protein was 0.5 to 1.0 mg/ml in column buffer. This was supplemented with 2 mM final  $\text{CaCl}_2$ . Factor Xa (0.01-0.02 mg per mg fusion protein) was added and was incubated at room temperature 18-24 hours. Cleavage was monitored by SDS-polyacrylamide gel electrophoresis.

### Bradford Protein Assay

Protein samples and standards (bovine serum albumin, Sigma) were diluted to 800  $\mu\text{l}$  in ddH<sub>2</sub>O (ddH<sub>2</sub>O was the blank). Two hundred  $\mu\text{l}$  of Bradford dye reagent concentrate (Biorad) was added to all and they were incubated at room temperature for 10 to 30 minutes. The absorbance of all was measured at 595 nm. The concentrations of protein in the samples were calculated from the curve generated by the standards.

### SDS-Polyacrylamide Gel Electrophoresis

SDS-PAGE was performed according to the method of Laemmli (1970). The gel system used was the mini Protean II (Bio-Rad Laboratories) which has a gel size of 8 x 7 cm. The spacer and combs used were 7.5 mm. A 10% separating polyacrylamide gel (10% acrylamide, 3% bis-acrylamide, 0.375 M Tris-HCl (pH 8.8), and 0.1% SDS with 10% ammonium persulfate (25  $\mu\text{l}$  per 5 ml) and TEMED (2.5  $\mu\text{l}$  per 5 ml) added to polymerize the gel) was poured into the apparatus to approximately 1 cm below the bottom of the comb. A stacking gel composed of 4.5% acrylamide, 1.2% bis-acrylamide, 0.125 M Tris-HCl (pH 6.8), and 0.1% SDS with 10% ammonium persulfate (25  $\mu\text{l}$  per 5 ml) and TEMED (5  $\mu\text{l}$  per 5 ml) to

polymerize the gel was poured on top of the polymerized separating gel. Samples were prepared by mixing the protein (up to 15  $\mu$ l) with one volume of 2 x sample buffer (0.2 M Tris-HCl, 100 mM DTT, 4% SDS, 10% glycerol, and 0.004% bromophenol blue). Samples were heated at 95°C for 5 minutes, cooled on ice and centrifuged briefly before being loaded onto the gel. Gels were electrophoresed in 1 x running buffer (0.025 M Tris-Base, 0.15 M glycine and 0.15% SDS) at a constant voltage setting of 200 volts for 45 minutes at 4°C. Gels were stained in Coomassie blue stain (methanol: glacial acetic acid: H<sub>2</sub>O = 9:2:9 with 0.126% Coomassie brilliant blue) for at least one hour up to overnight. The stain was poured off and reserved for reuse and the gel was destained in several courses of destain solution (methanol: acetic acid: H<sub>2</sub>O = 9:2:9) until the background was minimal. The gels were photographed on a light box using a green filter and Polaroid type 52 film at F-stop 5.6 for 1/30 of a second.

#### Spectrophotometric IMPDH Assay

The total assay volume was 400  $\mu$ l. Substrates (IMP, NAD<sup>+</sup>) and inhibitors if any (XMP, MPA) were mixed together in a microcentrifuge tube. The assay was started by the addition of enzyme in assay buffer (100 mM Tris-HCl pH 8.0, 75 mM KCl, 3 mM EDTA, 20  $\mu$ g/ml BSA final) plus dd H<sub>2</sub>O to bring the volume to 400  $\mu$ l. MPA was dissolved in DMSO and all assays with MPA present contained 5% DMSO final. The concentration of IMPDH in the assay mixture was: T333/S351 (wild-type) 8 nM; I333/S351 82 nM; T333/Y351 10 nM; I333/Y351 (double mutant) 80 nM. The reaction was incubated at 37°C in a temperature controlled spectrophotometer cuvette and monitored at 340 nm to measure the conversion of NAD<sup>+</sup> to NADH. A value for the optical density change over time was obtained and used to calculate the specific activity by the formula Absorbance = extinction coefficient x pathlength (cm) x concentration of product (mols/litre). The extinction coefficient of NADH is 6 200 M<sup>-1</sup> cm<sup>-1</sup>.

The initial velocity rates were obtained in the range of enzyme activity which was linear with respect to time. The amount of enzyme used in each assay was also in the linear range; ie, halving the amount of enzyme in the assay mixture resulted in a halving of the initial velocity rate.

The kinetic parameters were calculated as described in the appendix using "Grafit" Version 3.09. This software program allows the user to define his or her own equations; in this case, the equations were enzyme kinetic equations. For each group of initial velocity values (eg. inhibition of T333/ S351 IMPDH by XMP), all of the data obtained was analyzed as a whole and every data point was given equal weighting. After analysis, the initial velocities were plotted versus concentration of IMP. The curves drawn on the graphs were based on the kinetic parameters calculated by Grafit and the magnitude of concentration of inhibitor. The curves were not simply the best curve through each set of points, or in other words each individual concentration of inhibitor; again, the data was analyzed as a whole. All curves within the same graph are dependent on each other and on the calculated kinetic parameters. Upon inspection it may sometimes seem as though a better curve could have been drawn through a set of points, but this "better" curve would not be a representation of the data as a whole.

## **CHAPTER 4: Results**

### **Confirmation of Site-Directed Mutants by RFLP Analysis**

Two site-directed mutagenesis experiments were performed on I333/Y351 (double mutant) IMPDH cDNA which had been subcloned into the expression vector pMAL-c2. The first replaced Tyr351 with Ser, which involved a T to C nucleotide substitution at position 1052 (Table 5). This nucleotide substitution resulted in the generation of *Bsa* I restriction endonuclease site. The second replaced Ile333 with Thr, which involved a T to C nucleotide substitution at position 998. This nucleotide substitution resulted in the generation of a *Bsa* JI restriction endonuclease site. Site-directed mutagenesis was performed specifically on the double mutant and not the wild-type IMPDH so that the nucleotide substitution in each case could be monitored by the generation of a restriction site, not the abolishment of one, thus the changed nucleotide could be specifically identified. These nucleotide changes were monitored by RFLP analysis (Figures 12 A and B) performed simultaneously on T333/S351 (wild-type), I333/Y351 (double mutant), I333/S351, and T333/Y351 IMPDH. The restriction endonuclease maps are shown for *Bsa* I and *Bsa* JI (Figure 13).

**Figure 12\*. RFLP Analysis of Nucleotide Changes**

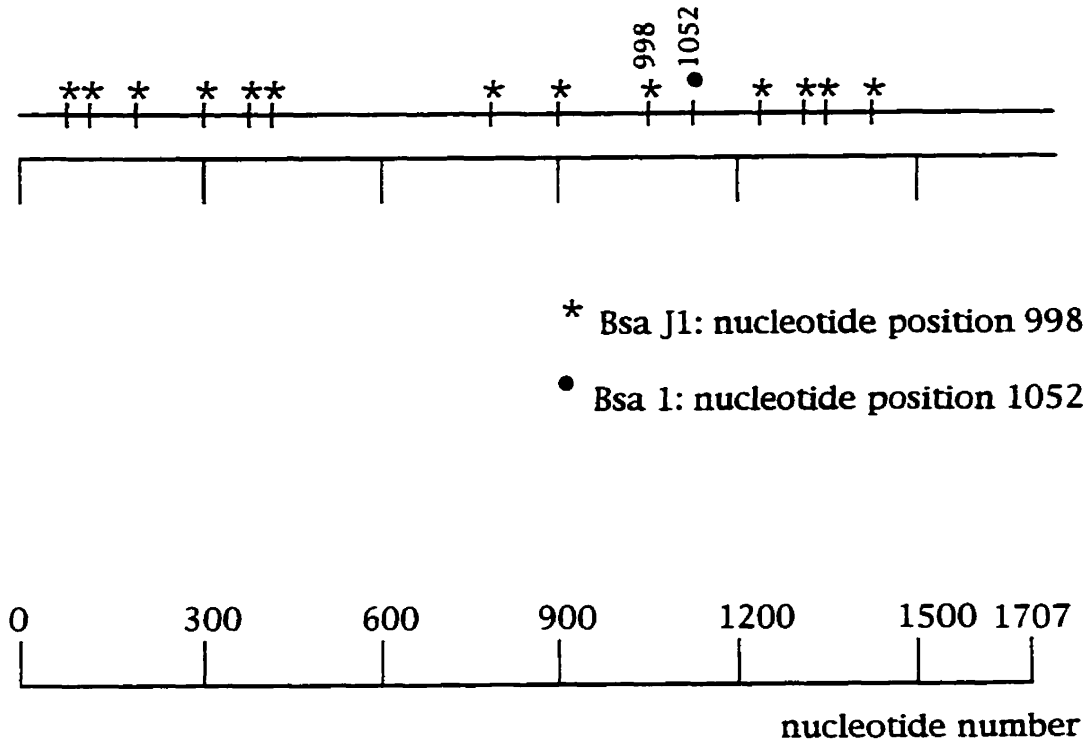
IMPDH cloned into pMAL was amplified via PCR with the primers IMP-2 and 3'-IMP (Table 5) to produce a 985 bp fragment.

A. Wild-type (T333/S351) IMPDH contains a *Bsa* I restriction endonuclease site, resulting in 527 and 458 bp products upon digestion of the 985 bp PCR product. The *Bsa* I site is not present in Tyr351 IMPDHs and thus the 985 bp PCR product remains undigested in these cases. Substitution of T with C at nucleotide position 1052 in the cDNA of Tyr351 IMPDHs results in Ser replacing Tyr at amino acid position 351 and the regeneration of the *Bsa* I restriction site.

B. Wild-type (T333/S351) IMPDH contains 13 *Bsa* J1 restriction endonuclease sites, resulting in (among others) 190 and 170 bp products upon digestion of the 985 bp PCR product. This particular *Bsa* J1 restriction site is not present in Ile333 IMPDHs and thus a 360 bp PCR product is observed instead of 190 and 170 bp products in these cases. Substitution of T with C at nucleotide position 998 in the cDNA of Ile333 IMPDHs results in Thr replacing Ile at amino acid position 333 and the regeneration of the *Bsa* J1 restriction site

\* refer also to Table 3 (table of nucleotide and amino acid substitutions) and Figure 13 (IMPDH restriction endonuclease map for *Bsa* I and *Bsa* J1).





\* Bsa J1: nucleotide position 998  
 ● Bsa I: nucleotide position 1052

stop codon is located at nucleotide 1609

**Figure 13. IMPDH Endonuclease Restriction Map for *Bsa* I and *Bsa* J1**

### Purification of Recombinant IMPDH

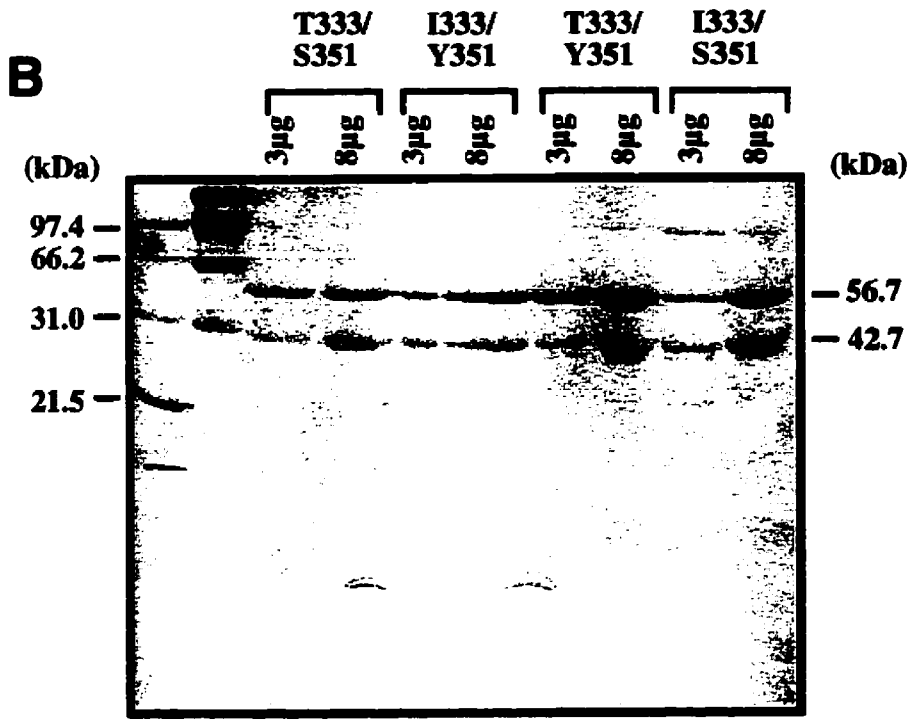
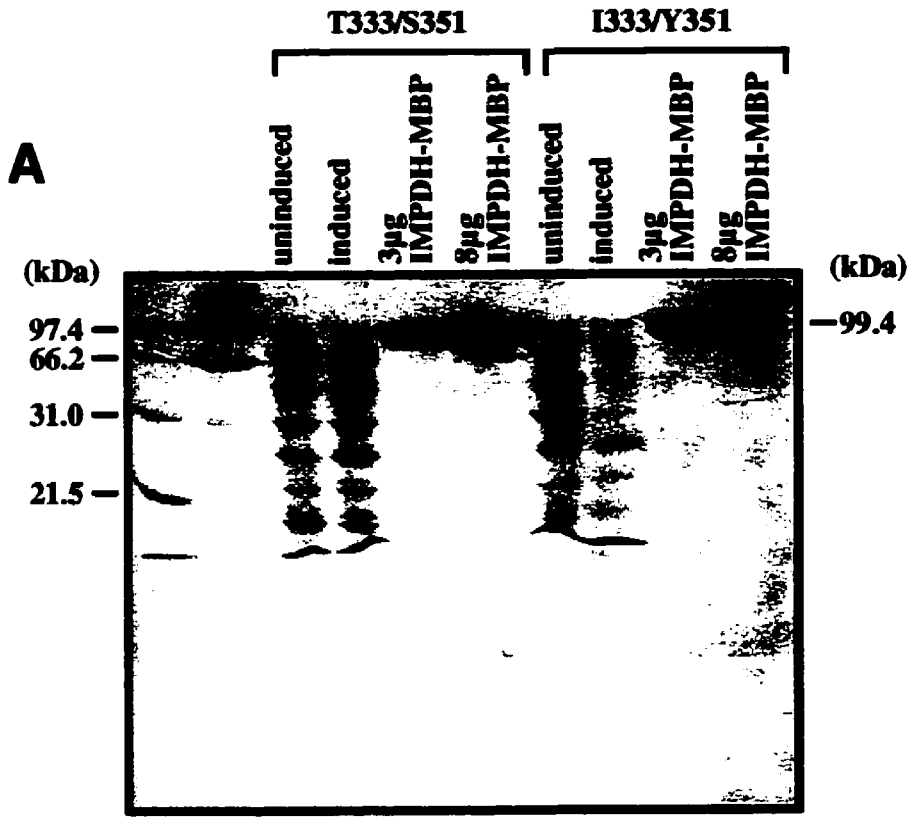
IMPDH-MBP fusion proteins were purified by affinity chromatography and analyzed on SDS-PAGE. The fusion protein could not be detected in the whole cell lysates of induced cells, but was readily visible after having been purified. Fusion protein (3 to 12 mg per litre *E. coli* culture) was purified, and it comprised up to 15% (but typically 5%) of the soluble proteins. The fusion proteins were quite pure (Figure 14 A).

The recombinant fusion proteins were cleaved with Factor Xa (thrombin) before being assayed. Uncut fusion proteins possessed IMPDH activity so this step may not have been necessary. Cleavage of all was almost complete (Figure 14 B). The cleaved fusion proteins were assayed directly for IMPDH activity.

**Figure 14. SDS-PAGE of Recombinant IMPDHs**

**A.** Wild-type (T333/S351) and double-mutant (I333/Y351) IMPDH. The gel contains cytoplasmic fractions of induced and uninduced transformed *E. coli* TB1 cells and amylose-purified IMPDH-MBP fusion proteins (3 and 8 $\mu$ g).

**B.** Wild-type (T333/S351), double mutant (I333/Y351) and each single mutant (I333/S351 and T333/Y351) IMPDH. These are the amylose-purified IMPDH-MBP fusion proteins which were then cleaved with Factor Xa. The 99.4 kDa fusion protein as shown in (A) was cleaved resulting in a 56.7 kDa IMPDH and a 42.7 kDa maltose binding protein. Two concentrations of the cleaved fusion proteins (3 and 8  $\mu$ g) are shown.



### IMPDH Kinetic Assays

Four sets of initial velocity IMPDH Assays were performed for T333/S351, I333/S351, T333Y351, and I333/Y351 IMPDHs. Each set of assays was analyzed by “Grafit” version 3.09 then plotted as initial velocity versus substrate concentration graphs.

The first set of assays involved varying concentrations of both substrates. They involved varying the concentration of one substrate (IMP) while holding the other ( $\text{NAD}^+$ ) at changing fixed concentrations to determine the  $K_m$  and the  $V_{max}$  for each substrate (Figure 15).

The second set of assays contained high ( $>0.5$  mM) changing fixed concentrations of  $\text{NAD}^+$  (substrate inhibition) and varying amounts of IMP in the reaction mix for determination of the mode of  $\text{NAD}^+$  inhibition at high concentrations, the  $K_m\text{IMP}$ , the  $V_{max}$ , and the  $K_i\text{NAD}^+$  (Figure 16).

The third set of assays contained changing fixed amounts of XMP (product inhibition) and varying amounts of IMP in the reaction mix to determine the  $K_m\text{IMP}$ ,  $V_{max}$ , and the  $K_i\text{XMP}$  (Figure 17).

The fourth set of assays contained changing fixed amounts of MPA and varying amounts of IMP in the reaction mix to determine the  $K_m\text{IMP}$ ,  $V_{max}$ , and  $K_i\text{MPA}$  (Figure 18).

The concentrations of IMPDH in the assay mixtures were : T333/S351 8 nM; I333/ S351 82 nM; T333/ Y351 10 nM; I333/ Y351 80 nM.

**Figure 15a). Initial Velocity of T333/S351 IMPDH**

The concentration of IMP varied (10, 15, 20, 35, and 60  $\mu\text{M}$ ) while  $\text{NAD}^+$  was held at changing fixed concentrations (0.05, 0.1, 0.15, 0.2, and 0.4 mM).

**Figure 15b). Initial Velocity of I333/S351 IMPDH**

The concentration of IMP varied (20, 40, 60, and 90  $\mu\text{M}$ ) while  $\text{NAD}^+$  was held at changing fixed concentrations (0.15, 0.2, 0.25 and 0.4 mM). The concentrations of IMP at 4.0 mM  $\text{NAD}^+$  were 20, 30, 40, 60, and 80  $\mu\text{M}$ .

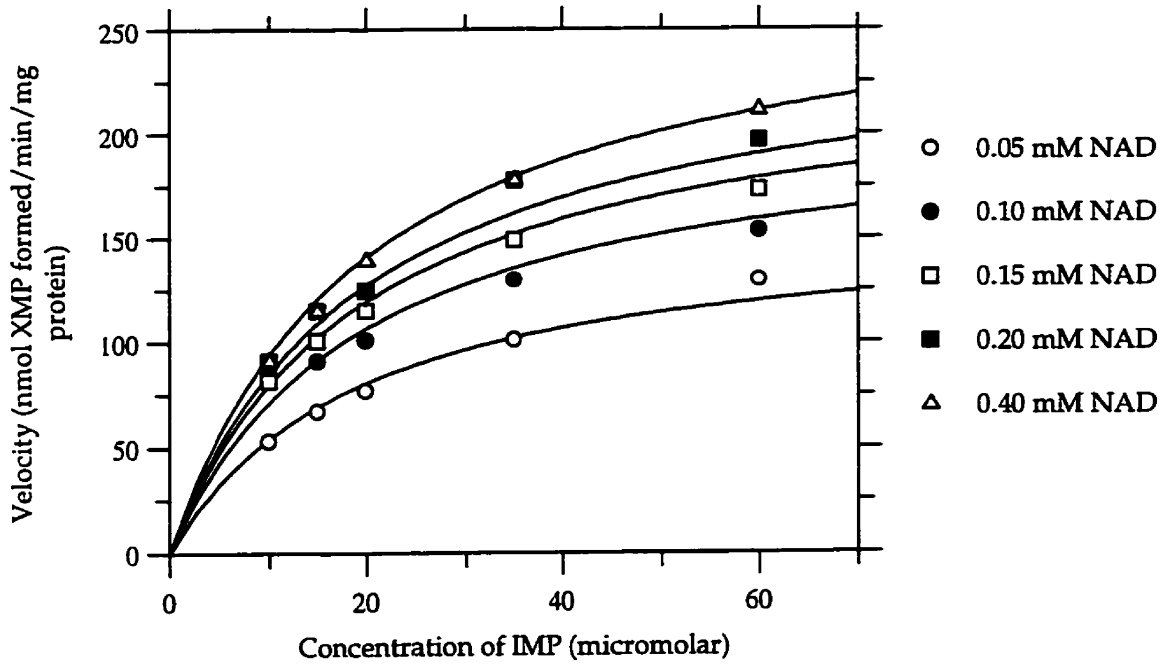
**Figure 15c). Initial Velocity of T333/Y351 IMPDH**

The concentration of IMP varied (100, 150, 200, 300, and 400 $\mu\text{M}$ ) while  $\text{NAD}^+$  was held at changing fixed concentrations (0.1, 0.15, 0.2, 0.3, and 0.4 mM).

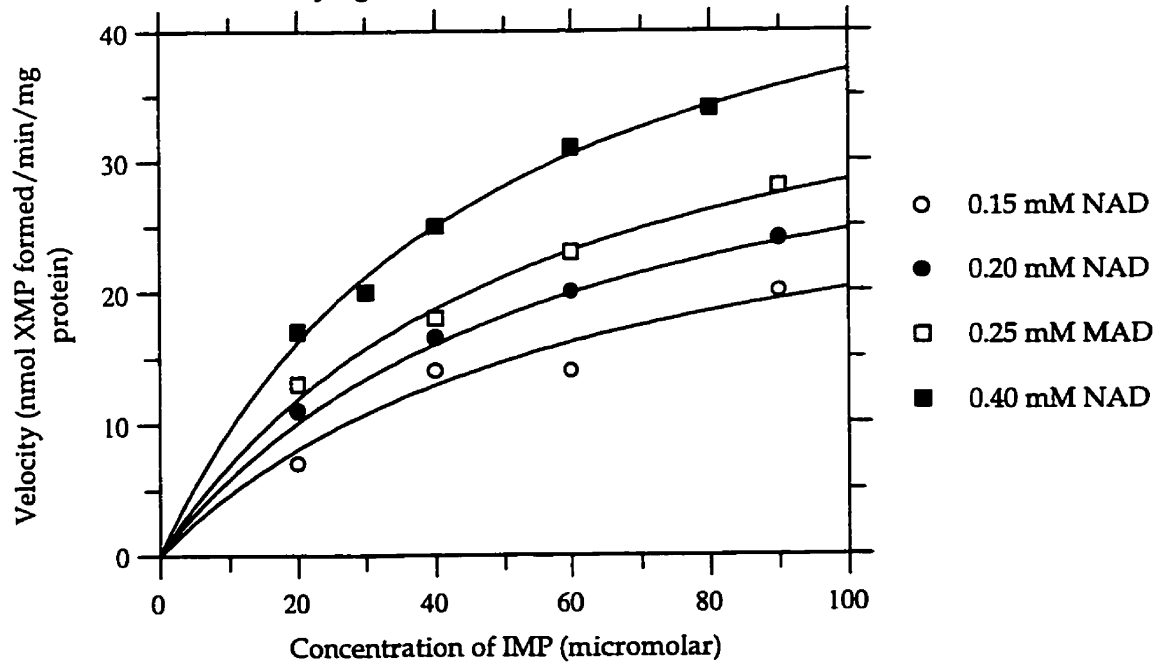
**Figure 15d). Initial Velocity of I333/Y351 IMPDH**

The concentration of IMP varied (50, 100, 200, and 300  $\mu\text{M}$ ) while  $\text{NAD}^+$  was held at changing fixed concentrations (0.075, 0.1, 0.15, 0.25, 0.4, and 1.0 mM).

**2 Substrate Kinetics for T333/ S351 IMPDH**  
 Varying [IMP], changing fixed [NAD]



**2 Substrate Kinetics for I333/ S351 IMPDH**  
 Varying [IMP], changing fixed [NAD]



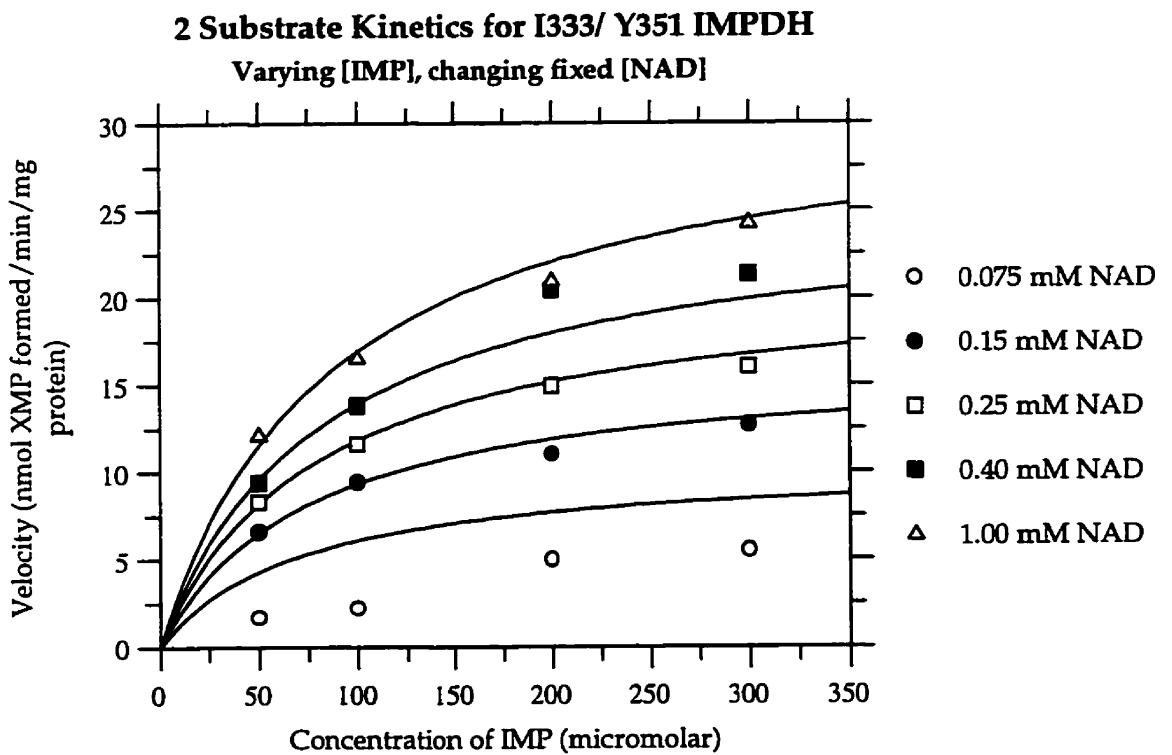
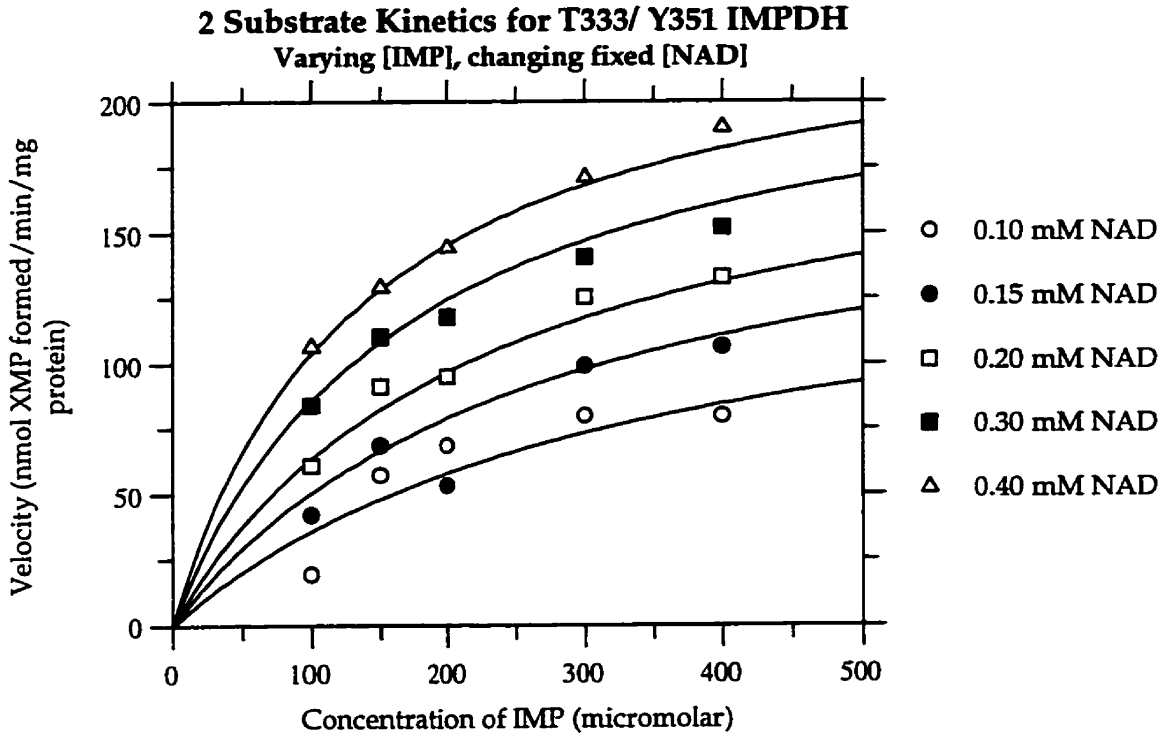


**Figure 16a). NAD<sup>+</sup> Uncompetitive Inhibition of T333/S351 IMPDH**

The concentration of IMP varied (10, 15, 20, 35, and 60  $\mu\text{M}$ ) while NAD<sup>+</sup> was held at changing fixed concentrations (0.4, 0.75, 1.0, and 2.5 mM).

**Figure 16b). NAD<sup>+</sup> Uncompetitive Inhibition of I333/S351 IMPDH**

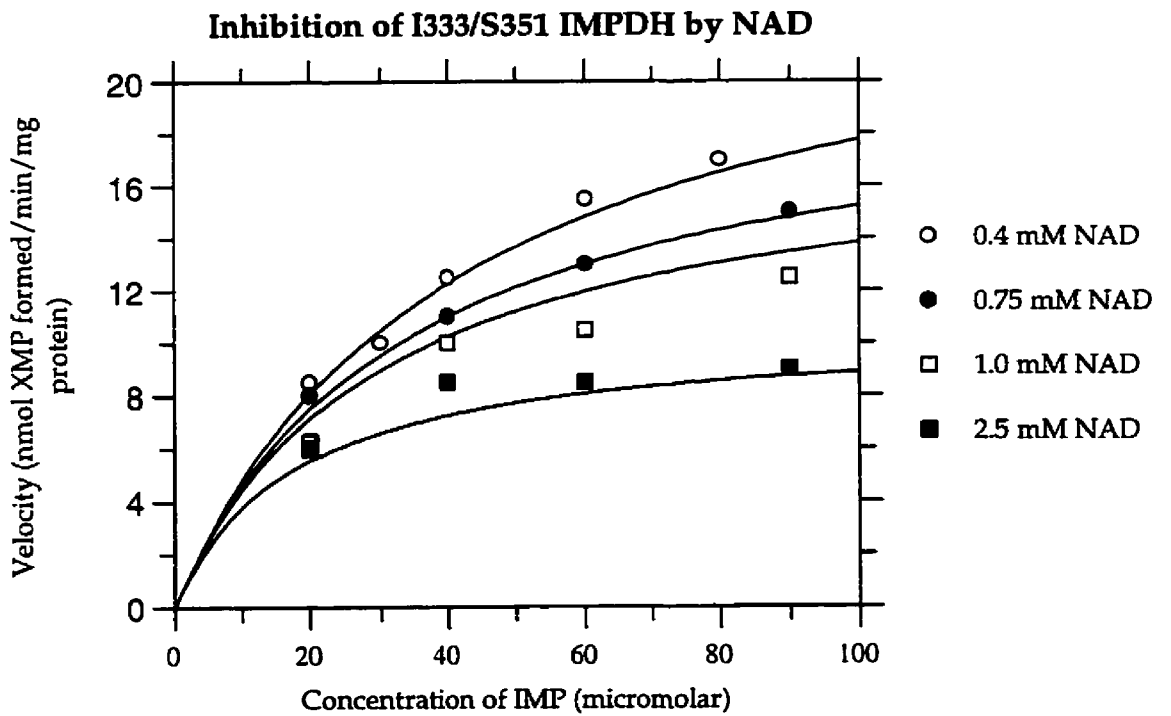
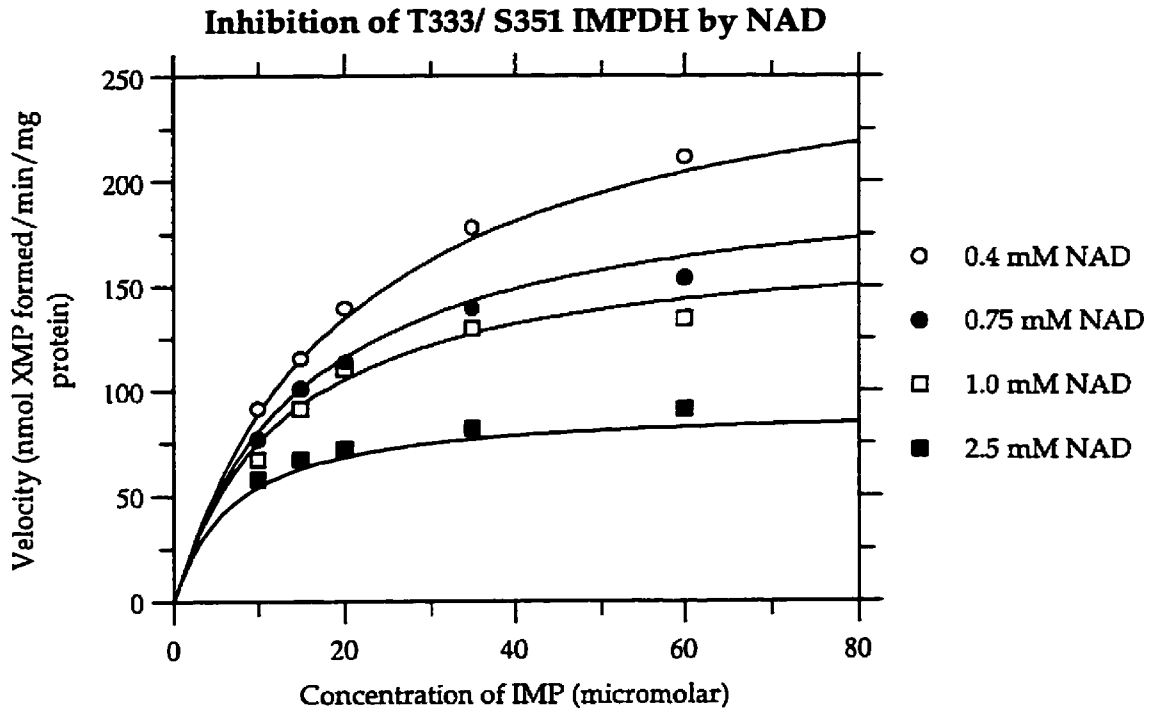
The concentration of IMP varied (20, 40, 60, and 90  $\mu\text{M}$ ) while NAD<sup>+</sup> was held at changing fixed concentrations (0.4, 0.75, 1.0, and 2.5 mM). The concentrations of IMP at 4.0 mM NAD<sup>+</sup> were 20, 30, 40, 60 and 80  $\mu\text{M}$ .

**Figure 16c). NAD<sup>+</sup> Uncompetitive Inhibition of T333/Y351 IMPDH**

The concentrations of IMP varied (100, 150, 200, 300, and 400  $\mu\text{M}$ ) while NAD<sup>+</sup> was held at changing fixed concentrations (0.4, 1.0, 1.8, and 2.5 mM).

**Figure 16d). NAD<sup>+</sup> Uncompetitive Inhibition of I333/Y351 IMPDH**

The concentrations of IMP varied (50, 100, 200 and 300  $\mu\text{M}$ ) while NAD<sup>+</sup> was held at changing fixed concentrations (1.0, 1.75, 2.5, 5.0, and 7.5 mM).



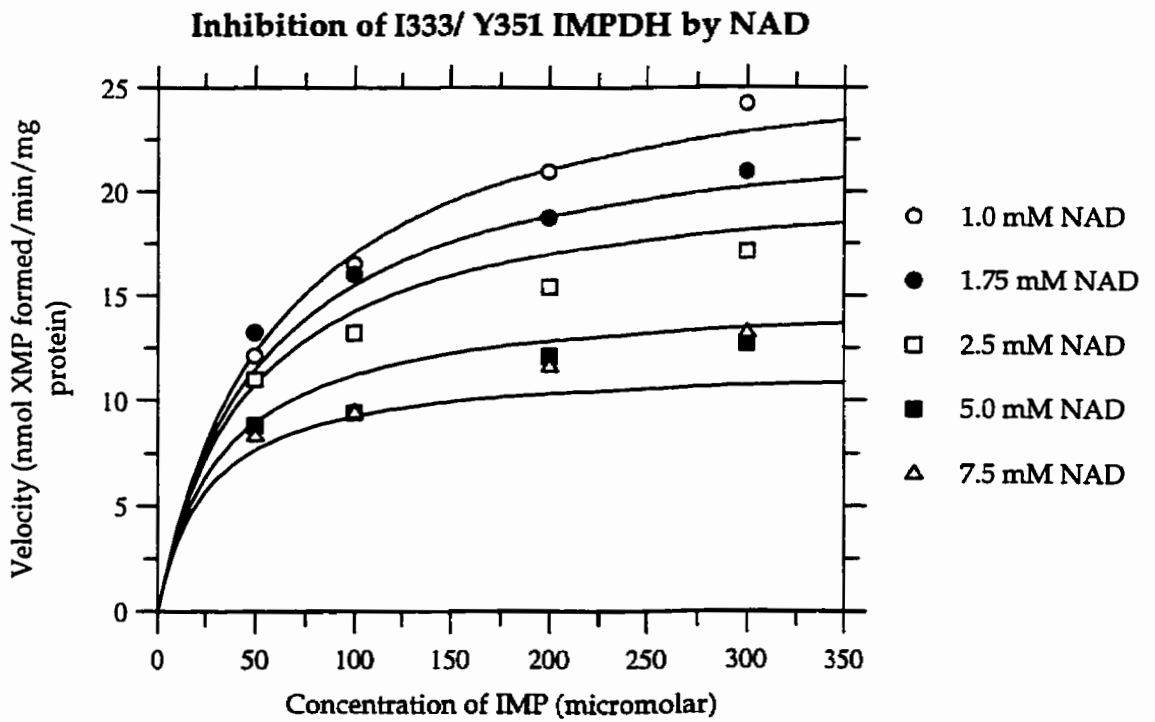
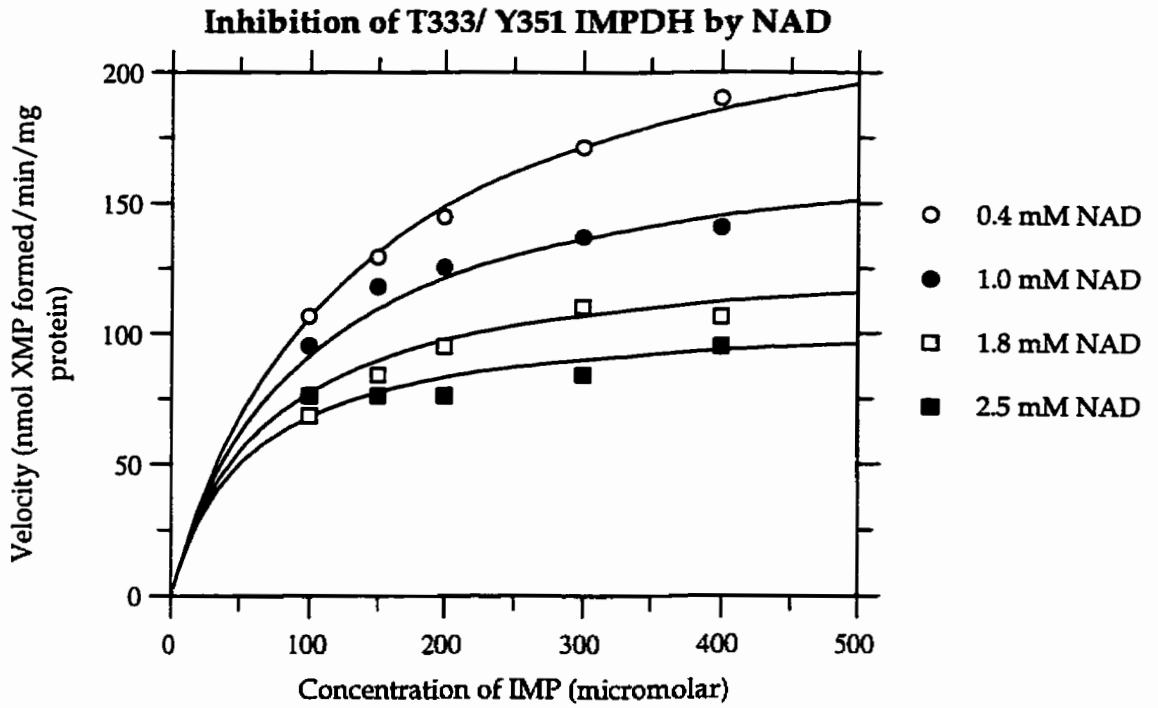


**Figure 17a). XMP Competitive Inhibition of T333/S351 IMPDH**

The concentration of IMP varied (10, 15, 20, 35, and 50  $\mu\text{M}$ ) while XMP was held at changing fixed concentrations (0, 40, 80, 120, 160, and 240  $\mu\text{M}$ ).

**Figure 17b). XMP Competitive Inhibition of I333/S351 IMPDH**

The concentration of IMP varied (20, 40, 60, and 90  $\mu\text{M}$ ) while XMP was held at changing fixed concentrations (0, 100, 250, 500, and 1000  $\mu\text{M}$ ).

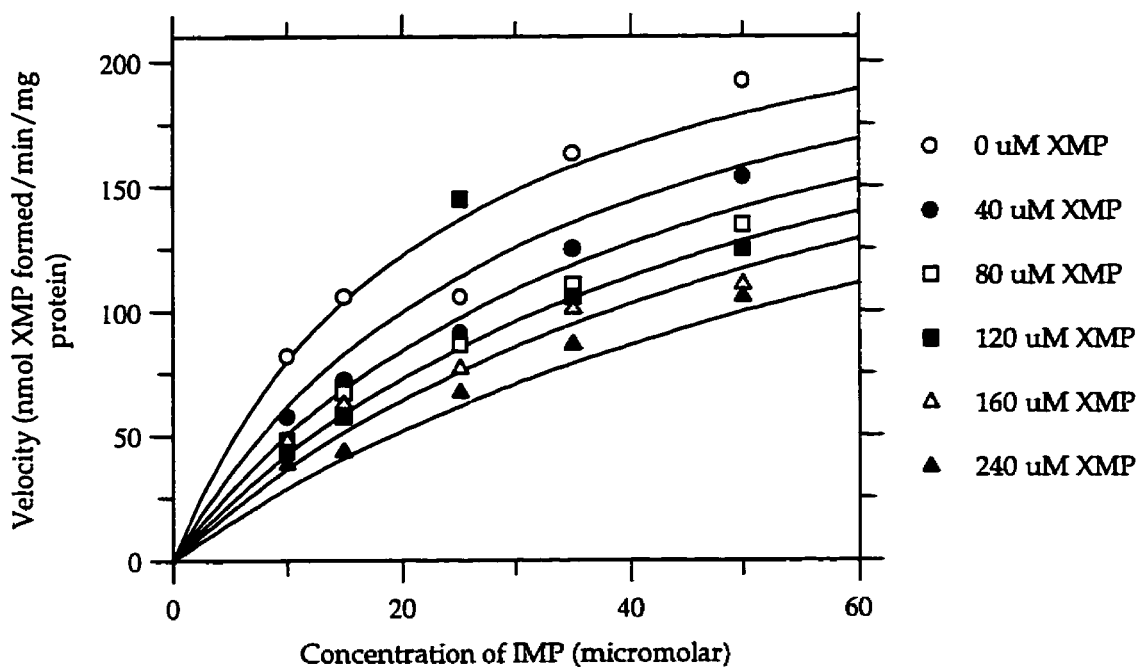
**Figure 17c). XMP Competitive Inhibition of T333/Y351 IMPDH**

The concentration of IMP varied (100, 150, 200, 300, and 400  $\mu\text{M}$ ) while XMP was held at changing fixed concentrations (0, 250, 500, 1000, and 2500  $\mu\text{M}$ ).

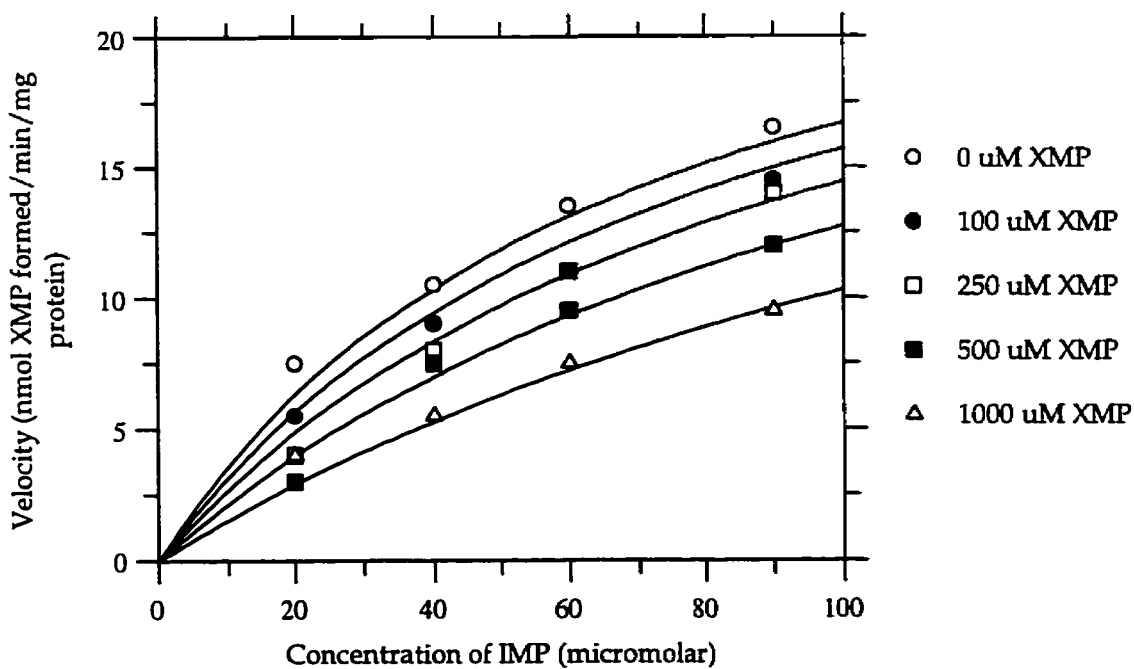
**Figure 17d). XMP Competitive Inhibition of I333/Y351 IMPDH**

The concentration of IMP varied (50, 100, 150, and 250  $\mu\text{M}$ ) while XMP was held at changing fixed concentrations (0, 100, 250, 500, and 1000  $\mu\text{M}$ ).

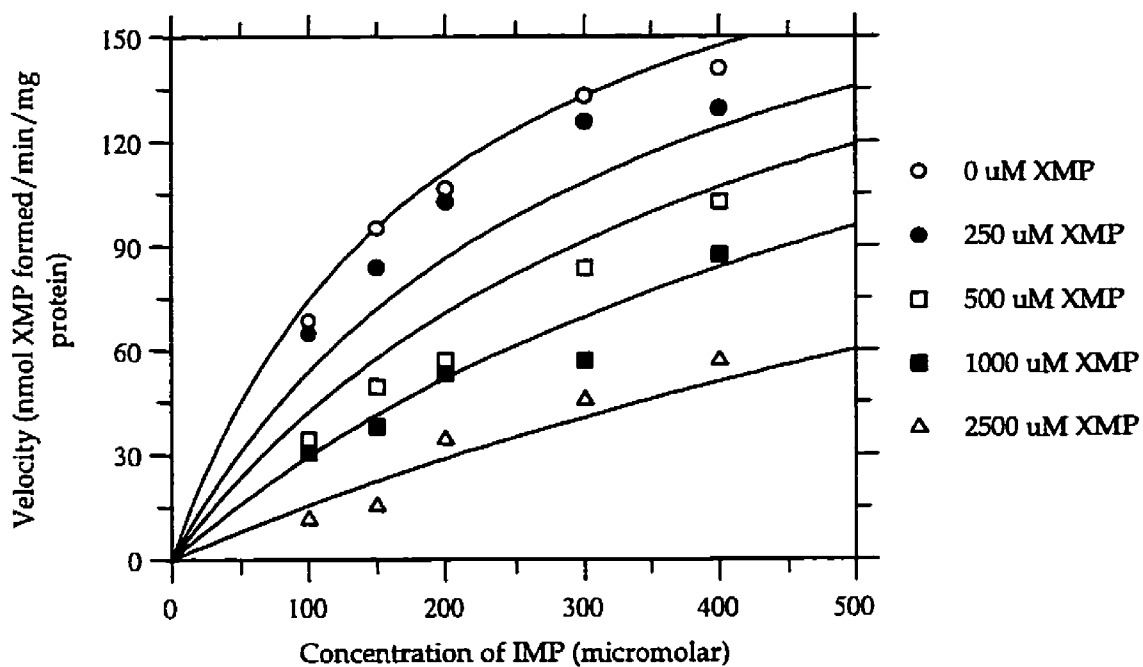
### Inhibition of T333/ S351 IMPDH by XMP



### Inhibition of I333/ S351 IMPDH by XMP



### Inhibition of T333/ Y351 IMPDH by XMP



### Inhibition of I333/ Y351 IMPDH by XMP

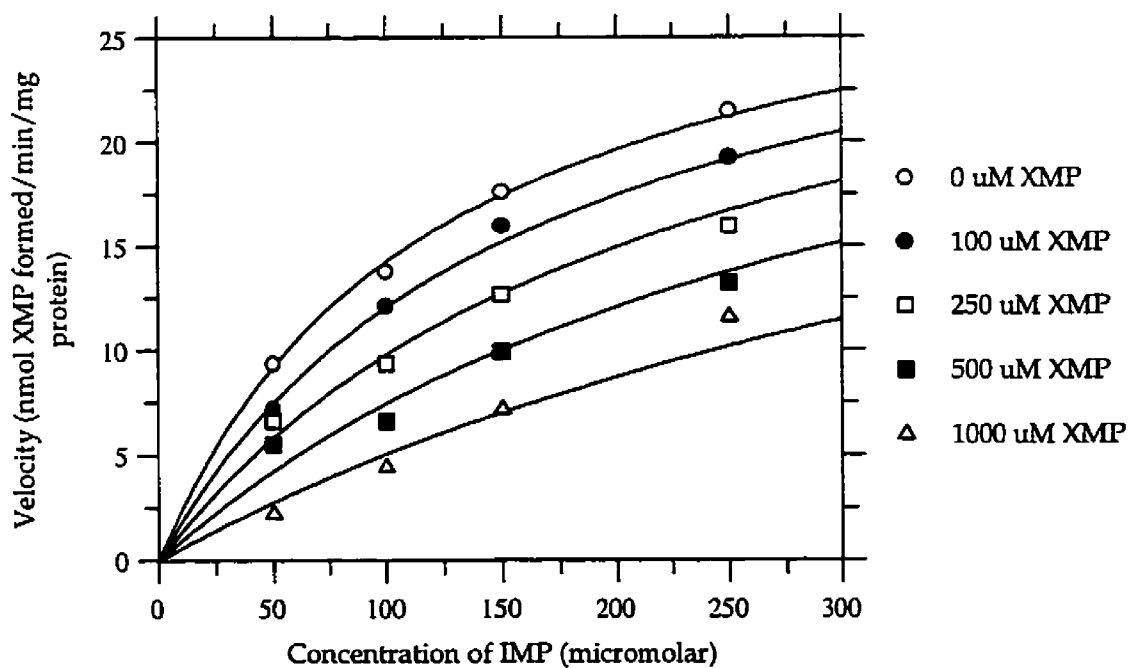


**Figure 18a). MPA Uncompetitive Inhibition of T333/S351 IMPDH**

The concentration of IMP varied (5, 10, 15, 25, and 40  $\mu\text{M}$ ) while MPA was held at changing fixed concentrations (0, 5, 10, 20, and 30 nM).

**Figure 18b). MPA Uncompetitive Inhibition of I333/S351 IMPDH**

The concentration of IMP varied (10, 15, 20, 40, and 80  $\mu\text{M}$ ) while MPA was held at changing fixed concentrations (0, 500, 1000, and 2500 nM).

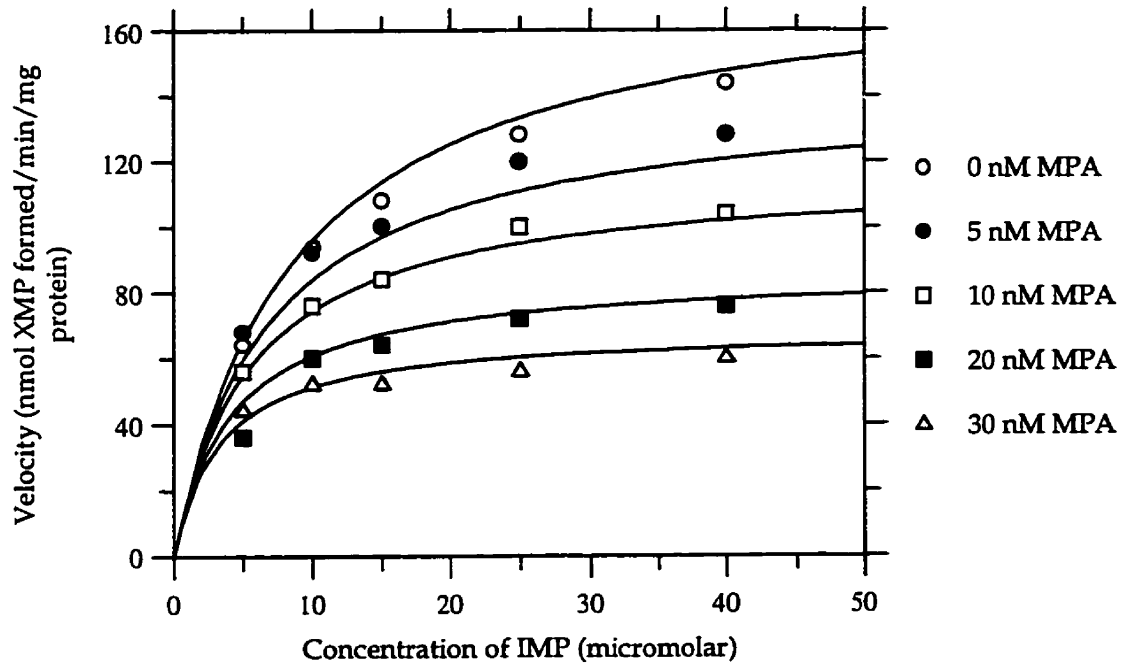
**Figure 18c). MPA Uncompetitive Inhibition of T333/Y351 IMPDH**

The concentration of IMP varied (50, 100, 150, 250, and 400  $\mu\text{M}$ ) while MPA was held at changing fixed concentrations (0, 10, 17.7, 20, 30, and 50 nM).

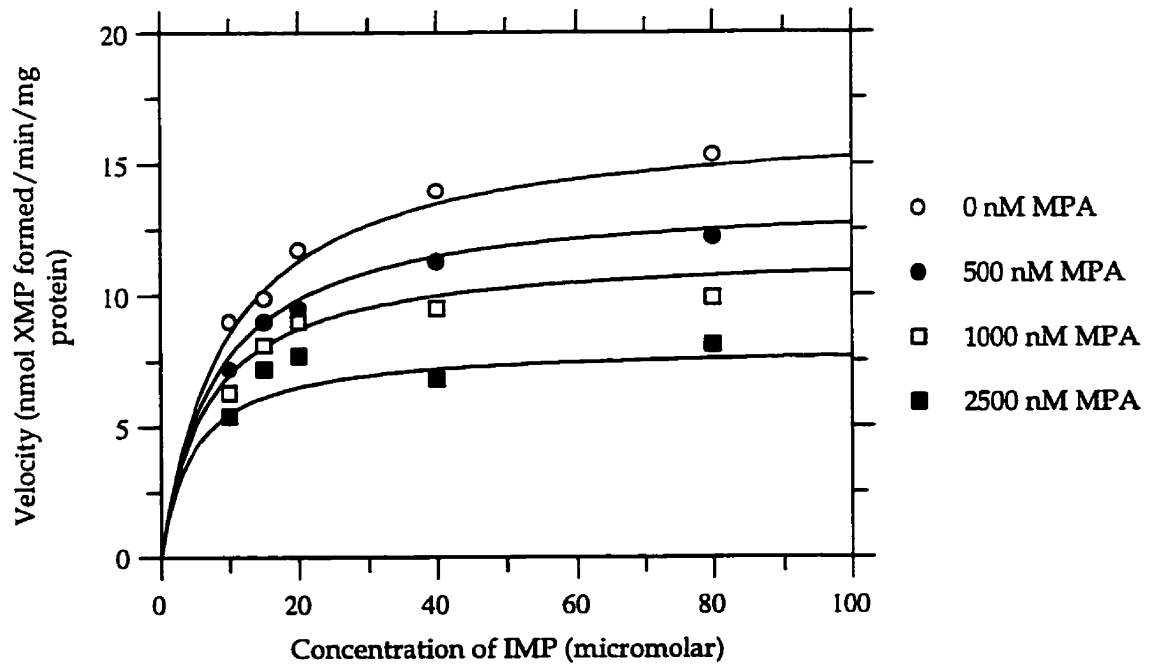
**Figure 18d). MPA Uncompetitive Inhibition of I333/Y351 IMPDH**

The concentration of IMP varied (25, 35, 50, 75, and 150  $\mu\text{M}$ ) while MPA was held at changing fixed concentrations (0, 1000, 2500, and 5000 nM).

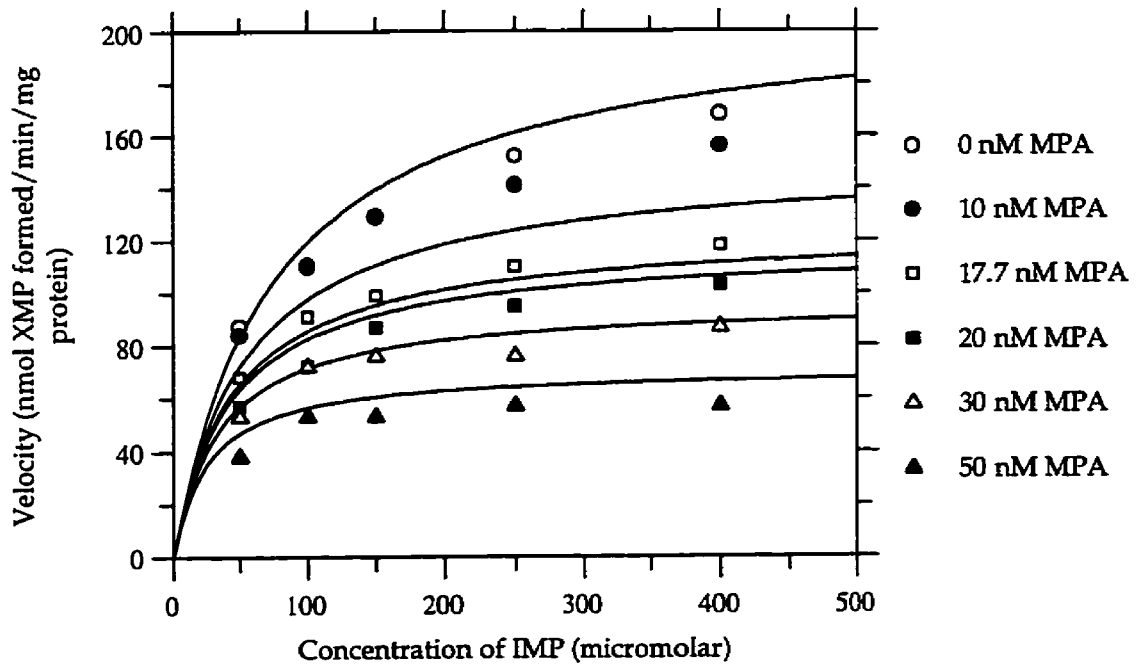
### Inhibition of T333/ S351 IMPDH by MPA



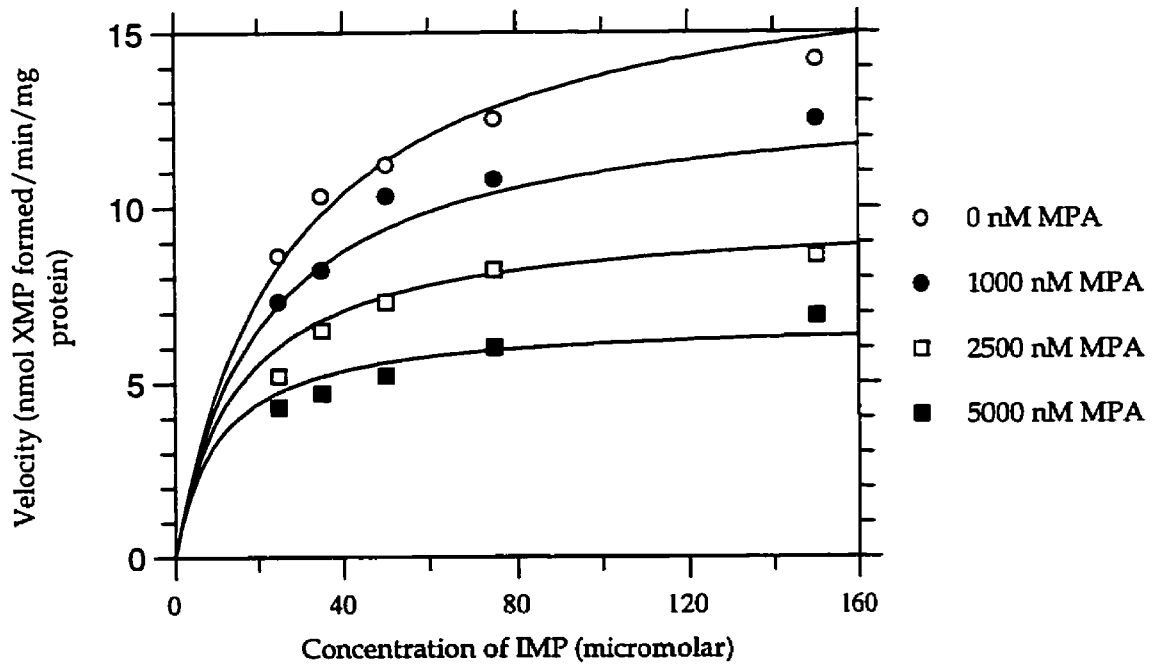
### Inhibition of I333/ S351 IMPDH by MPA



### Inhibition of T333/ Y351 IMPDH by MPA



### Inhibition of I333/ Y351 IMPDH by MPA



### Calculated Kinetic Parameters

The kinetic parameters  $K_m$ IMP,  $K_m$ NAD<sup>+</sup>,  $K_i$ XMP,  $K_i$ NAD<sup>+</sup>,  $K_i$ MPA and  $V_{max}$  were calculated using the program Grafit Version 3.09 from the initial velocities at known concentrations of substrates and inhibitors. The  $k_{cat}$  was calculated from the  $V_{max}$  and amount of IMPDH in the reaction mixture. All methods of calculations and formulae used are described in the Appendix. Calculations were performed on the data set as a whole; each data point was given equal weighting. The data were graphed as initial velocity versus concentration of IMP. The lines were drawn through the points by also treating the data as a whole and each line was interdependent with every line on the graph. Thus, sometimes an individual line was not the best line through the one set of data points, but it was the best line through the data points taking into account the mode of inhibition, concentrations of inhibitors, and every other line on the graph.

The calculated kinetic parameters are listed in Tables 6 and 7 and highlighted in Table 8. The calculations performed on the data used regression analysis; ie, kinetic parameters were calculated such that the smallest possible sum of the squared deviations of the experimental values from the calculated ones were produced. The quantity that is minimized is denoted by Chi-squared ("X<sup>2</sup>"). The value of X<sup>2</sup> includes the variance of the data point ( $\partial_i$ ) so that data points which have greater errors contribute less to the analysis. It is calculated as:  $X^2 = \sum[\Delta y_i / \partial_i]^2$  where  $\Delta y_i$  is the difference between the experimental and calculated y data values and  $i$  indicates the  $i$ th data value.

Table 6. Calculated Kinetic Parameters for Four Mouse Type II IMPDHs

ASSAY	IMPDH	Km IMP	Ki	(Chi) <sup>2</sup>	Vmax	kcat	kcat/Km <sub>IMP</sub>					
<b>XMP Inhibition</b>		$\mu\text{M IMP}$	$\mu\text{M XMP}$		$\text{nmols XMP/min/mg}$	(turnover/ s/IMPDH)	( $\text{mM}^{-2}\text{s}^{-1}$ )					
	<i>T333/S351</i>	22.4 \2.8	93 \9.6	44	259 \14	2.0	90					
	<i>I333/S351</i>	69.5 \12	661 \92	0.42	28 \2.5	0.20	2.9					
	<i>T333/Y351</i>	193 \46	432 \79	76	219 \23	1.6	8.2					
	<i>I333/Y351</i>	121 \15	301 \32	0.46	32 \1.8	0.23	1.9					
<b>NAD<sup>+</sup> Inhibition</b>		$\mu\text{M IMP}$	$\text{mM NAD}^+$		$\text{nmols XMP/min/mg}$							
	<i>T333/S351</i>	34 \4.2	0.66 \0.09	35	444 \38	3.2	95					
	<i>I333/S351</i>	58 \12	1.1 \0.2	0.56	35 \4.5	0.25	4.3					
	<i>T333/Y351</i>	177 \21	1.2 \0.1	24	330 \20	2.4	14					
	<i>I333/Y351</i>	79 \14	3.7 \0.6	1.4	35 \2.9	0.25	3.2					
<b>2 Substrates</b>	IMPDH	<b>Ka (IMP)</b>	<b>Kb (NAD<sup>+</sup>)</b>	<b>(Chi)<sup>2</sup></b>	<b>Vmax</b>	<b>kcat</b>	<b>kcat/Km<sub>IMP</sub></b>					
		$\mu\text{M IMP}$	$\text{mM NAD}^+$					$\text{nmols XMP/min/mg}$	(turnover/ s/IMPDH)	( $\text{mM}^{-2}\text{s}^{-1}$ )		
		<i>T333/S351</i>	20 \3.0					0.05 \0.01	44	317 \22	2.3	113
		<i>I333/S351</i>	35 \20					0.27 \0.17	0.98	91 \28	0.36	10
		<i>T333/Y351</i>	74 \37					0.17 \0.09	39	363 \78	2.8	38
<i>I333/Y351</i>	92 \28	0.20 \0.06	0.95	37 \4.0	0.27	2.9						

"\" represents "+/-"

Table 7: Mycophenolic Acid Inhibition of IMPDH

	<u>Uncompetitive</u>	<u>Noncompetitive</u>	<u>Tight-Binding</u>
<b>T333/ S351</b>			
$K_m$ IMP	8.7 /0.9	6.4 /0.7	8.3 /1.0
$K_i$ MPA	18.4 /1.5	27 /2	7.6 /0.9
$V_{max}$	180 /7	165 /6	
$(Chi)^2$	27	37	20
$k_{cat}$	1.4	1.3	
$k_{cat}/K_m$ IMP	161	203	
<b>I333/ S351</b>			
$K_m$ IMP	9.5 /1.1	7.6 /1.0	9.5 /1.1
$K_i$ MPA	2313 /231	3154 /350	2269 /229
$V_{max}$	16.7 /0.6	15.8 /0.6	
$(Chi)^2$	0.34	0.48	0.342
$k_{cat}$	0.13	0.12	
$k_{cat}/K_m$ IMP	13.7	16.1	
<b>T333/ Y351</b>			
$K_m$ IMP	75 /12	53 /8.3	72 /10
$K_i$ MPA	26 /2.9	36 /3.7	10.8 /2.3
$V_{max}$	209 /12	192 /9	
$(Chi)^2$	94	99	74
$k_{cat}$	1.6	1.5	
$k_{cat}/K_m$ IMP	21.6	28.1	
<b>I333/ Y351</b>			
$K_m$ IMP	28 /3.2	22 /1.9	27 /3.2
$K_i$ MPA	3141 /256	4479 /243	3109 /253
$V_{max}$	18 /0.7	16.6 /0.4	
$(Chi)^2$	0.26	0.15	0.25
$k_{cat}$	0.14	0.13	
$k_{cat}/K_m$ IMP	5.0	5.8	

Table 8. Summary of Mutation Effects in Mouse Type II IMPDH **$K_m$ IMP/ $K_m$ NAD<sup>+</sup>**

<u>IMPDH</u>	<u><math>K_m</math>IMP (μM)</u>	<u><math>K_m</math>NAD<sup>+</sup> (mM)</u>
T333/S351	20	0.05
I333/S351	35 (1.8x)	0.27 (5.4x)
T333/Y351	74 (3.7x)	0.17 (3.4x)
I333/Y351	92 (4.5x)	0.20 (4x)
Mutation Effects:	cumulative	I333 dominant Y351 important

 **$K_i$ XMP/ $K_i$ NAD<sup>+</sup>**

<u>IMPDH</u>	<u><math>K_i</math>XMP (μM)</u>	<u><math>K_i</math>NAD<sup>+</sup> (mM)</u>
T333/S351	93	0.66
I333/S351	661 (7x)	1.1 (2x)
T333/Y351	432 (4.5x)	1.2 (2x)
I333/Y351	301 (3x)	3.7 (5.5x)
Mutation Effects:	I333 dominant Y351 important	cumulative

 **$K_i$ MPA/ $k_{cat}$** 

<u>IMPDH</u>	<u><math>K_i</math>MPA (nM)</u>	<u>average <math>k_{cat}</math> (turnovers/s/IMPDH)</u>
T333/S351	7.6	2.2
I333/S351	2269 (300x)	0.24 (0.1x)
T333/Y351	10.8 (1.4x)	2.1 (0.9x)
I333/Y351	3109 (411x)	0.22 (0.1x)
Mutation Effects:	I333 dominant	I333 dominant

## **CHAPTER 5: Discussion**

A mouse IMPDH possessing altered kinetic properties including an increased  $K_i$  for the immunosuppressive drug mycophenolic acid (MPA) was identified in mouse neuroblastoma cells (Hodges *et. al.*, 1989, Lightfoot and Snyder, 1994) which had been stepwise selected for increased resistance to MPA. The identified IMPDH possessed two point mutations which resulted in the following two amino acid substitutions: Thr at position 333 was replaced with Ile and Ser at position 351 was replaced with Tyr. The purpose of the investigation presented here was to determine the extent to which each individual amino acid substitution was responsible for the observed changes in the kinetic parameters of the IMPDH. Site-directed mutagenesis was performed to generate each single mutant IMPDH. All four IMPDH species [T333/S351 (wild-type), I333/S351 (single mutant), T333/Y351 (single mutant), and I333/Y351 (double mutant)] were cloned, expressed, purified and assayed for activity. The values of  $K_m$ IMP,  $K_m$ NAD<sup>+</sup>,  $K_i$ XMP,  $K_i$ MPA,  $V_{max}$ ,  $k_{cat}$ , and  $k_{cat}/K_m$  were determined for all. The results were compared to those originally obtained for T333/S351 and I333/Y351 (Hodges *et. al.*, 1989) as well as to other published data. Unless otherwise noted, changes in observed kinetic parameters for the mutant IMPDHs are stated with respect to the corresponding kinetic parameters measured for T333/S351 (wild-type) IMPDH.

The only kinetic parameter determined for the MPA inhibition experiments which is discussed is the  $K_i$ MPA due to the fact that DMSO was present during those assays and seemed to have had the effect of decreasing the  $K_m$ IMP and lowering the  $V_{max}$ . The assay previously performed (Hodges *et. al.*, 1989) used a radiochemical IMP, giving a more sensitive assay than the spectrophotometric method used here. Another difference in the methods was that neither wild-type (T333/S351) nor double mutant (I333/Y351) had been expressed as fusion proteins previously (Hodges *et. al.*, 1989)

and that the T333/S351 IMPDH had been assayed from whole cell lysate, where it was estimated to have a 0.01% abundance.

#### Kinetic Parameters Obtained for T333/S351 (Wild-Type)

In short, all kinetic data obtained for the wild-type mouse IMPDH was in agreement with kinetic parameters previously reported for rodents and humans. The reaction mechanism (Figure 3) and molecular mechanism (Figure 6) can be referred to throughout the discussion.

The  $K_m$ IMP was determined to be in the range of 20 - 34  $\mu$ M. This was in agreement with that previously reported for mouse, 8 - 18  $\mu$ M (Hodges *et. al.*, 1989); human types I and II, 9 - 18  $\mu$ M (Carr *et. al.*, 1993, and Hager *et. al.*, 1995); Chinese hamster, 22 (Huberman *et. al.*, 1981); and rat, 12  $\mu$ M (Jackson *et. al.*, 1977).

The  $K_m$ NAD<sup>+</sup> was determined to be 0.05 mM which is in the vicinity of mouse, 0.025 mM (Hodges *et. al.*, 1989); human types I and II, 0.032 - 0.046 mM (Carr *et. al.*, 1993 and Hager *et. al.*, 1995); Chinese hamster, 0.029 mM (Huberman *et. al.*, 1981); and rat, 0.024 mM (Jackson *et. al.*, 1977).

XMP is a competitive inhibitor of IMPDH with respect to IMP and the  $K_i$ XMP was found to be 93  $\mu$ M, which was very close to mouse, 87  $\mu$ M (Hodges *et. al.*, 1989) and human types I and II, 80  $\mu$ M and 84  $\mu$ M respectively (Carr *et. al.*, 1993).

NAD<sup>+</sup> can display dead-end product inhibition at high (above 4 mM) concentrations. The  $K_i$ NAD<sup>+</sup> was approximately 0.66 mM. Most groups have looked at NADH as the inhibitor, but it is in fair agreement with the previously calculated  $K_i$ NAD<sup>+</sup> of 1.3 mM for the partially purified mouse IMPDH (Hodges *et. al.*, 1989).

As previously described, MPA produced uncompetitive inhibition with respect to IMP. The  $K_i$ MPA was determined to be 7.6 nM. Other reported MPA binding activities have been mouse, 1.4 nM (Hodges *et. al.*, 1989); human types I and II, 33 nM and 7.0 nM respectively (Carr *et. al.*, 1993), 11 nM and 6 nM respectively (Hager *et. al.*, 1994); and hamster, 9 nM (Sinchak *et. al.*, 1996).

The  $k_{cat}$  calculated was in the range of 2.0 - 3.2 turnovers per second per molecule IMPDH (the magnitude of  $k_{cat}$  is four times larger if it is expressed as turnover per second per active site). The human enzymes are estimated to be approximately 1.3 - 1.8 turnovers per second per molecule IMPDH (Carr *et. al.*, 1993, and Hager *et. al.*, 1995) or 0.4 turnovers per second per active site (Farazi *et.al.*, 1997), which corresponds to 1.6 turnovers per second per molecule IMPDH. The  $k_{cat}/K_m$  was determined to be in the range of 90 to 113  $\text{mM}^{-2} \text{s}^{-1}$  which is in very good agreement with that which had been obtained for the human enzymes, 83 and 140  $\text{mM}^{-2}\text{s}^{-1}$  for types I and II respectively (Carr *et. al.*, 1993) and 2 - 3 fold greater than that of Chinese hamster, which was approximately 35  $\text{mM}^{-2}\text{s}^{-1}$  (Sintchak *et. al.*, 1996).

#### Comparison of T333/S351 (Wild-Type) vs I333/Y351 (Double Mutant) Kinetic Data to that Previously Determined

There were four striking kinetic differences previously determined between T333/S351 (wild-type) and I333/Y351 (double mutant) IMPDHs (Hodges *et. al.*, 1989). I333/Y351 displayed a 4-fold increased  $K_m\text{NAD}^+$  (from 25 to 94  $\mu\text{M}$ ), a 4-fold increased  $K_i\text{XMP}$  (from 78 to 336  $\mu\text{M}$ ), a 2400-fold increased  $K_i\text{MPA}$  (from 1.4 to 3400  $\mu\text{M}$ ), and an estimated 10-fold decreased  $k_{cat}$  (the decreased  $k_{cat}$  was an estimate because the T333/S351 wild-type IMPDH was not fully purified). The changes in  $K_m\text{IMP}$  (8 to 18  $\mu\text{M}$ ) and  $K_i\text{NAD}^+$  (1.3 to 1.5 mM) were not considered significant. For the most part, the kinetic parameters presented here for the recombinant IMPDHs

are similar to those just described (Tables 6, 7 and 8); however, there were a two differences. A 4.5-fold increased  $K_m$ IMP was detected in I333/Y351 (double mutant) over T333/S351 (wild-type). This is consistent with the 3 to 4-fold increased  $K_i$ XMP observed in both studies. XMP is a competitive inhibitor of IMPDH with respect to IMP so it is reasonable that one or more mutations causing an increased  $K_i$ XMP would also translate to an increased  $K_m$ IMP. A detected 4-fold increased  $K_m$ NAD<sup>+</sup> was in agreement with the previous study, but a 5.5-fold increased  $K_i$ NAD<sup>+</sup> was detected as well, which points to a change in the NAD<sup>+</sup> binding site. This change could be due to an indirect long-distance effect. The estimated 10-fold decreased  $k_{cat}$  of I333/Y351 IMPDH was shown to be an accurate estimate, as it was also observed in the recombinant proteins.

#### Proposed Consequences of Mutations (See also Table 8)

##### $K_i$ MPA (Table 7)

MPA as an inhibitor of IMPDH was analyzed as an uncompetitive, a noncompetitive and a tight-binding inhibitor. It is possible that one or more mutations in an enzyme can change the mode of inhibition of an inhibitor. This is the reason that MPA was also analyzed as a noncompetitive inhibitor for all. For tight-binding analysis, both tight binding as an uncompetitive inhibitor and a noncompetitive inhibitor were calculated and they yielded identical results, so the results are simply discussed as tight-binding. Thus, for the purposes of discussing the changed  $K_i$ MPA, the mode of inhibition is irrelevant. However, it was essential to pick a mode of inhibition and values of kinetic parameters to graph the data.

By examination of the  $X^2$  values, it looks as though all sets of data have an approximately equal fit to uncompetitive and noncompetitive inhibition. Conversely, the  $K_m$ IMP values varied. The values of the  $K_m$ IMP for uncompetitive inhibition were very close to the  $K_m$ IMP values for tight binding inhibition, whereas the

$K_m$  IMP values for noncompetitive inhibition differed. An inhibitor should not affect the  $K_m$  values of substrates (it may affect the apparent  $K_m$  but not the actual calculated  $K_m$ ). Because of this, it was decided that the mode of MPA inhibition for all was uncompetitive and the curve fits on the graphs in figure 18 were drawn representing uncompetitive inhibition.

The most dramatic change in kinetic behaviour that had previously been noted from T333/S351 (wild-type) to I333/Y351 (double mutant) was the 2400-fold increased  $K_i$ MPA (Hodges *et. al.*, 1989). Using the model of tight-binding inhibition, an increased  $K_i$ MPA of 411-fold from T333/S351 to I333/Y351 was detected for the purified and cleaved fusion proteins. This increase seemed to be predominantly if not solely due to the mutation at position 333; the I333/S551 enzyme displayed a 300-fold increased  $K_i$ MPA while the T333/Y351 showed merely a 1.4-fold increased  $K_i$ MPA. It is possible that the S351Y mutation was the first to occur in the mouse NB cell line, offering it minimal resistance before the more effective mutation occurred, but at this point an increase in  $K_i$  of merely 1.4-fold is not significant enough on which to speculate. The T333I mutant Chinese hamster IMPDH has been obtained and has shown a 260-fold increased  $K_i$  MPA over the Thr 333 wild-type (Sinchak *et. al.*, 1996), which is in agreement with the results presented here. The crystal structure (Figure 8) revealed that Thr 333 is directly involved in binding the -OH of mycophenolic acid, so mutating it to Ile 333 would abolish the -OH on the side chain and presumably decrease the enzyme's affinity for MPA. The only kinetic parameter presented in the study for the single mutant Chinese hamster IMPDH was the  $K_i$ MPA (Sintchak *et. al.*, 1996).

#### $K_m$ NAD<sup>+</sup> and $K_i$ NAD<sup>+</sup>

It has been hypothesized that MPA binds to the nicotinamide subsite of the NAD<sup>+</sup> binding site of IMPDH (Hedstrom and Wang, 1990). This could mean then that Thr 333 is involved in hydrogen bonding to the

nicotinamide moiety of  $\text{NAD}^+$ . If this is the case, then one would expect that I333/S351 IMPDH should show different kinetic parameters in response to  $\text{NAD}^+$  binding than T333/S351 (wild-type) IMPDH. This is indeed the case. A 5.4-fold increased  $K_m\text{NAD}^+$  (which is possibly because the -OH of T333 is no longer present to participate in hydrogen bonding) and a slight increase (2-fold) in the  $K_i\text{NAD}^+$  was observed. One would expect that if the mutation S351Y has no effect on the enzyme, then the  $\text{NAD}^+$  kinetic parameters of T333/Y351 IMPDH should resemble those of T333/S351 (wild-type) and that the enzyme containing both mutations, I333/Y351, should resemble I333/S351. This is not the case. The S351Y mutation also has altered kinetic parameters. The T333/Y351 IMPDH possesses an increased  $K_m\text{NAD}^+$  of 3.4-fold and a 2-fold increased  $K_i\text{NAD}^+$ . It is possible that these properties are due to perturbations of the tertiary structure of IMPDH caused by the introduction of a phenyl moiety at position 351 and not due to a direct effect. A perturbation in the tertiary structure could change the environment of the  $\text{NAD}^+$  binding site. To ascertain with minimal doubt what is occurring at the structural level, one would need to obtain a crystal structure of IMPDH with the S351Y mutation and compare it to that of the wild-type IMPDH.

The  $K_i\text{NAD}^+$  of I333/Y351 is 5.5-fold higher than the  $K_i\text{NAD}^+$  T333/S351, which exceeds the cumulative effects of each single mutation. It might be expected then that the  $K_m\text{NAD}^+$  for I333/Y351 (double mutant) should represent the cumulative effects of each single mutation as well. This is not the case; the increased  $K_m\text{NAD}^+$  for I333/Y351 is only 4-fold, which lies between I333/S351 (5.4-fold) and T333/Y351 (3.4-fold).

### $K_m\text{IMP}$

A 4.5-fold increased  $K_m\text{IMP}$  was detected in the I333/Y351 (double mutant) IMPDH. This appears to be a cumulative effect of each single mutation. The  $K_m\text{IMP}$  of I333/S351 is 1.8-fold higher than

that of T333/S351 (wild-type) and the  $K_m$ IMP of T333/Y351 is 3.7-fold higher, as determined by initial velocity studies with both substrates at varying concentrations and no inhibitors present. Neither Thr 333 nor Ser 351 has been implicated in IMP binding in wild-type hamster IMPDH (Sintchak *et al.*, 1996); however, Thr 333 is in close proximity to the active site Cys 331. The effect of Tyr 351 on IMPDH affinity for IMP could be due to the introduction of a bulky phenyl moiety, as was discussed above. If the environment of the active site had changed due to tertiary perturbations, then it may be possible that the affinity of IMPDH for IMP would be lowered, so the Tyr at position 351 has an indirect effect.

#### $K_i$ XMP

In accordance with the increased  $K_m$ IMP, an increased  $K_i$ XMP (3-fold) in the I333/Y351 (double mutant) IMPDH was detected. It seems as though the T333I mutation contributes significantly. There was a 4.5-fold increased  $K_i$ XMP detected for the T333/Y351 enzyme. The surprising result is that the T333I mutation increased the  $K_i$ XMP 7-fold; this mutation had less effect on the  $K_m$ IMP. It would be tempting to hypothesized that Ile at position 333 is less favourable to XMP binding than Thr 333 at that position, but the crystal structure does not implicate Thr 333 in IMP or, presumably, XMP binding.

#### $k_{cat}$ and $K_m$ IMP/ $k_{cat}$

There was an approximate 10-fold decreased  $k_{cat}$  for I333/Y351 (double mutant) when compared to T333/S351 (wild-type). This decrease in  $k_{cat}$  seemed to be solely due to the T333I mutation; T333/Y351 had a similar  $k_{cat}$  value to wild-type and I333/S351 had a similar  $k_{cat}$  as the double mutant. It is possible that the decreased  $k_{cat}$  may be partly attributed to the interaction of the amino acid at position 333 with  $NAD^+$ ; Thr 333 of the wild-type IMPDH could have a role in  $NAD^+$  binding (discussed above). Alternatively, it has also been hypothesized that the -OH of MPA which interacts with Thr 333

mimics a water molecule. Thr 333 may play a role in catalysis at the point of hydrolysis. Replacement of it with Ile would then possibly lower the rate of hydrolysis and thus the overall rate of catalysis.

$K_m$ IMP/ $k_{cat}$  values were calculated for all four species of IMPDH. For all mutants, there was a vast decrease in this value: 11 to 30-fold for I333/S351, 3 to 11-fold for T333/Y351, and 30 to 47-fold for I333/Y351. The double mutant appears to be the least catalytically efficient IMPDH of the four studied.

### Thr 333 and Ser 351 Across Species

IMPDH consists of two domains: a larger alpha/beta barrel domain and a subdomain which is inserted between the second alpha helix and third beta strand of the barrel (Sinchak *et. al.*, 1996). Thr 333 is located in an alpha-helix portion of the active site loop of IMPDH, which starts just after strand beta-6 of the alpha/beta barrel domain. When MPA is bound to IMPDH, the side-chain of Thr 333 is in close proximity to the side-chains of Gln 441 and Gly 362, which also interact with MPA (Figure 8; Sinchak *et. al.*, 1996). Thr 333 is conserved across all species to date (Table 4), from bacteria and protozoa to humans, suggesting that it has an essential role in IMPDH. This study has implicated its importance in the catalytic rate and mycophenolic acid sensitivity. Substitution of Thr 333 by Ile resulted in a 10-fold decrease in  $k_{cat}$  and 300-fold increase in  $K_i$ MPA. Thr 333 has not been implicated in IMP binding, yet it is close to Cys 331, and substitution of a polar side-chain (of Thr) with a nonpolar side chain (of Ile) may have affected the environment of the active site and could possibly be the reason for the observed increased  $K_m$ IMP of I333/S351 over T333/S351. It is possible that Thr 333 plays a role in  $NAD^+$  binding since it is invariable across species and substitution with Ile resulted in a 6.5-fold decreased affinity for  $NAD^+$ . Thr 333 may also be involved in catalysis since replacement of it caused a 10-fold decreased  $k_{cat}$  and it is

hypothesized to interact with a water molecule.

Ser 351 is located in the alpha-six helix of the alpha/beta barrel domain of IMPDH. Substitution of Ser 351 with Tyr resulted in a 3 to 4-fold increase in both  $K_m$ IMP and  $K_m$ NAD<sup>+</sup>. Sensitivity of the enzyme to MPA and its catalytic efficiency were not greatly affected by this substitution, but the  $K_i$ XMP was increased 4.5-fold. Ser 351 is variable across species (Table 4), present in *D. melanogaster*, hamster, human type II and mouse type II. *B. Subtilis*, *P. furiosus*, *L. donovani*, human type I and mouse type I possess Ala at this position. *E. coli* possesses Val, *T. foetus* has Asn, and *A. thaliana* has a Cys at position 351. Ala is uncharged and the rest of the amino acids, including the original Ser and substituted Tyr of mouse type II IMPDH, contain uncharged polar side-chains. Because of this, the effects of Tyr at position 351 on the  $K_m$ IMP,  $K_m$ NAD<sup>+</sup>, and  $K_i$ XMP may be due to its bulky side chain; amino acids found naturally at amino acid position 351 are much less bulky than Tyr.

### Conclusions

The kinetic properties of four species of mouse type II IMPDH were studied. Substitution of Thr 333 with Ile resulted in an increased  $K_m$ IMP, an increased  $K_m$ NAD<sup>+</sup>, an increased  $K_i$ XMP, an increased  $K_i$ NAD<sup>+</sup>, an increased  $K_i$ MPA, and a decreased  $k_{cat}$ . This mutation proved to be the dominant mutation in both the increased mycophenolic acid resistance and the decreased  $k_{cat}$ . Substitution of Ser 351 with Tyr resulted in an increased  $K_m$ IMP, an increased  $K_m$ NAD<sup>+</sup>, an increased  $K_i$ XMP, and an increased  $K_i$ NAD<sup>+</sup>. The  $K_i$ MPA and  $k_{cat}$  were not significantly affected by this mutation. T333I seemed to be the dominant mutation in the  $K_m$ NAD<sup>+</sup> effect, but each mutation (T333I and S351Y) was cumulative in the  $K_i$ NAD<sup>+</sup> effect (Table 8). This could mean that the determinants in NAD<sup>+</sup> binding as a substrate and binding as inhibitor differ in some aspects. It would

be interesting to obtain the crystal structures of IMPDH bound simultaneously to  $\text{IMP}_{(\text{ox})}$  and  $\text{NAD}^+$  and determine the amino acids important in binding  $\text{NAD}^+$  both as a substrate and as an inhibitor. This could be done for both the wild-type and T333I single mutant IMPDH to see if there are any differences in  $\text{NAD}^+$  binding.

Obtaining the above crystal structures may aid in the generation of better IMPDH MPA-based inhibitors. It has been proposed that MPA mimics the nicotinamide portion of  $\text{NAD}^+$  plus a water molecule (Sintchak *et. al.*, 1996); thus, determining the amino acids important in binding  $\text{NAD}^+$  would aid in decisions regarding modifications to MPA as an IMPDH inhibitor. Presently this is an area of interest for the following reasons. Mycophenolic acid is rapidly metabolized *in vivo* (Shaw *et. al.*, 1995) and undergoes recycling in the liver (Allison and Eugui, 1993). The drug products accumulate in the gastrointestinal tract which contributes to side-effects (Shaw *et. al.*, 1995). An increased half-life *in vivo* would mean that a lower dosage could be given and this could alleviate some of the GI side-effects. Novel IMPDH inhibitors could be synthesized based on the interaction of MPA and  $\text{NAD}^+$  with wild-type and mutant IMPDHs.

## **References**

Abraham, E.P. (1945). The effect of mycophenolic acid on the growth of *Staphylococcus aureus* in heart broth. *Biochemistry Journal* **39**: 398-408.

Abrams, R. and Bentley, M. (1959). Biosynthesis of nucleic acid purines. III. Guanosine 5'-phosphate formation from xanthosine 5'-phosphate and L-glutamine. *Archives of Biochemistry and Biophysics* **79**: 91-110.

Allison, A.C., Hovi, T., Watts, R.W.E., and Webster, A.B.D. (1977). The role of *de novo* purine synthesis in lymphocyte transformation. *Ciba Foundation Symposium* **48**: 207.

Allison, A.C., and Eugui, E.M. (1993). Immunosuppressive and other effects of mycophenolic acid and an ester prodrug, mycophenolate mofetil. *Immunology Review* **136**: 5-28.

Amemiya, H.S., Suzuki, H., Watanabe, R., Hayashi, R., and Niiya, S. (1989). Synergistically enhanced immunosuppressive effect by combined use of cyclosporine and mizoribine. *Transplantation Proceedings* **12**: 956.

Anderson, J.H., and Sartorelli, A.C. (1968). Inosinic acid dehydrogenase of Sarcoma 180 cells. *The Journal of Biological Chemistry* **243**: 4762-4768.

Antonino, L., and Wu, J.C. (1994). Human IMP dehydrogenase catalyzes the dehalogenation of 2-fluoro- and 2-chloroinosine 5'-monophosphate in the absence of NAD<sup>+</sup>. *Biochemistry* **33**: 1753-1759.

Antonino, L., Straub, K., and Wu, J.C. (1994). Probing the active site

of human IMP dehydrogenase using halogenated purine riboside 5'-monophosphates and covalent modification reagents. *Biochemistry* **33**: 1760-1765.

Alsberg, C.L., and Black, O. F. (1913). Contribution to the study of maize deterioration. U.S. Department of Agriculture Plant Industry Bulletin **270**: 7-48.

Atkins, C.A., Shelp, B.J., and Storer, P.J. (1985). Purification and properties of IMP dehydrogenase from nitrogen-fixing nodules of cowpea. *Archives of Biochemistry and Biophysics* **236**: 807-814.

Aviv, H., and Leder, P. (1972). Purification of biologically active globin messenger RNA by chromatography on oligothymidylic acid-cellulose. *Proceedings of the National Academy of Sciences, USA* **69**: 1408-1412.

Bacus, S., Kiguchi, K., Chin, D., King, C. R., and Huberman, E. (1990). Differentiation of cultured human breast cancer cells (AU-565 and MCF-7) associated with loss of cell surface HER-2/neu antigen. *Molecular Carcinogens* **3**: 350-362.

Beck, J.T., Zhao, S. and Wang, C.C. (1994). Cloning, sequencing, and structural analysis of the DNA encoding IMP dehydrogenase from *Trichomonas foetus*. *Experimental Parasitology* **78**: 101-112.

Birnboim, H.C. and Doly, J. (1979). A rapid alkaline extraction procedure for screening recombinant plasmid DNA. *Nucleic Acids Research* **7**: 1513.

Birkinshaw, F.H., Raistrick, H., and Ross, D.F. (1952). Studies in the biochemistry of microorganisms. The molecular constitution of mycophenolic acid, a metabolic product of *Penicillium brevicompactum dierckx*. III. Further observations on the structural

formula for mycophenolic acid. *Biochemistry Journal* **50**: 630-634.

Brox, L.W. and Hampton, A. (1968). IMP dehydrogenase, kinetic mechanism and evidence for selective reaction of the 6-chloro analog of IMP with a cysteine residue at the IMP site. *Biochemistry* **7**: 2589-2596.

Carr, S.F., Papp, E., Wu, J.C., and Natsumeda, Y. (1993). Characterization of human type I and type II IMP dehydrogenases. *The Journal of Biological Chemistry* **268**: 27286-27290.

Catapano, C.V., Dayton, J.S., Mitchell, B.S. and Fernandes, D.J. (1995). GTP Depletion induced by IMP dehydrogenase inhibitors blocks RNA-primed DNA synthesis. *Molecular Pharmacology* **47**: 948-955.

Cha, S. (1975). Tight-binding inhibitors-1; kinetic behaviour. *Biochemical Pharmacology* **24**: 2177-2185.

Cohen, M.B. and Sadee, W. (1983). Contributions of the depletions of guanine and adenine nucleotides to the toxicity of purine starvation in the mouse T lymphoma cell line. *Cancer Research* **43**: 1587-1591.

Collart, F.R. and Huberman, E. (1988). Cloning and sequence analysis of the human and chinese hamster IMP dehydrogenase cDNAs. *The Journal of Biological Chemistry* **263**: 15769-15772.

Collart, F.R. and Huberman, E. (1990). Expression of IMP dehydrogenase in differentiating HL-60 cells. *Blood* **75**: 570-576.

Collart, F.R., Chubb, C.B., Mirkin, B.L., and Huberman, E. (1992). Increased IMP dehydrogenase gene expression in solid tumor tissues and tumor cell lines. *Cancer Research* **52**: 5826-5828.

Collart, F.R., Osipiuk, J., Trent, J., Olsen, G.J., and Huberman, E. (1996).

Cloning, characterization and sequence comparison of the gene coding for IMP dehydrogenase from *Pyrococcus furiosus*. *Gene* **174**: 209-216.

Collart, F.R., Osipiuk, J., Trent, J., Olsen, G.J., and Huberman, E. (1996). Cloning and characterization of the gene encoding IMP dehydrogenase from *Arabidopsis thaliana*. *Gene* **174**: 217-220.

Chomczynski, P. and Sacchi, N. (1987). Single-Step Method of RNA Isolation by Acid Guanidium Thiocyanate-Phenol-Chloroform Extraction. *Analytical Biochemistry* **162**, 156-159.

Crabtree, G.W. and Henderson, J.F. (1971). Rate-limiting steps in interconversion of purine ribonucleotides in Ehrlich Ascites tumor cells *in vitro*. *Cancer Research* **31**: 985-991.

Dayton J.S. and Mitchell, B.S. (1993). Type I IMP dehydrogenase: evidence for a single functional gene in mammalian species. *Biochemical and Biophysical Research Communications* **195**: 897-891.

Dayton, J.S., Lindsten, T., Thompson, C.B., and Mitchell, B.S. (1994). Effects of human T lymphocyte activation on IMP dehydrogenase expression. *Journal of Immunology* **152**: 984-991.

Eugui, E.M., Almquist, S.J., Muller, C.D., and Allison, A.C. (1991). Immunosuppressive effects of mycophenolic acid *in vitro*: role of deoxyguanosine nucleotide depletion. *Scandinavian Journal of Immunology* **33**: 161-173.

Farazit, T., Leichman, J., Harris, T., Cahoon, M., and Hedstrom, L. (1997). Isolation and Characterization of Mycophelic Acid-resistant Mutants of Inosine 5'-Monophosphate Dehydrogenase. *The Journal of Biological Chemistry* **272**: 961-965.

Fleming, M.A., Chambers, S.P., Connelly, P.R., Nimmesgern, E., Fox, T., Bruzzese, F.J., Hoe, S.T., Fulghum, J.R., Livingston, D.J., Stuver, C.M., Sintchak, M.D., Wilson, K.P., and Thompson, J.A. (1996). Inhibition of IMPDH by Mycophenolic Acid: Dissection of Forward and Reverse Pathways Using Capillary Electrophoresis. *Biochemistry* **35**: 6990-6997.

Florey, H.W., Gilliver, K., Jennings, M.A., and Sanders, A.G. (1946). Mycophenolic acid, an antibiotic from *Penicillium brevi-compactum dierckx*. *Lancet* **1**: 46-49.

Franklin, T.J. and Cooke, J.M. (1969). The inhibition of nucleic acid synthesis by mycophenolic acid. *Biochemistry Journal* **113**: 515-524.

Gharehbaghei, K., Sreenath, A., Hao, A., Paull, K., Szekeres, T., Cooney, D.A., Krohn, K., and Jayaram, H.N. (1994). Comparison of biochemical parameters of benzamide riboside, a new inhibitor of IMP dehydrogenase, with tiazofurin and selenazofurin. *Biochemical Pharmacology* **48**: 1413-1419.

Gilbert, H.J., Lowe, C.R., and Drabble, W.T. (1979). IMP dehydrogenase of *Escherichia coli*. *Biochemistry Journal* **183**: 481-494.

Glesne, D.A., Collart, F.R., and Huberman, E. (1991). Regulation of IMP dehydrogenase gene expression by its end products, guanine nucleotides. *Molecular Cell Biology* **11**: 5417.

Glesne, F., Collart, F., Varkony, T., Drabkin, H. and Huberman, E. (1993). Chromosomal localization and structure of the human type II IMP dehydrogenase gene. *Genomics* **16**: 274-277.

Gosio, B. (1896). Bateriologiche e chimiche sulle alterazioni del mais. *riv. Igiene Sanita Publica Ann.* **7**: 825-868.

Gruber, H.E., Jansen, I., Willis, R.C. and Seegmiller, J.E. (1985). Alterations of IMP branchpoint enzymes in cultured human lymphoblasts. *Biochimica et Biophysica Acta* **846**: 135-144.

Gu, J.J., Kaiser-Rogers, K., Rao, K., and Mitchell, B.S. (1994). Assignment of human type I IMP dehydrogenase gene (IMPDH) to chromosome 7q31.3-q32. *Genomics* **24**: 179-181.

Hager, P.W., Collart, F.R., Huberman, E., and Mitchell, B.S. (1994). Recombinant human IMP dehydrogenase type I and type II proteins: purification and characterization of inhibitor binding. *Biochemical Pharmacology* **49**: 1323-1329.

Hedstrom, L. and Wang, C.C. (1990). Mycophenolic acid and thiazole adenine dinucleotide inhibition of *Tritrichomonas foetus* IMP dehydrogenase: implications on enzyme mechanism. *Biochemistry* **29**: 849-854.

Hodges, S.D., Fung, E., McKay, D.J., Renaux, B.S., and Snyder, F.F. (1989). Increased activity, amount, and altered kinetic properties of IMP dehydrogenase from mycophenolic acid-resistant neuroblastoma cells. *The Journal of Biological Chemistry* **264**: 18137-18141.

Holmes, E.W., Pehlke, D.M., and Kelley, W.N. (1974). Human IMP dehydrogenase kinetic and regulatory properties. *Biochimica et Biophysica Acta* **364**: 209-217.

Huberman, E., McKeown, C.K., and Friedman, J. (1981). Mutagen-induced resistance to mycophenolic acid in hamster cells can be associated with increased IMP dehydrogenase activity. *Proceedings of the National Academy of Sciences, USA* **78**: 3151-3154.

Huete-Perez, J.A., Wu, J.C., Whitby, F.G., and Wang, C.C. (1995).

Identification of the IMP binding site in the IMP dehydrogenase from *Trichomonas foetus*. *Biochemistry* **34**: 13889-13894.

Hupe, D.J., Azzolina, B.A., and Behrens, N.D. (1986). IMP dehydrogenase from the intracellular parasitic protozoan *Eimeria tenella* and its inhibition by mycophenolic acid. *The Journal of Biological Chemistry* **261**: 8363-8369.

Ish-Horowicz, D. and Burke, J.F. (1981). Rapid and efficient cosmid cloning. *Nucleic Acids Research* **9**: 2989.

Jackson, R.C. and Weber, G. (1975). IMP dehydrogenase, an enzyme linked with proliferation and malignancy. *Nature* **256**: 331-333.

Jackson, R.C., Morris, H.P. and Weber, G. (1977). Partial purification, properties, and regulation of IMP dehydrogenase in normal and malignant rat tissues. *Biochemistry Journal* **166**: 1-10.

Jayaram, H.N., Gharehbaghi, K., Jayaram, N.H., Rieser, J., Krohn, K. and Paull, K.D. (1992). Cytotoxicity of a new IMP dehydrogenase inhibitor, benzamide riboside, to human myelogenous leukemia K562 cells. *Biochemistry and Biophysics Residence Communications* **186**: 1600-1606.

Jayaram, H.N., Dion, R.L., Glazer, R.I., Johns, D.G., Robins, R.K., Srivastava, P.C. and Cooney, D.A. (1982). Initial studies on the mechanism of action of a new oncolytic thiazole nucleoside, 2- $\beta$ -ribofuranosylthiazole-4-carboxamide. *Biochemical Pharmacology* **31**: 2371-2380.

Kanzake, N. and Miyagawa, K. (1990). Nucleotide sequence of the *Bacillus subtilis* IMP dehydrogenase gene. *Nucleic Acids Research* **18**: 6710.

- Kharabanda, S.M., Serman, M.L., Spriggs D.R., and Kufe, D.W. (1988). Effects of tiazofurin on protooncogene expression during HL60 differentiaion. *Cancer Research* **46**: 5965-5968.
- Kuchi, K., Collart, F.R., Henning-Chubb, C., and Huberman, E. (1990). Induction of cell differentiation in melanoma cells by inhibitors of IMP dehydrogenase; altered patterns of IMP dehydrogenase expression and acitivity. *Cell Growth and Differentiation* **1**: 259-270.
- Kiguchi, K., Collart, F.R., Henning-Chubb, C., and Huberman, E. (1990). Cell differentiation and altered IMP dehydrogenase expression induced in human T-lymphoblastoid leukemia cells by mycophenolic acid and tiazofurin. *Experimental Cell Research* **187**: 47-53.
- Koloski, J., Blair, O.C., and Sartorelli, A.C. (1986). Alterations in glycoprotein synthesis and guanosine triphosphate levels associated with the differentiation of HL-60 leukemia cells produced by inhibitors of IMP dehydrogenase. *Cancer Research* **46**: 2314-2319.
- Konno, Y., Natsumeda, Y., Nagai, M., Yamaji, Y., Ohno, S., Koichi, S., and Weber, G. (1991). Expression of human IMP dehydrogenase types I and II in *Escherichia coli* and distribution in human normal lymphocytes and leukemic cell lines. *The Journal of Biological Chemistry* **266**: 506-509.
- Kumagai, N., Benedict, S.H., Mills, G.B., and Gelfand, E.W. (1987). Requirements for the simultaneous presence of phorbol esters and calcuim ionophores in the expression of human T lymphocyte proliferation-related genes. *Journal of Immunology* **139**: 1393.
- Laemmli. (1970). Cleavage of structural proteins during the assembly of the head of bacteriophage T4. *Nature* **227**: 680-685.
- Lightfoot, T., and Snyder, F. F. (1994). Gene amplification and dual

point mutations of mouse IMP dehydrogenase associated with cellular resistance to mycophenolic acid. *Biochimica et Biophysica Acta* **1217**: 156-162.

Link, J. O. and Straub, K. (1996). Trapping of an IMP dehydrogenase-substrate covalent intermediate by mycophenolic acid. *Journal of the American Chemical Society* **118**, 2091-2092.

Lowe, J.K., Brox, L, and Henderson, J.F. (1977). Consequences of inhibition of guanine nucleotide synthesis by mycophenolic acid and virazole. *Cancer Research* **37**: 736-743.

Malinoski, F., and Stollar, V. (1981). *Virology* **110**: 281-291.

Mitchell, B.S., Dayton, J.S., Turka, L.A. and Thompson, C.B. (1992). IMP dehydrogenase inhibitors as immunomodulators. *Annals of the New York Academy of Sciences* **685**: 217-224.

Nagai, M., Natsumeda, Y., Konno, Y., Hoffman, R., Irino, S., and Weber, G. (1991). Selective up-regulation of type II IMP dehydrogenase messenger RNA in human leukemias. *Cancer Research* **51**: 3886-3890.

Nagai, M., Natsumeda, Y., and Weber, G. (1992). Proliferation-linked regulation of type II IMP dehydrogenase gene in human normal lymphocytes and HL-60 leukemic cells. *Cancer Research* **52**: 258-261.

Natsumeda, Y., Ikegame, T., Murayma, K., and Weber, G. (1988). *De novo* guanylate synthesis in the commitment to replication in hepatoma 3824A cells. *Cancer Research* **48**: 507-511.

Natsumeda, Y., Ohmo, S., Kawasaki, H., Konno, Y., Weber, G., and Suzuki, K. (1990). Two distinct cDNAs for human IMP

dehydrogenase. *The Journal of Biological Chemistry* **265**: 5292-5295.

Olah, E., Natsumeda, Y., Ikegami, T., Kote, Z., Horanyi, M., Szelenyi, J., Paulik, E., Kremmer, T., Hollan, J., Sugar, J., and Weber, G. (1988). Induction of erythroid differentiation and modulation of gene expression by tiazofurin in K-562 leukemia cells. *Proceedings of the National Academy of Sciences, USA* **85**: 6533-6537.

Robins, R.K. (1982) *Nucleosides Nucleotides* **1**, 35-44.

Sakaguchi, K.M., Tsujino, M., Yoshizawa, M., Mizuno, K., and Hayano, K. (1975). Action of Bredenin [mizoribine] on mammalian cells. *Cancer Research* **35**: 1643-1648.

Seeds, N.W., Gilman, A.G., Amano, T., and Nirenburg, M.W. (1970). Regulation of Axon Formation by Clonal Lines of a Neural Tumor. *Proceedings of the National Academy of Sciences, USA*. **66**, 160-167.

Senda, M., and Natsumeda, Y. (1994). Tissue-differential expression of two distinct genes for human IMP dehydrogenase. *Life Sciences* **54**: 1917-1936.

Shaw, L.M., Sollinger, H.W., Halloran, P., Morris, R.E., Yatscoff, R.W., Ransom, J., Tsina, I., Keown, P., Holt, D.W., Lieberman, R., Jaklitsch, A., and Potter, J. (1995). Mycophenolate mofetil: a report of the consensus pannel. *Therapeutic Drug Monitoring* **17**: 690-699.

Sidi, Y., Panet, C., Wasserman, L., Cyjon, A., Novogrodsky, A., and Nordenberg, J. (1988). Growth inhibition and induction of phenotypic alterations in MCF-7 breast cancer cells by an IMP dehydrogenase inhibitor. *Breast Journal Cancer* **58**: 61-63.

Sifri, C.D., Wilson, K., Smolik, S., Forte, M., and Ullman, B. Cloning and

sequence analysis of a *Drosophila melanogaster* cDNA encoding IMP dehydrogenase. *Biochimica et Biophysica Acta* **1217**: 103-106.

Sintchak, M.D., Fleming, M.A., Futer, O., Raybuck, S.A., Chambers, S.P., Caron, P.R., Murcko, M.A., and Wilson, K.P. (1996). Structure and mechanism of IMP dehydrogenase in complex with the immunosuppressant mycophenolic acid. *Cell* **85**: 921-930.

Snyder, F.F. and Henderson, J.F. (1973). Effects of elevated intracellular ATP and GTP concentrations on purine ribonucleotide synthesis and interconversion. *Canadian Journal of Biochemistry* **51**: 943-948.

Sollinger, H.W. (1995). Mycophenolate mofetil for the prevention of acute rejection in primary cadaveric renal allograft recipients. *Transplantation* **60**: 225-232.

Streeter, D.G., Witowski, J.T., Gyaneshwar, P.K., Sidwell, R.W., Bauer, R.J., Robins, R.K., and Simon, L.N. (1973). Mechanism of 1- $\beta$ -D-ribofuranosyl-1,2,4-triazole-3-carboxamide (Virazole), a new broad-spectrum antiviral agent. *Proceedings of the National Academy of Sciences, USA* **70**, 1174-1178.

Thomas, M.S., and Drabble, W.T. (1985). Nucleotide sequence and organization of the *gua* promoter region of *Escherichia coli*. *Gene* **36**: 45-53.

Tiedeman, A.A., and Smith, J.M. (1991). Isolation and sequence of a cDNA encoding mouse IMP dehydrogenase. *Gene* **97**: 289-293.

Tricot, G.J., Jayaram, H.N., Lapis, E., Natsumeda, Y., Nichols, C.R., Kneebone, P., Heerema, N., Weber, G., and Hoffman, R. (1989). Biochemically directed therapy of leukemia with tiazofurin, a selective blocker of IMP dehydrogenase activity. *Cancer Research*

49: 3696-3701.

Turka, L.A., Dayton, J., Sinclair, C., Thompson, C.B., and Mitchell, B.S. (1991). Guanine ribonucleotide depletion inhibits T cell activation: mechanism of action of the immunosuppressive drug mizoribine. *Journal of Clinical Investigations* **87**: 940.

Verham, R., Meek, T.D., Hedstrom, L., and Wang, C.C. (1987). Purification, characterization and kinetic analysis of IMP dehydrogenase of *Tritrichomonas foetus*. *Molecular Biochemistry of Parasitology* **24**: 1-12.

Weber, G. (1983). Biochemical strategy of cancer cells and the design of chemotherapy: G.H.A. Clowes memorial lecture. *Cancer Research* **43**, 3466-3492.

Webster, H.K. and Whaun, J.M. (1982). Antimalarial Properties of Bredinin. *Journal of Clinical Investigation* **70**: 461-469.

Wilson, K., Collart, F., Huberman, E., Stringer, J. and Ullman, B. (1991). Amplification and molecular cloning of the IMP dehydrogenase gene of *Leishmania donovani*. *The Journal of Biological Chemistry* **266**: 1665-1671.

Wu, J.C., Carr, S.F., Antonino, L.C., Papp, E., and Pease, J.H. (1996). Formation and rate-determining hydrolysis of a covalent intermediate by human type II IMP dehydrogenase. *FASEB Journal*, A1337

Xiang, B., Taylor, J., and Markham, G.D. (1996). Monovalent cation activation and kinetic mechanism of IMP dehydrogenase. *The Journal of Biological Chemistry* **271**: 1435-1440.

Yamada, Y., Natsumeda, Y., and Weber, G. (1987). Purification of IMP

Dehydrogenase from Rat Hepatoma 3942A. *Life Sciences* **40**: 2277-2282.

Yamafi, Y., Natsumeda, Y., Yamade, Y., Iroino, S., and Weber, G. (1990). Synergistic action of tiazofurin and retinoic acid on differentiation and colony formation of HL-60 leukemia cells. *Life Sciences* **46**: 435-442.

Zimmermann, A.G., Spsychala, J. and Mitchell, B.S. (1995). Characterization of the human IMP dehydrogenase type II gene. *The Journal of Biological Chemistry* **270**: 6808-6814.

## Appendix: Enzyme Kinetics

The following is a brief explanation of terms used when enzyme kinetics was discussed followed by a list of the formulae used to calculate the kinetic parameters.

$K_m$  is an apparent dissociation constant that may be treated as the overall dissociation constant of all enzyme-bound species. In all cases, the  $K_m$  is equal to the substrate concentration at which the velocity of the reaction is equal to half of the maximal velocity. Since enzymes have a high affinity for their substrates, binding the substrate is not usually the rate-limiting step; thus, the  $K_m$  is often thought of as the concentration of substrate which half-saturates the enzyme.

$K_i$  is the dissociation constant for the complex containing the inhibitor. Its value depends on the mode of inhibition (discussed below).

$k_{cat}$  is the catalytic constant, often referred to as the turnover number. It represents the maximum number of substrate molecules converted to products per active site (or per enzyme) per unit time, or the number of times the enzyme "turns over" per unit time.

$k_{cat}/K_m$  is the specificity constant. It relates the reaction rate to the concentration of free rather than total enzyme. It determines the specificity of the enzyme for competing substrates.

### Initial Velocity Studies

Initial velocity studies allow the investigator to learn details about the enzyme mechanism. The concentration of products are essentially equal to zero; thus, the rate equation for the reaction is

simplified.

It may be useful to refer to figure 3 for the reaction mechanism of IMPDH. For the case of the ordered bi-bi mechanism of IMPDH, E = IMPDH, A = IMP, B = NAD<sup>+</sup>, S = variable substrate, and I = XMP, NAD<sup>+</sup> at high concentrations, or MPA. All data was analyzed using the following formulae before being plotted as double reciprocals (Lineweaver-Burk plots). For the case of an ordered bi-bi reaction (as in IMPDH), the initial velocity equation when [A] is varied and B is held at changing fixed concentrations is:

$$v = \frac{V_{\max} [A] [B]}{K_{ap}K_mB + K_b[A] + K_mA[B] + [A] [B]}$$

where A is the first substrate which binds and B is the second. From the known values of [E]<sub>0</sub>, [A], [B], and enzyme rate (which is measured), the values of K<sub>m</sub>A, K<sub>m</sub>B, k<sub>cat</sub> and V<sub>max</sub> (which is equal to k<sub>cat</sub> [E]<sub>0</sub>) can be determined. K<sub>ap</sub> is the apparent constant. With increasing concentrations of B, K<sub>ap</sub> either decreases or remains the same for an ordered mechanism and increases for a ping-pong mechanism. The Lineweaver-Burk plots are 1/velocity vs 1/[variable substrate] and yield a series of lines which join to the left of the vertical axis. The vertical intercept represents the reciprocal velocity at infinite substrate concentration { = (1/V<sub>max</sub>) (1 + K<sub>m</sub>B/[B]) when A is the variable substrate } and the slope is a measure of how quickly the reaction slows down as the substrate concentration decreases from infinity to zero { = (K<sub>m</sub>A/V<sub>max</sub>) (1 + K<sub>i</sub>A K<sub>m</sub>B/[B]K<sub>m</sub>A) }.

### Enzyme Inhibition

There are three main types of reversible enzyme inhibitors: competitive, uncompetitive and noncompetitive.

### Competitive Inhibition

An inhibitor is competitive with respect to a substrate if its binding to the enzyme is mutually exclusive with the binding of the substrate. They could resemble each other and bind to the same site, there could be steric hindrance preventing the simultaneous binding of both, or they could bind to overlapping sites. Increasing concentrations of substrate can overcome the inhibition. The rate equation for competitive inhibition is

$$v = \frac{V_{\max}[S]}{[S] + K_m (1 + [I]/K_i)}$$

Inhibitor I and substrate S compete for binding to the enzyme. The apparent  $K_m$  is affected (apparently increased by a factor of  $1 + [I]/K_i$ ). The  $V_{\max}$  is not affected since infinitely high concentrations of S displace all I from the enzyme; however, when inhibitor is present, a greater concentration of substrate is needed to attain the  $V_{\max}$ . The slope of the double reciprocal plot is equal to  $[K_m/V_{\max}(1 + [I]/K_i)]$  and the vertical intercept is  $(1/V_{\max})$ . The series of nonparallel lines intercept on the vertical axis since the  $V_{\max}$  is unaffected with a competitive inhibitor present. The  $K_i$  is equivalent to the concentration of I required to double the slope of the double reciprocal plot.

### Uncompetitive Inhibition

An inhibitor is uncompetitive with respect to a substrate when it cannot bind to the same form of the enzyme to which the substrate binds. The pattern of inhibition disappears when the concentration of substrate is extrapolated to zero because the enzyme form to which the inhibitor binds is not present when there is no substrate

present. The rate equation for uncompetitive inhibition is

$$v = \frac{V_{\max}[S]/(1 + [I]/K_i)}{[S] + K_m/(1 + [I]/K_i)}$$

Inhibitor I binds to ES but not to E; no EI complex forms. The slope of the double reciprocal plot is equal to  $K_m/V_{\max}$  and the y-intercept is equal to  $1/V_{\max}(1 + [I]/K_i)$ . The inhibitor decreases  $V_{\max}$  and the apparent  $K_m$  equally; therefore the slope is unaffected. The degree of uncompetitive inhibition increases as [S] increases, because the [ES] also increases and the uncompetitive inhibitor binds only to ES. The double reciprocal plots are thus a series of parallel lines. The  $K_i$  is equal to the [I] which doubles the vertical intercept value of the double reciprocal plot.

#### Noncompetitive Inhibition

Noncompetitive inhibition was not examined in this study but is worth mentioning in the appendix for the sake of completion. An inhibitor is noncompetitive with respect to substrate if the inhibitor and substrate bind randomly and independently at different sites on the enzyme. The ESI complex is not active. The velocity equation for uncompetitive inhibition is

$$v = \frac{V_{\max}([S]/K_m)}{1 + [S]/K_m + [S][I]/K_m K_i}$$

I and S can bind simultaneously to the enzyme and do not compete for the same site. Both the slope and intercept terms of the reciprocal plot are affected by a noncompetitive inhibitor. The result is a series of nonparallel lines which meet left of the vertical axis. The slope of

each line is equal to  $K_m/V_{max}(1 + [I]/K_i)$  and the intercept is  $1/V_{max}(1 + [I]/K_i)$ . In classical noncompetitive inhibition, the apparent  $K_m$  is unaffected and  $V_{max}$  is decreased by a factor of  $(1 + [I]/K_i)$ . When  $[I] = K_i$ , 50% inhibition is observed at all  $[S]$ . It is more common that the dissociation constant of  $S$  from  $EIS$  is different than that from  $ES$ . In this case, both  $K_m$  and  $V_{max}$  are decreased and the type of inhibition is termed mixed.

### Substrate Inhibition

This type of inhibition usually occurs when the substrate combines with the wrong enzyme form and so is apparent only at high substrate concentrations. In the case of IMPDH,  $NAD^+$  at high concentrations was able to bind to  $E-IMP_{(ox)}$  after  $NADH$  had been released, resulting in a dead-end complex that could not be hydrolyzed to products.  $NAD^+$  was treated as an uncompetitive inhibitor in the analysis.

### Tight-Binding Inhibition

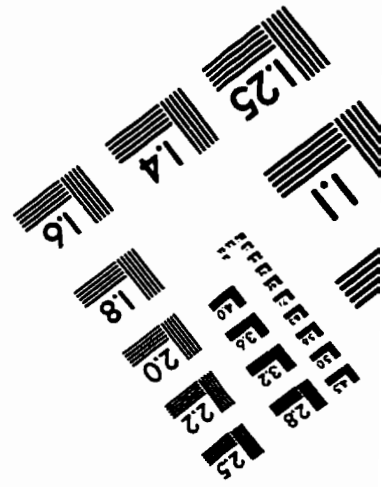
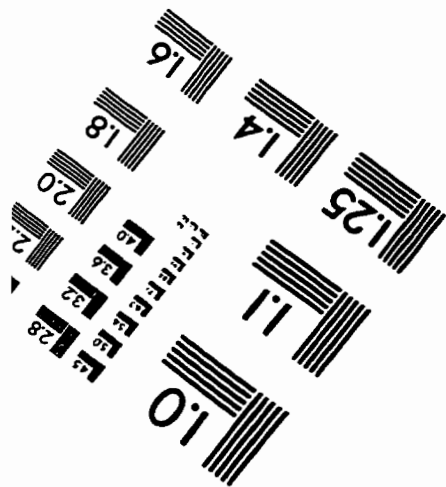
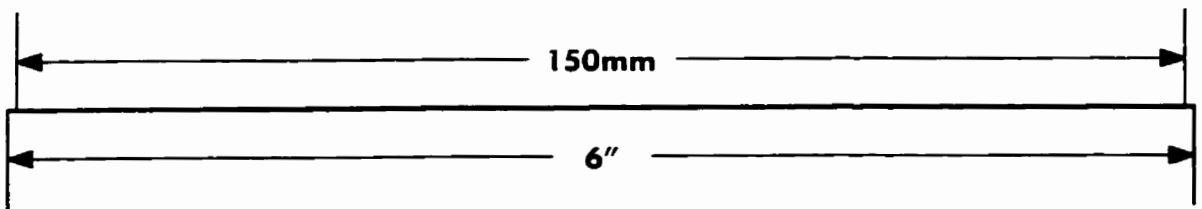
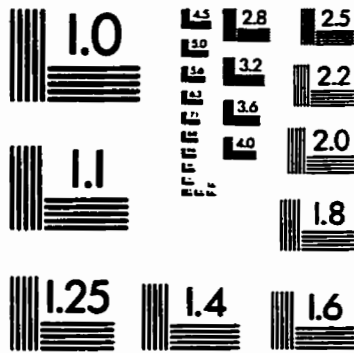
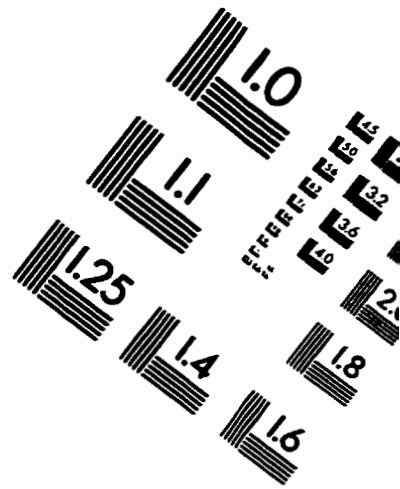
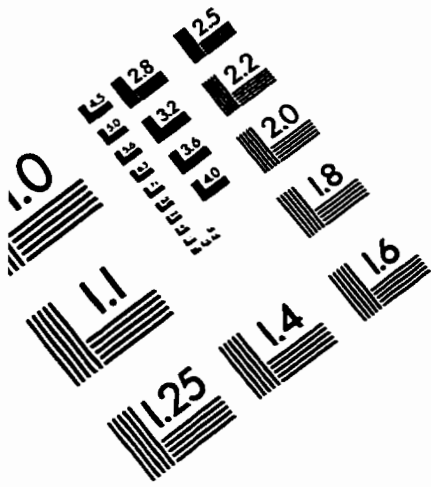
The above inhibitions assume that there is no significant depletion of inhibitor when it binds to  $E$ . This is not true if the inhibitor has a very high affinity for  $E$ . In this case, a very small concentration of inhibitor is used in initial velocity studies and thus may be relatively significantly depleted upon binding to enzyme. MPA is a tight-binding uncompetitive inhibitor of IMPDH. The initial velocity equation used for MPA is

$$v = \frac{k_{cat}[E]_0[S]/(1 + [I]/(K_i + v/k_{cat}))}{[S] + K_m/(1 + [I]/(K_i + v/k_{cat}))}$$

MPA is also a dead-end inhibitor of IMPDH, meaning that it combines with the enzyme to form a complex which cannot undergo any

further conversion and the reaction is not "backed up".

# IMAGE EVALUATION TEST TARGET (QA-3)



APPLIED IMAGE, Inc  
1653 East Main Street  
Rochester, NY 14609 USA  
Phone: 716/482-0300  
Fax: 716/288-5989

© 1993, Applied Image, Inc., All Rights Reserved